

**SPRAY CHARACTERISTICS OF EMULSIFIED  
BIODIESEL-DIESEL BLENDS IN A CONSTANT  
VOLUME COMBUSTION CHAMBER**

**A Thesis Submitted to  
the Graduate School of Engineering and Sciences of  
İzmir İnstitute of Technology  
in Partial Fulfillment of the Requirements for the Degree of**

**MASTER OF SCIENCE**

**in Mechanical Engineering**

**by  
Yusufcan TEZEL**

**December 2020  
İZMİR**

## ACKNOWLEDGEMENTS

There are many people who supported me in various ways while I was working on this Master thesis. I would like to thank everyone who helped me directly or indirectly.

First of all, I would like to express my deep and sincere gratitude to my research supervisor Assoc. Prof. Dr. Ünver Özkol for his coaching and assistance during my thesis. Also, I would like to express my appreciation to my prior advisor Asst. Prof. Dr. Alvaro Diez Rodriguez for his support.

I would like to acknowledge to examining committee members who are Assoc. Prof. Dr. Nurdan Yıldırım and Asst. Prof. Dr. Güray Yıldız for their valuable comments and suggestions. I would also like to thank my colleagues and friends at İzmir Institute of Technology for their friendship and support. Besides, I would like to special thank to Anılcan Ulu for his help and sharing his experience with me from the beginning of my studies.

Also, I am thankful to my lovely friend Ecem Sert for her love, understanding and continuing support.

Finally, and most importantly, I am extremely grateful to my mother Nazan Tezel, my father Mustafa Nevzat Tezel and my brother Mehmet Can Tezel for their love, caring, sacrifices and endless support.

# ABSTRACT

## SPRAY CHARACTERISTICS OF EMULSIFIED BIODIESEL-DIESEL BLENDS IN A CONSTANT VOLUME COMBUSTION CHAMBER

Over the last decades, various studies have been carried out by the researchers to find out an alternative fuel that can overcome emission problems caused by diesel fuel which affect the environment and human health significantly. Due to emulsified biodiesel-diesel blend (EBB) fuels are being a possible alternative fuel for diesel, in this study, it was aimed to investigate the macroscopic spray parameters such as spray penetration length and cone angle of different EBB fuels, namely B20W15 and B20W5, containing 15% and 5% water by volume, respectively. In order to examine the spray characteristics of B20W15 and B20W5, the experiments were carried out by means of constant volume combustion chamber and utilizing shadowgraph technique with a high speed camera. Experiments were performed with 600 bar and 800 bar injection pressure while the ambient pressure was 0 bar, 5 bar and 10 bar, respectively. After experiments were fulfilled, the recorded images of test fuels were processed via ImageJ program.

The results showed that stability of the emulsion can be obtained when HLB value was 8 and surfactant concentration was 5% by volume. It was understood that increment in water concentration in the emulsion caused deterioration in emulsion stability while it led higher viscosity, higher density, longer spray penetration lengths and narrower cone angles. It was observed that B20W5 resulted wider spray cone angles and shorter spray penetration lengths than B20W15 under 0,5 and 10 bar chamber pressure with injections pressures of 600 and 800 bar. Also, it was understood that both EBB lead longer spray penetration lengths and narrower spray cone angles compared to reference diesel while they lead vice versa compared to reference biodiesel. The reason of spray geometry difference between diesel and EBB fuels can be associated with the higher viscosity and density of EBB fuels compared to diesel. As a result, considering that B20W5 reduce the use of fossil fuels, and no significant difference compared to diesel in terms of spray geometry, it can be said that B20W5 may be a promising alternative fuel for the future.

***Keywords:*** *Emulsion, Stability, Spray Characteristics*

## ÖZET

### SABİT HACİMLİ YANMA ODASINDA EMÜLSİFİYE BİYODİZEL-DİZEL KARIŞIMLARIN PÜSKÜRTME ÖZELLİKLERİ

Son yıllarda, araştırmacılar tarafından çevreyi ve insan sağlığını önemli ölçüde etkileyen dizel yakıtının neden olduğu emisyon problemlerinin üstesinden gelebilecek alternatif bir yakıt bulmak için çeşitli çalışmalar yapılmıştır. Emülsiyonlaştırılmış biyodizel-dizel karışım (EBK) yakıtlarının dizel için olası bir alternatif yakıt olması sebebi ile, bu çalışmada hacimlerinin sırasıyla %15'i ve %5'i su olan B20W15 ve B20W5 olarak adlandırılan farklı EBK yakıtlarının püskürtme uzunlunluğu ve püskürtme açısı gibi makroskopik püskürtme parametrelerinin incelenmesi amaçlanmıştır. B20W15 ve B20W5'in püskürtme özelliklerini incelemek için deneyler, sabit hacimli yanma odası ve yüksek hızlı kamera ile gölgelendirme tekniği kullanılarak gerçekleştirilmiştir. Deneyler, 600 bar ve 800 bar enjeksiyon basıncıyla yapılırken ortam basıncı sırasıyla 0 bar, 5 bar ve 10 bar idi. Deneyler tamamlandıktan sonra, test yakıtlarının kaydedilen görüntüleri ImageJ programı ile işlendi.

Sonuçlar, emülsiyon stabilitesinin HLB değeri 8 ve yüzey aktif madde konsantrasyonu hacmen %5 olduğunda elde edilebileceğini gösterdi. Emülsiyondaki su konsantrasyonundaki artış, emülsiyon stabilitesinde bozulmaya neden olurken, daha yüksek viskozite, daha yüksek yoğunluk, daha uzun püskürtme uzunluklarına ve daha dar püskürtme koni açılarına yol açtığı anlaşılmıştır. B20W5'in 0,5 ve 10 bar oda basınçları altında 600 ve 800 bar enjeksiyon basınçlarıyla B20W15'e göre daha geniş püskürtme konisi açılarına ve daha kısa püskürtme penetrasyon uzunlukları sağladığı gözlemlenmiştir. Ayrıca, her iki EBK'nin referans dizele kıyasla daha uzun püskürtme penetrasyon uzunlukları ve daha dar püskürtme konisi açılarına neden olduğu, referans biyodizele kıyasla ise tam tersine sebep olduğu anlaşılmıştır. Dizel ve EBK yakıtlarının arasındaki püskürtme geometrisi farkının nedeni, EBK yakıtlarının dizele kıyasla daha yüksek viskozitesi ve yoğunluğu ile ilişkilendirilebilir. Sonuç olarak, B20W5'in fosil yakıt kullanımını azalttığı ve püskürtme geometrisi açısından dizel ile kıyaslandığında önemli bir fark olmadığı göz önüne alındığında, B20W5'in gelecek için umut verici bir alternatif yakıt olabileceği söylenebilir.

**Anahtar Sözcükler:** Emülsiyon, Stabilité, Püskürtme Özellikleri

# TABLE OF CONTENTS

LIST OF FIGURES .....	vii
LIST OF TABLES .....	ix
LIST OF ABBREVIATIONS .....	x
LIST OF SYMBOLS .....	xi
CHAPTER 1. INTRODUCTION .....	1
CHAPTER 2. LITERATURE SURVEY .....	4
2.1. Internal Combustion Engines.....	4
2.1.1. Combustion Processes in Diesel Engine.....	6
2.1.2. Engine Emissions in Diesel Engine .....	8
2.1.2.1. Nitrogen Oxide (NO <sub>x</sub> ) .....	8
2.1.2.2. Hydrocarbon (HC) .....	9
2.1.2.3. Particulate Matter (PM).....	9
2.1.2.4. Carbon Monoxide (CO) .....	10
2.2. Injection System and Its Effect on Emissions.....	10
2.2.1. Fuel Injectors.....	12
2.2.2. Nozzle .....	14
2.3. Fundamentals of Liquid Sprays .....	16
2.3.1. Primary Breakup Regimes .....	18
2.3.2. Secondary Breakup Regimes .....	21
2.3.3. Spray Patterns.....	22
2.3.4. Spray Characteristics.....	23
2.3.5. Spray Measurement Methods.....	31
2.4. Fuel types for CI Engine .....	33
2.4.1. Emulsified Diesel .....	33
2.4.2. Biodiesel.....	34
2.4.2.1. Emissions of Biodiesel.....	35

2.4.2.2. Engine Performance of Biodiesel.....	37
2.4.2.3. Drawbacks of Biofuels.....	38
2.4.3. Emulsified Biodiesel-Diesel Blends .....	39
2.4.3.1. Effect on Engine Performance .....	40
2.5.3.2. Effect on Emissions.....	42
2.5. Preparation of Blend Biodiesel-Diesel Emulsion .....	44
2.5.1. Emulsion Stability .....	45
2.5.1.1 Role of Water & Surfactant Concentration on Emulsion Stability .....	46
 CHAPTER 3. EXPERIMENTAL DESIGN & METHODOLOGY.....	 52
3.1. Experimental Test Apparatus.....	53
3.2. The Preparation of Emulsion of Biodiesel-Diesel Blend.....	58
3.3. Methodology .....	60
 CHAPTER 4. RESULTS & DISCUSSIONS .....	 64
4.1. Stabilities of Emulsions .....	64
4.2. Examination of Spray Penetration Length.....	67
4.3. Examination of Spray Cone Angle .....	73
 CHAPTER 5. CONCLUSION .....	 78
5.1. Conclusions .....	78
5.2. Suggestions for Future Works.....	80
 REFERENCES .....	 81

# LIST OF FIGURES

<b><u>Figure</u></b>	<b><u>Page</u></b>
Figure 2.1: Example of a Spark Ignition internal combustion engine with four stroke cycle .....	4
Figure 2.2: Heat release rate of the CI engine with respect to combustion process .....	7
Figure 2.3: Sketch of common-rail injection system .....	11
Figure 2.4: Cross-section of a fuel injector .....	12
Figure 2.5: Types of nozzles: Single hole, pintle hole, multiple hole, and pintaux .....	14
Figure 2.6: VCO nozzle and sac hole nozzle .....	15
Figure 2.7: Demonstration of different nozzle hole geometries .....	16
Figure 2.8: The illustration of full cone spray .....	17
Figure 2.9: Demonstration of the primary and secondary breakup .....	17
Figure 2.10: The schematic of the primary break-up regimes .....	18
Figure 2.11: Jet break-up regimes according to Ohnesorge number .....	19
Figure 2.12: Cavitation and turbulence inside of the nozzle .....	20
Figure 2.13: Secondary breakup regimes according to Weber number .....	22
Figure 2.14: Demonstration of different spray patterns.....	22
Figure 2.15: Demonstration of macroscopic spray parameters .....	24
Figure 2.16: Schematic view of a shadowgraph system .....	32
Figure 2.17: Distribution of feedstocks used in the scientific articles .....	34
Figure 2.18: Transesterification reaction of triglyceride .....	35
Figure 2.19: Emission difference between diesel, biodiesel and biodiesel blend.....	35
Figure 2.20: Illustration of secondary atomization due to micro explosion phenomenon.....	40
Figure 2.21: Illustration of three phase emulsion and two phase emulsion .....	45
Figure 2.22: The stability of the three phase emulsion with respect to different HLB and different water concentrations .....	47
Figure 3.1: Illustration of experimental test apparatus .....	52
Figure 3.2: Schematic of the experimental test apparatus .....	53
Figure 3.3: The demonstration of CVCC.....	54

<b><u>Figure</u></b>	<b><u>Page</u></b>
Figure 3.4: The components of fuel injection system, respectively; fuel pump (at the bottom of the table), fuel tank (on the left of the table), common rail (at the middle of the table).....	55
Figure 3.5: Indication of located injector as horizontally .....	56
Figure 3.6: Illustration of optical system from different views .....	57
Figure 3.7: Materials for preparation B20W15 and B20W5; distilled water, surfactants, diesel and biodiesel .....	58
Figure 3.8: Changing colour of the mixture during the addition of water .....	59
Figure 3.9: The sample of blended emulsion fuel at the end of the preparation process .....	60
Figure 3.10: Demonstration of images during the measurement process.....	62
Figure 4.1 (a): Spray penetration lengths with injection pressures of 600 bar and 800 bar at 0 bar ambient pressure .....	68
Figure 4.1 (b): Spray penetration lengths with injection pressures of 600 bar and 800 bar at 5 bar ambient pressure .....	68
Figure 4.1 (c): Spray penetration lengths with injection pressures of 600 bar and 800 bar at 10 bar ambient pressure .....	68
Figure 4.2 (a): Spray penetration lengths with 600 bar injection pressure under 0 bar, 5 bar and 10 bar ambient pressure .....	69
Figure 4.2 (b): Spray penetration lengths with 800 bar injection pressure under 0 bar, 5 bar and 10 bar ambient pressure .....	69
Figure 4.3 (a): Spray cone angles with injection pressures of 600 bar and 800 bar at 0 bar ambient pressure .....	73
Figure 4.3 (b): Spray cone angles with injection pressures of 600 bar and 800 bar at 5 bar ambient pressure .....	74
Figure 4.3 (c): Spray cone angles with injection pressures of 600 bar and 800 bar at 10 bar ambient pressure .....	74
Figure 4.4 (a): Spray cone angles with 600 bar injection pressure under 0 bar, 5 bar and 10 bar ambient pressure .....	75
Figure 4.4 (b): Spray cone angles with 800 bar injection pressure under 0 bar, 5 bar and 10 bar ambient pressure .....	75



## LIST OF TABLES

<b><u>Table</u></b>	<b><u>Page</u></b>
Table 2.1: Piezo injectors vs solenoid injectors.....	13
Table 2.2: Summarization of studies related with spray characterization in CI engine.....	28
Table 2.3: Comparison of optical techniques .....	32
Table 2.4: Properties of Span 80 and Tween 80.....	46
Table 2.5: O/W/O Emulsions with different concentration ratios of water, surfactant and HLB value .....	49
Table 4.1: Stabilization of emulsions with different concentration of ingredients.....	65
Table 4.2: Properties of fuels.....	66

## LIST OF ABBREVIATIONS

ICE.....	Internal Combustion Engine
SI.....	Spark Ignition
CI.....	Compression Ignition
TDC.....	Top Dead Center
BDC.....	Bottom Dead Center
BP.....	Brake Power [kW]
BTE.....	Brake Thermal Efficiency
BSFC.....	Brake Specific Fuel Consumption [g/kW.h]
HRR.....	Heat Release Rate [W]
EBB.....	Emulsified Blend Biodiesel-Diesel
CVCC.....	Constant Volume Combustion Chamber
RCM.....	Rapid Compression Machines
CPFR.....	Constant Pressure Flow Rig
RCYM.....	Rapid Cycling Machine
LIF.....	Laser Induced Fluorescence
PIV.....	Particle Image Velocimetry
PDPA.....	Phase Doppler Particle Anemometry
PCV.....	Pressure Control Valve
VCV.....	Volume Control Valve
PWM.....	Pulse with Modulation
DAQ.....	Data Acquisition Card
SPL.....	Spray Penetration Length [mm]
SCA.....	Spray Cone Angle [degree]
SMD.....	Sauter Mean Diameter
CPO.....	Crude Palm Oil

## LIST OF SYMBOLS

W/O.....	Water in Oil
O/W.....	Oil in Water
W/O/W.....	Water in Oil in Water
O/W/O.....	Oil in Water in Oil
HLB <sub>ST</sub> .....	Combined Hydrophilic-Lipophilic Balance of Tween 80 and Span 80
HLB <sub>T</sub> .....	Hydrophilic-Lipophilic Balance of Tween 80
HLB <sub>S</sub> .....	Hydrophilic-Lipophilic Balance of Span 80
W <sub>T</sub> .....	Weight of Tween 80 [N]
W <sub>S</sub> .....	Weight of Span 80 [N]
BX.....	X% Biodiesel in Blended Biodiesel-Diesel
WY.....	Y% Water by Volume
Z.....	Ohnesorge Number
Re.....	Reynolds Number
We.....	Weber Number
<i>u</i> .....	Velocity [m/s]
<i>D</i> .....	Diameter [m]
$\rho$ .....	Density [kg/m <sup>3</sup> ]
$\sigma$ .....	Surface Tension [N/m]
$\mu$ .....	Dynamic Viscosity [(N.s)/m <sup>2</sup> ]
$\dot{m}$ .....	Mass Flow Rate [kg/s],[g/h]
LCV.....	Lower Calorific Value [kJ/kg]
<i>N</i> .....	Crankshaft Rotational Speed [rev/s]
<i>T</i> .....	Torque [N.m]
$n_{brakethermal}$ .....	Brake Thermal Efficiency
CO.....	Carbon Monoxide

CO <sub>2</sub> .....	Carbon Dioxide
HC.....	Hydrocarbon
PM.....	Particulate Matter
NO <sub>x</sub> .....	Nitrogen Oxide

# CHAPTER 1

## INTRODUCTION

Nowadays, diesel fuels have been usually utilized in various sectors like agriculture, transportation and industries as major source of energy when their high efficiency and lower fuel consumptions are taken account of. For decades, the emissions released from burned diesel fuel has adverse effects on the environment, consequently on human health as well. Also, rising vehicle population and depletion of petroleum reserves has been led researchers to find out an alternative fuel instead of fossil fuel that can overcome these significant issues.

Thangavelu et al. (2016) [1] stated that biofuels such as biodiesels and bioethanols are most distinguished alternative fuels for replacing petroleum-based fuels in internal combustion engines (ICE). Thangavelu et al. (2016) [1] pointed out that bioethanols are produced from bioenergy crops and high octane number, low vapor pressure, high heat of vaporization, beign renewable of them lead to be considered as alternative fuel for gasoline.

Meanwhile, biodiesels was thought as one of the possible alternative fuel for diesel fuel due to their closer properties to diesel. The biggest advantage of biodiesel compared to diesel is beign a renewable fuel and composing of animal fats and vegetable oils. Borovalı (2019) [2] showed that, Turkey produced 120.000m<sup>3</sup> of biodiesel while Germany, France, Spain, Italy and Greece produced 2.610.000m<sup>3</sup>, 1.700.000m<sup>3</sup>, 1.200.000m<sup>3</sup>, 560.000m<sup>3</sup>, 130.000m<sup>3</sup> of biodiesel respectively at 2018. Borovalı (2019) [2] reported that during these productions at 2018, the most used feedstock in EU was canola oil, which was 42% of the total feedstock. On the other hand, cottonseed oil was the most used feedstock in Turkey as 32% of the total feedstock.

According to Hoekman and Robbins (2012) [3], Canakci (2007) [4] and Chauhan et al, (2012) [5], eventough biodiesels contribute the reduction in most of emissions, the higher oxygen concent in their structure have been leading to increase in NO<sub>x</sub>. Thus, another possible alternative fuel has been thought as emulsificated blend biodiesel-diesel

(EBB), which can reduce the extra NO<sub>x</sub> caused by biodiesels. Kumar et al. (2009) [6], Elsanusi et al. (2017) [7] and Karabektas et al. (2016) [8] explained this with decreased combustion temperature due to water content inside of the mixture. Also, Avulapati et al. (2016) [9] and Hagos et al. (2011) [10] reported that another important advantage of water is promoting the combustion process through the occurrence of microexplosion phenomenon which results in disintegration of the fuel droplets as very fine formation.

The spray's geometric characteristics of a fuel takes an significant role on the combustion process, and consequently affecting to engine performance and emission levels, when the mixture of air and fuel is taken consider. For this reason, in this study, it was aimed that examination of spray's geometric characteristics such as spray penetration length (SPL) and spray cone angle (SCA) of B20W5 and B20W15, which contains 80% diesel and 20% biodiesel (B20) with a concentration of 5% water (W5) and 15% water (W15) respectively, and comparison the results of both EBB fuels with reference diesel and reference biodiesel fuel.

For the following chapters, researches in the literatures related with the spray investigation of EBB fuels are explained. Firstly, basics of internal combustion engines and combustion process of Compression Ignition (CI) engines are explained. For the following, the injection system of CI engine and fundamentals of liquid sprays are expressed. Meanwhile, the measurement methods of macroscopic and microscopic spray parameters including several test rigs with optical techniques, especially shadowgraph technique are mentioned. In addition, studies has been done before for macroscopic spray parameters of test fuels are summarized in table. Next, fuel types of CI engines are compared to each others according to engine performance and emission levels. After that, preparation of EBB is represented. Besides, various studies which investigates the parameters that affects emulsion stability such as concentration of water, concentration of surfactant, value of hydrophilic-lipophilic balance (HLB), type of mixer, speed and time of mixing are summarized in another table.

In Chapter 3, the experimental test apparatus and methodology performed including image processing during this study is described, detailly. Also, the preparation of emulsion and requirement materials are clarified.

In Chapter 4, the results obtained from this study is given deatilly. First, stability of various emulsions are discussed and maximum stability obtained during the trials are mentioned. After that, the results of spray penetration length and spray cone angle of emulsified biodiesel-diesel blends are given respectively by means of various graphs and the results of each other are disscussed detailly.

In Chapter 5, the conclusion of this study and recommendation for future works is presented.

## CHAPTER 2

### LITERATURE SURVEY

#### 2.1. Internal Combustion Engines

Naber and Johnson (2014) [11] defined that internal combustion engine (ICE) is an engine that enables to convert chemical energy to mechanical energy where the combustion occurs through the mixture of air and fuel. This combustion of mixture produces high amount of chemical energy due to high temperature and pressure inside of the combustion chamber, and that occurred chemical energy is transformed to mechanical energy by the help of pistons through crank-slider mechanism. Illustration of the four-stroke IC engine includes compression, combustion, power, and exhaust processes is shown in the Figure 2.1 below.

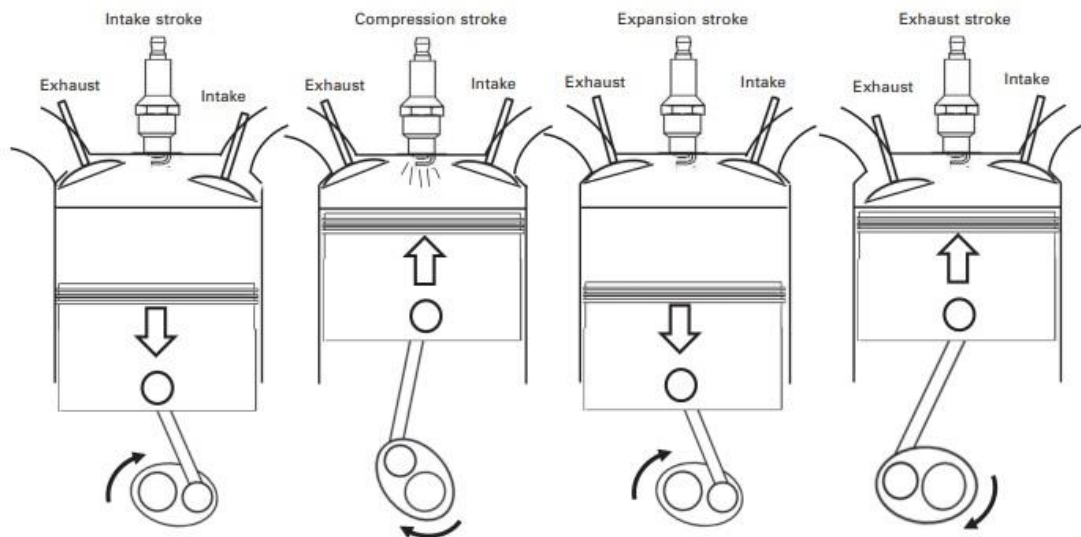


Figure 2.1: Example of a Spark Ignition internal combustion engine with four stroke cycle [11]



As it can be seen on the Figure 2.1, Naber and Johnson (2014) [11] expressed that ignition occurs when the air and fuel is compressed due to piston upward motion, and this ignition makes the piston rapidly accelerate to the downward. So that, the energy comes from reciprocating piston movement transferred to rotational energy via rotational shaft, which is called as crankshaft.

Naber and Johnson (2014) [11] stated that there are two main engine technologies, which are spark ignition (SI) engines and compression ignition (CI) engines. SI engines have sparks to ignite air and fuel mixture where CI engines have not. The fuel-air mixture is drawn into combustion chamber as homogeneous in the SI engine and the mixture is ignited via spark plugs at the end of the piston upward motion, which is called top dead centre (TDC). On the other hand, fuel is injected when the air is compressed at the end of the compression stroke in CI engines. CI engines provide the required energy via autoignition of the fuel under high temperature and pressure chamber. At this point, fuel is ignited spontaneously without any sparks because air has already high enough temperature to ignite the fuel. Then, flame starts to propagate across the combustion chamber.

Tindal and Uyehara (1988) [12] mentioned that interval time between start of injection of the fuel and first portion of the ignition takes generally 1 ms. During this time, fuel enters to the cylinder and breaks up into smaller droplets, and some portion vaporizes before ignition occurs. Sprayed fuel must with air so that a self-ignition occurs. This mixing of the air and fuel, which depends to characteristics of the fuel spray such as SPL and SCA, is critically significant for the combustion process and obviously emissions related with combustion for diesel engines.

In general, the terms of brake power (BP), brake thermal efficiency (BTE), and brake specific fuel consumption (BSFC) are utilized to compare performances of different engines. In the following sections, the performance different type of fuels will be compared with respect to these terms. Therefore, basic explanations of these terms are expressed below for the next sections.

Nirmala et al. (2020) [13] defined brake power (BP) as the total power generated by the engine at output shaft. Also, they mentioned that it can be expressed as the total useful

energy generated per second via an engine. According to J.B. Heywood (1988) [14], formulation of BP is shown as equation 2.1.

$$Brake\ Power\ [kW] = 2 \times \pi \times N \left[ \frac{rev}{s} \right] \times T[N.m] \times 10^{-3} \quad [Eqn\ 2.1]$$

where,  $N$  is equal to crankshaft rotational speed (rev/s) and  $T$  is equal to Torque (N.m).

Moreover, Nirmala et al. (2020) [13] expressed brake thermal efficiency (BTE) as the ratio of power output generated by the engine to chemical energy that supplied from the fuel. According to J.B. Heywood (1988) [14], equation 2.2 indicates the formulation of brake thermal efficiency.

$$n_{brakethermal} = \frac{(Brake\ Power)[kW]}{(\dot{m}_{fuel}) [kg/s] \times LCV[kj/kg]} \quad [Eqn\ 2.2]$$

where,  $(\dot{m}_{fuel})$  is equal to mass of the fuel supplied as kg/s, and  $LCV$  is equal to Lower Calorific Value of the fuel as kj/kg.

Brake specific fuel consumption (BSFC) takes a significant role when comparing the efficiency and performance of an engine. Nirmala et al. (2020) [13] defined it as the ratio of the total fuel consumption to BP. According to J.B. Heywood (1988) [14], the equation 2.3 indicates the formulation of BSFC.

$$BSFC = \frac{(\dot{m}_{fuel}) [g/h]}{Brake\ Power\ [kW]} \quad [Eqn\ 2.3]$$

where,  $(\dot{m}_{fuel})$  is equal to mass of the fuel supplied, as g/h.

### 2.1.1. Combustion Processes in Diesel Engine

The combustion process in diesel engine is typically falls into several stages, which is shown in the Figure 2.2. As it can be seen from the figure, the horizontal axis represents crank angle where vertical axis represents heat release rate (HRR). Start of the injection is marked as point **a**. An important point is that the heat release is not observed

shortly after the injection start at point **b**. According to J.B. Heywood (1988) [14], this time interval is called as ignition delay period and fuel droplets are begun vaporized and then started to mix with air during this time. The ignition starts with beginning of the pre-mixed phase when delay period is over. Meanwhile, flame begins the propagate towards the combustion chamber, and heat release rate is rapidly increased.

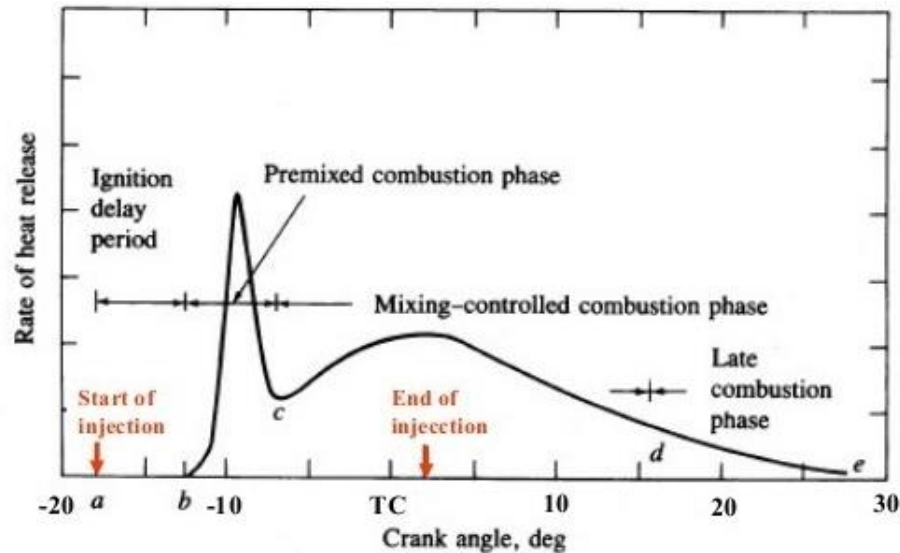


Figure 2.2: Heat release rate of the CI engine with respect to combustion process [15]

Heat release rate is controlled in the mixing-controlled combustion phase, at the beginning of this phase fuel has been still injected to the chamber. This injected fuel causes increase in the heat release rate since the fuel has been still injected. After a while later, heat release tends to decrease due to the end of injection. No other peak is observed during this phase.

J.B. Heywood (1988) [14] stated that combustion does not stop even fuel injection is completed due to several reasons. One of them is that some of the fuel may not burned completely, or some portion of the fuel may exist as soot in the chamber and its energy can still be released during this phase. The completed combustion is provided by late combustion phase.

## **2.1.2. Engine Emissions in Diesel Engine**

According to J.B. Heywood (1988) [14], the emissions of the diesel engines contain large spectrum of organic and inorganic compounds. Typically, diesel engine pollutants are hydrocarbons (HC), carbon monoxide (CO), nitrogen oxides (NO<sub>x</sub>), and particulate matters (PM). The formations of these emissions are powerfully dependent on the fuel distribution. In this section, the situations in which emissions occur and in which cases they increase, or decrease are explained. In the following sections, these pollutants of biodiesel and emulsified biodiesel will be examined detailly.

### **2.1.2.1. Nitrogen oxides (NO<sub>x</sub>)**

J.B. Heywood (1988) [14] represented that nitrogen dioxide (NO<sub>2</sub>) and nitric oxide (NO) are generally grouped together while NO is determinant. The main source of NO is the oxidation of atmospheric nitrogen. J.B. Heywood (1988) [14] reported that critical time for the NO<sub>x</sub> is when the burned gas temperatures are at maximum. Also, Rounce et al. (2012) [16] investigated the emissions from biodiesel combustions and increased NO<sub>x</sub> was associated with increased cylinder pressures, injection advance and the amount of injected fuel. Besides, Sayin et al. (2009) [17] studied effect of injection timing on the exhaust emissions with using diesel methanol blends. It was observed that retarding the injection timing results in lower peak temperatures due to reduced peak cylinder pressures, which in turn results in some reduction of NO<sub>x</sub> formation. Moreover, Mohamed Shameer et al. (2017) [18] summarized the various studies which investigate the effect of injection timing on engine emissions and the study stated that most of the studies found out that advancing the injection timing leads to increment in NO<sub>x</sub> emissions due to increased cylinder temperature.

### **2.1.2.2. Hydrocarbon (HC)**

J.B. Heywood (1988) [14] expressed the hydrocarbon emissions (HC) as result of incomplete combustion of hydrocarbon fuels. The reason was attributed to the nonuniform distribution of the air-fuel mixture inside the chamber. It was reported that, some area in the chamber can be presence as lean or rich for proper combustion. Nirmala et al. (2020) [13] examined performance and emission characteristics of different biodiesels. It was pointed out that the availability of O<sub>2</sub> in the fuel takes important role on the unburned hydrocarbons. They observed lower HC emissions with biodiesel fuels which contains higher oxygen than diesel. In addition, Raheman and Kumari (2014) [19] investigated combustion characteristics and emissions of emulsified jatropha biodiesel blend. It was found out that increase in HC was observed when the engine load is increased. Moreover, Mohamed Shameer et al. (2017) [18] showed that most of the researchers usually found out that advancement in injection timing leads to decrease in HC emissions while retarding in injection timing results in opposite. Also, Panneerselvam et al. (2015) [20] summarized the studies that examines the effect of injection timing on emissions and it is understood that density and viscosity of the fuel have a strong effect on the HC emissions.

### **2.1.2.3. Particulate matter (PM)**

J.B. Heywood (1988) [14] clarified that the reason of occurrence particulate matters in the exhaust is generally caused by unburned hydrocarbons. Also, Sayin et al. (2009) [17] reported that advanced injection timing leads to reduce in PM emissions because earlier injection timing provides higher cylinder temperatures which results in decrease in PM. Besides, they emphasized that between the particles, soot is the most distinguishable one such that the results are often converted to soot by opacimeters during the PM measurements. It was stated that the presence of soot increase in which occurrence of lack of oxygen in the chamber and the formation of soot is related with the engine load. More fuel is injected as the engine load increases which results increment in PM.

#### **2.1.2.4. Carbon monoxide (CO)**

Raheman and Kumari (2014) [19] explained that carbon monoxide (CO) is resulted from incomplete combustion and the reason of unburned fuel was associated with the lack of oxygen, poor atomization, or nonhomogeneous fuel distribution inside the chamber, which results in occurrence of CO. Also, Canakci et al. (2013) [21] investigated effect of alcohol-gasoline blends on the exhaust emissions of an SI engine and both Raheman and Kumari (2014) [19] and Canakci et al. (2013) [21] pointed out that the amount of CO emission existing in the exhaust represents lost chemical energy. Besides, Raman et al. (2019) [22] studied performance, combustion and emissions of rapeseed oil biodiesel. Raman et al. (2019) [22] observed lower CO emissions at higher engine loads compared to lower engine loads. Moreover, Panneerselvam et al. (2015) [20] reported that, most studies found less CO when the injection timing is advanced.

### **2.2. Injection System and Its Effect on Emissions**

According to Gupta et al. (2011) [23], injection systems take big part in reducing engine emissions and improving fuel economy. Carsten Baumgarten (2013) [24] defined the task of the injection system as achieving high degree of atomization in order to provide adequate evaporation in short time and achieving appropriate spray penetration in order to use full air. Besides, it was stated that fuel injection system must be able to calculate required amount of fuel according to engine speed and load, and it must be able to inject that fuel at proper time. Also, Carsten Baumgarten (2013) [24] reported that there are two main groups of high pressure injection systems which are common rail system and unit injector system. The difference was basically explained that, injection pressure is not dependent on the engine speed and generation of the pressure and the injection are not coupled in the common rail systems. On the other hand, in the unit injector systems, pressure generation and the injection event occur synchronously, and unit injector systems are driven by a camshaft which is mechanically coupled with the engine. This

difference provides higher flexibility of injection and mixture formation to the common rails when compared to unit injector systems.

Gupta et al. (2011) [23] expressed that common-rail injection system consists of fuel tank, fuel pump, injector, common rail and electronic unit. The illustration given in Figure 2.3 is an example of common rail injection system that includes its subsystems.

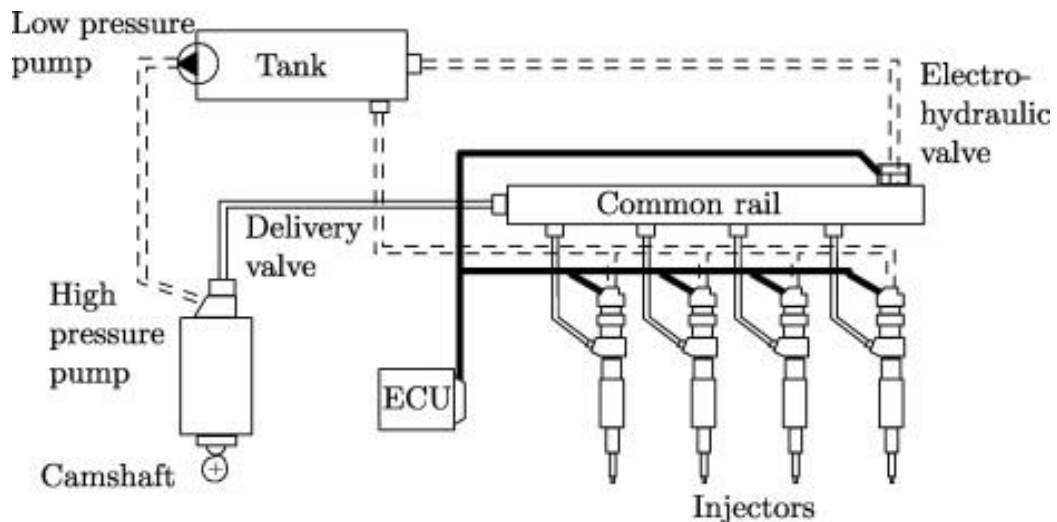


Figure 2.3: Sketch of common-rail injection system [23]

In the common rail systems, Carsten Baumgarten (2013) [24] clarified that, high pressure fuel pump provides pressurized fuel continuously to the common rail and this pressurized fuel is stored in the rail. Pressure sensor that is mounted on the common rail regulates the desired rail pressure through an additional valve which controls the mass flow of excess fuel back to the fuel tank. Therefore, rail pressure does not depend on the engine speeds. As it can be seen from figure 2.3, short pipes provide the connection between the rail and injectors. Also, it was reported that, injection pressure can be kept at desired level by the common rail since the injection duration and injection timing which those are independent of the pressure generation are controlled by solenoid valves.

As mentioned in the previous sectioned, Sayin et al. (2009) [17], Mohamed Shameer et al. (2017) [18] and Panneerselvam et al. (2015) [20] investigated the effect of

injection timing on diesel engines fuelled with different fuels. Mohamed Shameer et al. (2017) [18] reviewed various articles that investigated the effect of injection timing and injection pressure on emissions characteristics of diesel engines fuelled with different biodiesels. Mohamed Shameer et al. (2017) [18] reported that most studies found out that, at advanced injection timings, longer ignition delay leads to raise in amount of burned fuel and low gas temperatures in premixed phase which results in increment in the NO<sub>x</sub> emission. Besides, study indicated that most of the authors reported that advancement injection timing resulted in decrease in CO, HC and PM. Also, it was pointed out that most of the authors concluded that increasing injection pressure of biodiesel resulted in decrease in CO, HC, PM and NO<sub>x</sub>.

### 2.2.1. Fuel Injectors

According to study [25], fuel injectors are utilized for atomizing the fuel into very fine droplets to result better mixing thus to acquire better combustion. Fuel injectors consist of main parts such as spring, pump plunger, solenoid valve and nozzle as it is shown in the Figure 2.4.

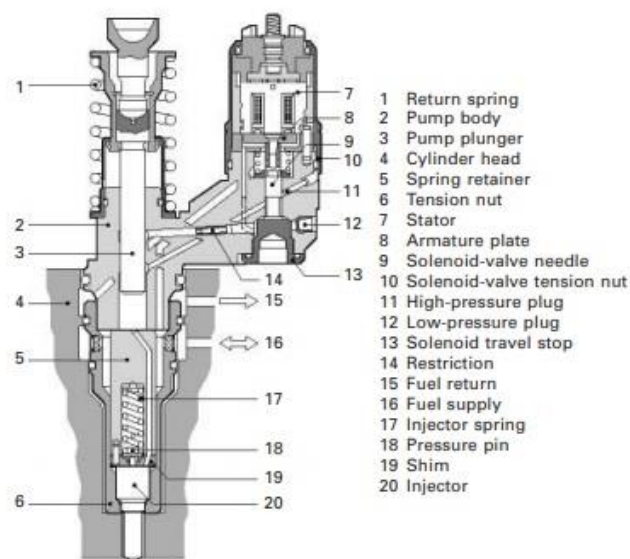


Figure 2.4: Cross-section of a fuel injector [26]



Horrocks et al. (2009) [26] stated there are two types of injectors, which are piezo and solenoid injectors, respectively. Both has advantages and disadvantages according to their applications. The comparison of both injectors is expressed in the Table 2.1. According to Horrocks et al. (2009) [26], the piezo actuators provide faster response than conventional solenoids approximately four times which gives positive effect on the smaller pilot injections. These injections take essential role on the engine emissions when the requirements of emissions standard are taken consider.

Table 2.1: Piezo injectors vs solenoid injectors [26]

<b>Injector Actuator</b>	<b>Volume Generation</b>	<b>Density of Engine Power</b>	<b>Engine Emissions Requirement</b>	<b>Cost</b>
Solenoid	Very High	Low /Average	Low / Average	Low
Piezo	Low / Medium	High	High	High

Carsten Baumgarten (2013) [24] expressed that there are three phases during the injection process. In the first phase, the pressurized fuel is supplied from the fuel pump it enters the injector via passing through the common rail where pressure fluctuations settle down due to larger cross section. Here, build up pressure of the fuel applies enough force on needle which pushes against the spring to lift the nozzle valve. The injection of the fuel starts via a small orifice under high pressure when the valve is opened. During this phase, while the needle is opening, small cross-sectional area cause increase in fuel velocity. Increased speeds of the fuel results in drastically low static pressures which creates cavitation. At this point, flow of fuel through nozzle hole is turbulent flow due to high speeds and cavitation. Carsten Baumgarten (2013) [24] explained the reason why initial spray angle near the nozzle is generally large is based on the low axial velocity and radial velocity fluctuations. On the other hand, narrower initial spray angles can be obtained when the needle is opened faster. Consequently, needle speed plays an essential role establishing the spray angle at the beginning of the injection. At the end of the injection, the spring pushes the valve back on its seat. During this phase, velocity is decreasing to zero that results in deterioration of the spray.

### 2.2.2. Nozzle

Carsten Baumgarten (2013) [24] reported that most significant part of the injection system is the nozzle and the main functions that nozzle should carry out are atomization, distribution of the fuel, prevent fuel impact on the piston wall, and mixing air and fuel.

Research [25] specified that atomization of the fuel is very important for a proper air and fuel mixture in order to obtain efficient combustion which directly effects the performance and emissions of an engine. Also, fuel should be distributed as uniformly as possible inside of the combustion chamber so that more surface area is provided, resulting in better combustion as it allows larger number of molecules to contact each other. Distribution of the fuel also depends on the density of the air and properties of the fuel. Besides, fuel should not strike to cylinder and piston because fuel may be decomposed which results in increasing carbon deposits.

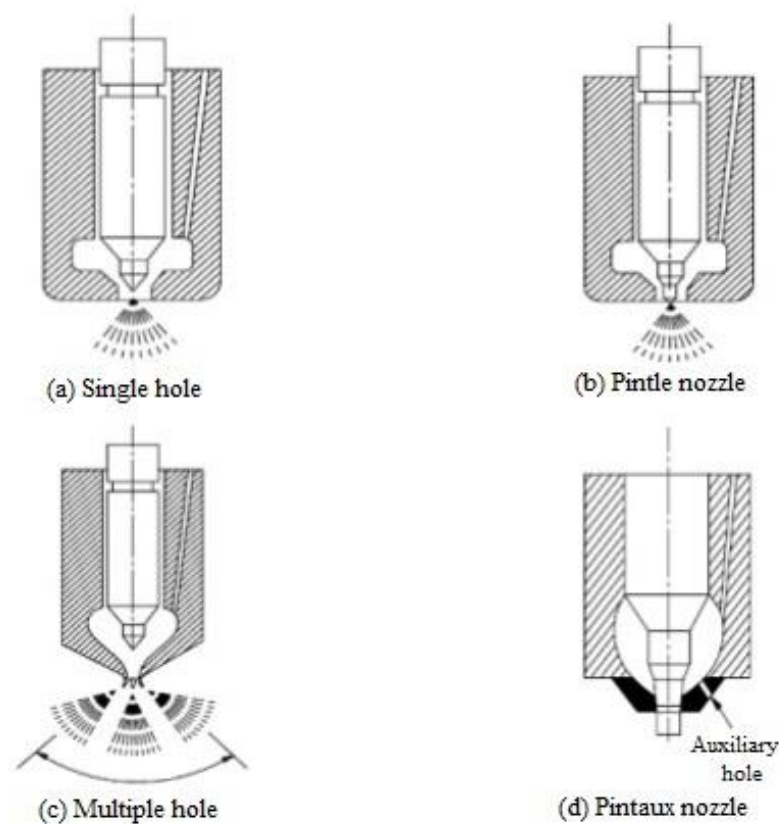


Figure 2.5: Types of nozzles: Single hole, pintle hole, multiple hole and pintaux [83]

According to research [25], there are four common nozzle types which are single hole, pintle nozzle, multi-hole nozzle, and pintaux nozzle as shown in the Figure 2.5. Study [25] expressed that there is a single hole at the centre of the nozzle body in the single hole nozzles, which is opened and closed through the nozzle valve. The size of the hole is typically about 0.2 mm, and the injection pressure is about 8~10 MPa where the spray cone angle is around 15°. However, the problem with the single hole nozzle is that they may tend to drip the fuel, and it is hard to obtain good mixing if the velocity is not high enough due to a narrow spray cone angle.

According to research [25], pintle nozzles also provide sprays under running low injection pressures like single hole nozzles which is around 8~10 MPa but the advantage of this nozzle compared to single hole is they do not tend to drip fuels. Another advantage is that this type of nozzles prevents generating undesired carbon deposition on the nozzle hole. Also, the spray cone angle is higher than single hole nozzle.

Besides, study [25] indicated that multi-hole nozzles consist of several holes as understand from its name. The size of the holes is around 35 ~ 200 $\mu$ m, and the number of holes vary from 4 to 18. Compared to pintle and single hole nozzle, this type of nozzles can run under high injection pressures around 18MPa.

Moreover, study [25] stated that pintaux nozzle is a kind of pintle nozzle. The difference is that it has an extra hole in the nozzle body which is called as auxiliary hole as it can be seen from the Figure 5. A small amount of fuel is injected via this extra hole shortly before the main injection. Also, high amounts of fuel can be injected through this additional hole at low speeds. The biggest advantage of this nozzle is better cold starting performance.

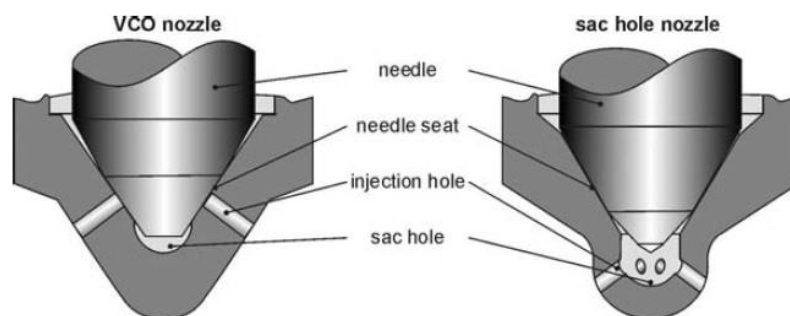


Figure 2.6: VCO nozzle and sac hole nozzle [24]

In addition to these, Carsten Baumgarten (2013) [24] clarified that two main nozzle types in direct injection diesel engines are the sac hole nozzle and the valve covered orifice nozzle (VCO) which are shown in the Figure 2.6.

Besides, Carsten Baumgarten (2013) [24] expressed that in the sac hole nozzle, there is more volume below the needle seat compared to covered orifice nozzle seat as shown in the Figure 2.6. This volume is beneficial for producing symmetric overall spray, but it has negative effect on the HC emissions because some of the fuel volume between the needle seat and the combustion chamber may leak through the cylinder after injection is finished. So that, this volume should be kept as small as possible. In the opposite case, soot formation and HC may increase due to late evaporation of the fuel. Furthermore, Carsten Baumgarten (2013) [24] pointed out that there are different nozzle hole geometries nowadays depending on the application. They are called as cylindrical hole, k-nozzle, and ks-nozzle as shown in the Figure 2.7. While cylindrical hole produces the strongest cavitation, ks-nozzles are designed to suppress the cavitation. The spray breaks up with a large spray divergence near the nozzle is observed in the cylindrical hole. On the other hand, large spray penetration lengths are produced in the ks-nozzles.

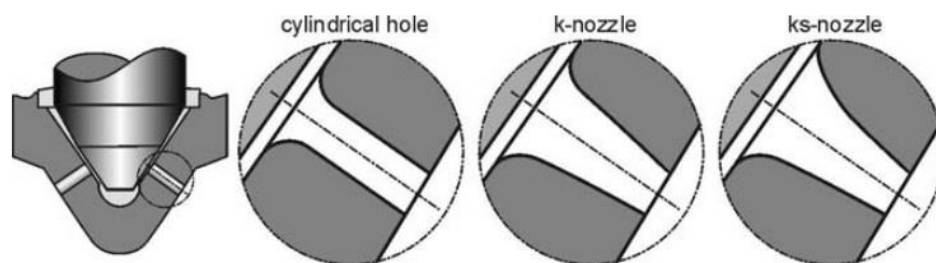


Figure 2.7: Demonstration of different nozzle hole geometries [24]

### 2.3. Fundamentals of Liquid Sprays

According to Helge von Helldorff and Micklow (2019) [27], spray modelling and droplet breakup which consist of spray penetration length and spray cone angle become more significant when simulating the internal combustion engines. The particle breakup

process is typically divided as Primary Breakup and Secondary Breakup as it can be seen on Figure 2.8.

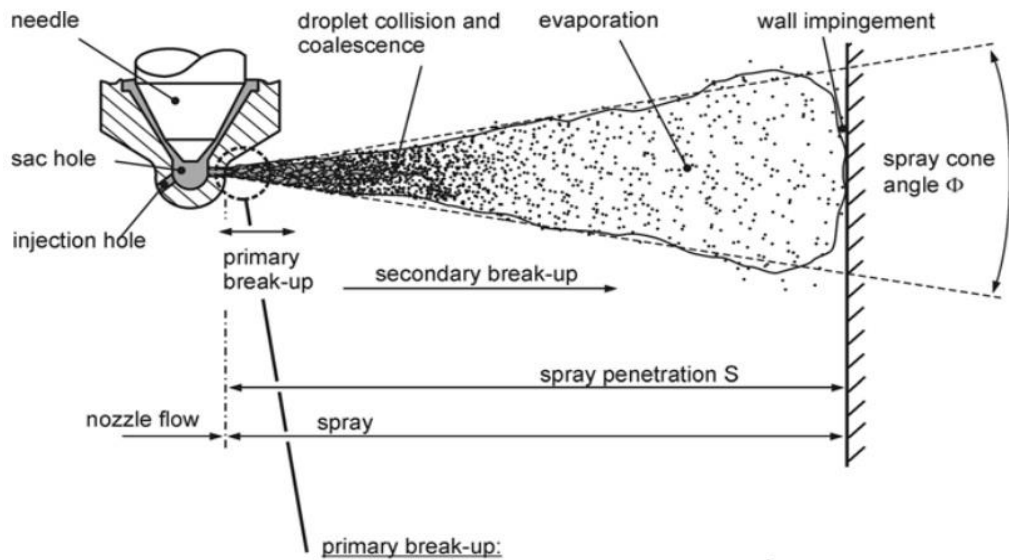


Figure 2.8: The illustration of full cone spray [24]

Helge von Helldorff and Micklow (2019) [27] expressed that the primary breakup regime starts from at the end of the nozzle exit. The secondary break-up regime begins where the primary fuel particles are disintegrated into fine particles. In the primary break-up process, the cylindrical liquid comes from nozzle exit is converted into distinct particles due to the surface tension and forces related to injector nozzle geometry and aerodynamic effects. In the secondary breakup regime, the disintegrated particles further break up into much smaller particles as shown in the Figure 2.9.

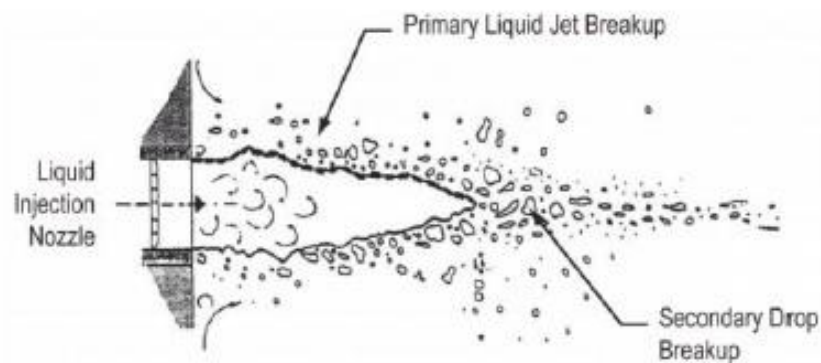


Figure 2.9: Demonstration of the primary and secondary breakup [28]

### 2.3.1. Primary Breakup Regimes

Carsten Baumgarten (2013) [24] stated that there are several primary breakup mechanisms of a liquid jet, which depends on the relative velocity and properties of the liquid, and properties of the surrounding gas and these mechanisms can be divided as Rayleigh regime, wind-induced regime and atomization regimes as seen in Figure 2.10.

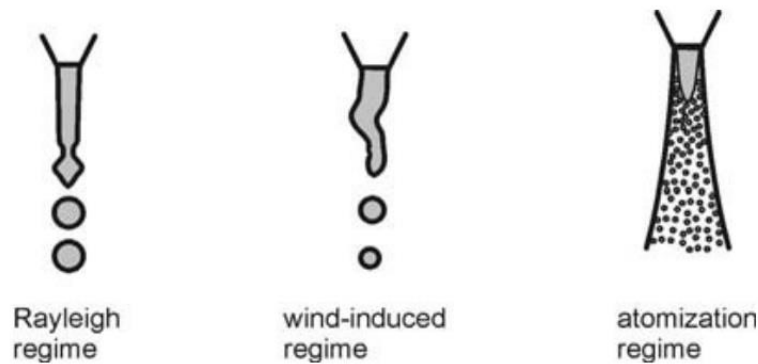


Figure 2.10: The schematic of the primary break-up regimes [24]

Carsten Baumgarten (2013) [24] expressed that these regimes can be distinguished with the utilization of the Weber and Reynolds numbers where they are defined as;

$$We_l = \frac{u^2 D \rho_l}{\sigma} \quad \text{and} \quad Re = \frac{u D \rho_l}{\mu_l} \quad [\text{Eqn 2.4 and Eqn 2.5}]$$

Here,  $u$  and  $\rho$  are velocity (m/s) and density ( $\text{kg/m}^3$ ) of the liquid,  $D$  is hole diameter of nozzle (m),  $\sigma$  is surface tension (N/m) at the liquid gas interface,  $\mu_l$  is the dynamic viscosity of the liquid ( $(\text{N.s})/\text{m}^2$ ).

Carsten Baumgarten (2013) [24] showed that the velocity of the jet can be eliminated to be able to obtain a dimensionless Ohnesorge number as shown below. Spray regimes are shown on a Ohnesorge Reynolds number chart in the Figure 2.11 below.

$$Z = \frac{\sqrt{We_l}}{Re} = \frac{u_l}{\sqrt{\sigma \rho_l D}} \quad [\text{Eqn 2.6}]$$

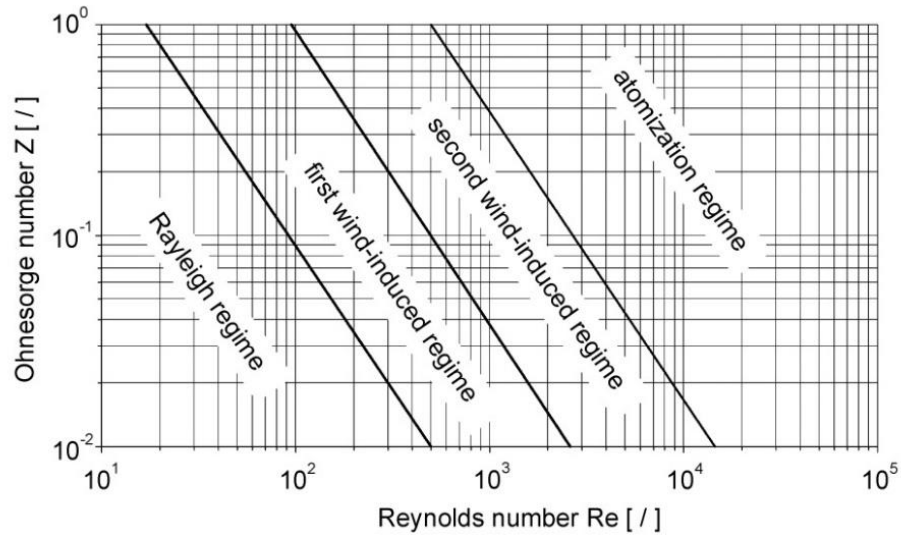


Figure 2.11: Jet break-up regimes according to Ohnesorge number [24]

Carsten Baumgarten (2013) [24] and Helge von Helldorff and Micklow (2019) [27] explained these regimes, respectively. In the Rayleigh breakup regime, the formation of jet is not observed at very low velocities. An increment in the velocity results in stretched unbroken jet length. After breaking up process, the diameter of droplets become larger than nozzle diameter due to restored surface tension of particles. Low spray angle and long primary breakup lengths are occurred in this regime due to the large liquid column lengths.

The breakup length is decreasing when the velocity of the jet is increased further. The surface tension force becomes stronger in the first wind induced regime due to aerodynamic forces. The diameter of the droplets is about the same size as the nozzle exit.

They clarified that when the flow inside the nozzle turns into turbulent then jet break up occurs in the second wind induced regime. Diameter of droplets is generally smaller than the nozzle diameter, and breakup length is decreasing when the Reynold number is increasing.

In the atomization regime, spray is developed as conical and disintegration begins subsequently jet leaves the nozzle. Droplets, which are smaller than the nozzle diameter

in this regime, are disintegrated from the surface of the liquid due to the air friction effects which results in reducing the size of the liquid cone as shown in the Figure 2.9.

Carsten Baumgarten (2013) [24] emphasized that cavitation and turbulence are two significant breakup mechanisms which both are generated inside of the nozzle before the liquid jet leaves nozzle as shown in the Figure 2.12.

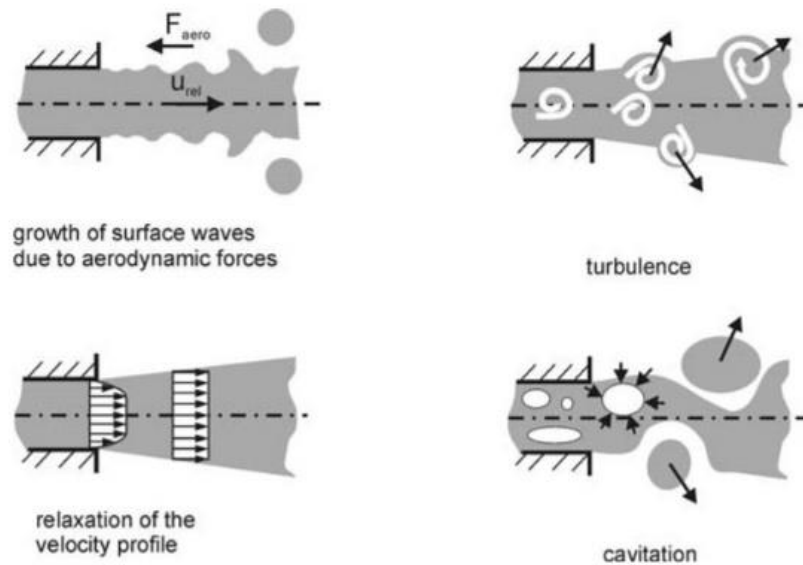


Figure 2.12: Cavitation and turbulence inside of the nozzle [24]

According to Carsten Baumgarten (2013) [24], when the turbulent liquid jet leaves the nozzle, some of the very small waves on the outer layer of the liquid surface become more powerful due to aerodynamic shear forces, and these small waves can overcome the surface tension if they are amplified high enough. Thus, the outer jet liquid breaks up as form of small droplets. Therefore, the turbulence breakup is one of the significant breakup mechanisms when the high pressure sprays are considered.

Bekdemir (2008) [29] explained that cavitation is developed due to decrease of static pressure below its vapor pressure. The formation of the vapour bubbles can be seen where the pressure is lower than vapour pressure, and it has positive effect to the primary break up because they implode at the end of the nozzle due to high ambient pressure inside of the chamber thus creating a high fluctuating velocities and pressures. Also, nozzle geometry such as inlet edges takes an important role on the formation of these bubbles in the liquid flow.



### 2.3.2. Secondary Breakup Regimes

Carsten Baumgarten (2013) [24] reported that in the secondary breakup regimes, the existing fuel droplets occurred in the primary breakup regime separates into even smaller droplets particles due to the aerodynamic forces which occurs due to the relative velocity between droplet and surrounding gas. These forces cause instable growing of waves on the liquid surface, and these waves wear the surface which is leading into further breakups. The separated droplets are again exposed to aerodynamic forces to disintegrate into more smaller particles. On the other hand, surface tension force opposes to these instabilities in order to keep the droplet as spherical. Surface tension force and relative velocity becomes larger when the droplet size becomes smaller. The relation is expressed via gas phase Weber number where  $\rho_g$  is the gas density,  $u_{rel}$  is the relative velocity between gas and droplet,  $d$  is the droplet diameter before breakup,  $\sigma$  is the surface tension between gas and liquid.

$$We_g = (\rho_g \cdot u_{rel}^2 \cdot d) / \sigma \quad [\text{Eqn 2.7}]$$

Carsten Baumgarten (2013) [24] indicated that there are several secondary breakup regimes according to Weber numbers, which are vibrational breakup, bag breakup, streamer breakup, stripping breakup, and catastrophic breakup. The all breakups are shown in the Figure 2.13, respectively.

According to Carsten Baumgarten (2013) [24], the vibrational breakup happens near the Weber value of 12, and there is no breakup below this critical Weber value. In the bag break up mode, both large and small droplets are seen in the same time during the breaking up occurrence. The critical Weber value of breaking up in this regime is around 20 while it is 50 for bag-streamer regime. The droplet diameter gradually decreases because of the fine droplets are still separating from the boundary layer due to shear forces in the stripping regime. Lastly, larger and smaller droplets are seen during the breaking up in the catastrophic breakup mode.

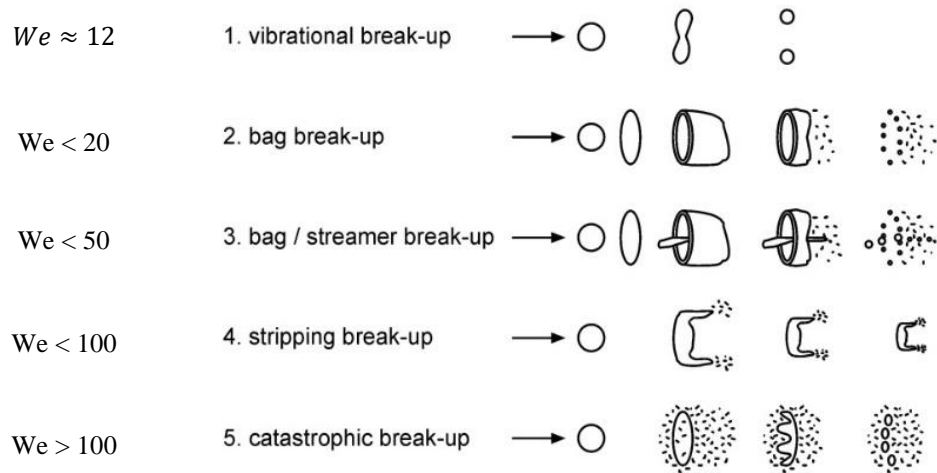


Figure 2.13: Secondary breakup regimes according to Weber number [24]

Carsten Baumgarten (2013) [24] reported that when the engine spray is taken under consideration all these modes are seen on the engine but most of the breakup is occurred near the nozzle at high Weber numbers which gets smaller as further downstream due to lower velocity and lower droplet diameter. As a result of this, less and less disintegration occurs as spray move downstream.

### 2.3.3. Spray Patterns

Yao et al. (2015) [30] stated that there are basically three spray patterns, which are full cone, hollow cone, and flat fan as shown in the Figure 2.14, respectively. Each of these patterns has their own characteristics and applications.

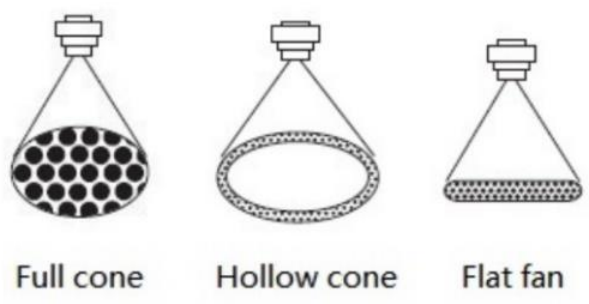


Figure 2.14: Demonstration of different spray patterns [30]

Yao et al. (2015) [30] expressed that pattern appearance of the flat fan spray is generated by the elliptical orifice. The sizes of the droplets are larger than the cone sprays. However, large, and equally distributed droplets with high flow rates are occurred through the full cone angle, and benefit of the full cone angle is that able to maintain its spray pattern under high pressures.

According to Carsten Baumgarten (2013) [24], hollow cone patterns are generally utilized for conventional gasoline engines. The more liquid is concentrated at the outer edge of the pattern on the other hand less in the centre as shown in the figure. The diameter of the droplets is small in this pattern which has positive effect on the atomization when the fuel and air mixing is taken consider.

#### **2.3.4. Spray Characteristics**

Soid and Zainal (2011) [31] expressed two types of spray behaviour, which are macroscopic and microscopic spray parameters, respectively. Macroscopic parameters consist of spray cone angle and spray penetration while microscopic parameters consist of velocity, droplet size and scaler field. The main focus of this thesis is that investigate the macroscopic spray behaviours of emulsified blend biodiesel-diesels such as the spray tip penetration length and spray cone angle as shown in the Figure 2.15. Soid and Zainal (2011) [31] emphasized that in order to acquire more efficient combustion, higher spray cone angles and longer penetration lengths are preferred without spray-wall contact when the air and fuel mixture is considered.

Suh et al. (2007) [32] defined spray cone as the angle between two straight lines which is drawn from the nozzle tip. Meanwhile, spray tip penetration was expressed as the distance between beginning of the nozzle tip and maximum distance that spray can further along its axis as shown in the Figure 2.15. Amir Khalid et al. (2017) [33] showed that density and viscosity have a remarkable effect on the spray development.

There are many studies in literature utilizing test rigs with optical diagnostic tools with intent to understand better the spray behaviours. In the studies various fuels such as diesel, biodiesel, blend biodiesel-diesel, emulsified diesel and emulsified biodiesels were

examined in terms of their spray behaviour. Table 2.2 summarized some parts of these studies which related with macroscopic spray parameters.

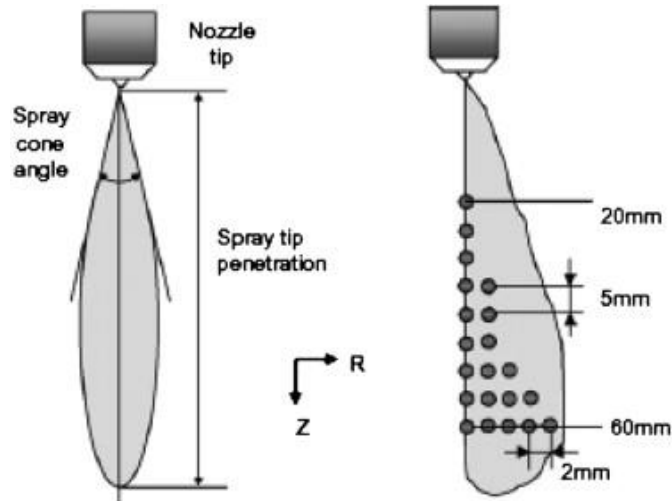


Figure 2.15: Demonstration of macroscopic spray parameters [32]

If spray penetration length is examined, according to studies of Amir Khalid et al. (2017) [33], Yu et al. (2017) [34], Nguyen et al. (2020) [35], Lee et al. (2017) [36], Gao et al. (2009) [37] and Mohan et al. (2014) [38], it can be said that biodiesels and blended biodiesels (containing diesel) lead to longer penetration lengths compared to diesels. According to authors, the reason is generally correlated to higher viscosity and density of the biodiesel. For instance, Amir Khalid et al. (2017) [33] studied with crude palm oil (CPO) biodiesel blends and their emulsions with water range up to 5% and 15%. The highest penetration length while comparing the biodiesel and diesel was obtained as 138.9 mm with CPO15 due to its higher viscosity. Yu et al. (2017) [34] examined the internal flow and spray characteristics for diesel and biodiesel in the study and it shows that the average velocity at the end of the nozzle for diesel is higher than that of biodiesel because of lower viscosity of diesel which results in occurrence of higher mass flow rates. However, this phenomenon leads to spray atomization rapidly hence prevent the development of spray tip penetration. Besides, Nguyen et al. (2020) [35] and Gao et al. (2009) [37] found out that spray penetration length increases as biodiesel concentration is increased in the blended fuel since the higher viscosity prohibits the spray to disintegrate which results in larger droplets. As a result, larger size of spray droplets with

higher momentum because of high density results in longer penetrations. For instance, Nguyen et al. (2020) [35] found out increasing blend ratio of biodiesel resulted in increment in penetration length from 1.2% to 9.9% at 50 bar injection pressure. In addition to these, Lee et al. (2017) [36] studied with blends of Karanja biodiesels, and research showed that increasing biodiesel concentration leads to longer penetrations and the reason is associated with higher viscosity of the biodiesels. Also, Mohan et al. (2014) [38] investigated spray characteristics of waste cooking oil biodiesel (B100) and its blend with diesel (B20). The highest spray penetration length was acquired with the B100 and the reason was correlated with the higher viscosity and surface tension of the biodiesel. Moreover, Nguyen et al. (2020) [35], Agarwal et al. (2014) [39] and Park et al. (2016) [40] showed that increment in injection pressure leads longer penetration since raise in the injection pressure caused in increase initial velocity and momentum at nozzle exit which in turns results in further tip penetration lengths. For instances, Agarwal et al. (2014) [39] found that increasing injection pressure from 300 bar to 1000 bar resulted 13.23 mm increase in the penetration length. Meanwhile, Agarwal et al. (2014) [39] indicated that increment in ambient pressure causes shorter penetration. Agarwal et al. (2014) [39] explained that raise in ambient pressure results in increased flow resistance between the spray and air inside the chamber, which results in shorter penetration lengths.

Furthermore, Amir Khalid et al. (2017) [33], Park et al. (2016) [40], Y. S. Lin and Lin (2011) [41], A. Khalid et al. (2014) [42], Huo et al. (2014) [43] and Song and Lee (2020) [44] investigated the spray characteristics of emulsified fuels. Park et al. (2016) [40] and Y. S. Lin and Lin (2011) [41] indicated that emulsified fuels with water results in longer penetration lengths compared to diesel. Also, Amir Khalid et al. (2017) [33] and A. Khalid et al. (2014) [42] pointed out that raise in the water concentration in the mixture results in longer spray penetration lengths. Amir Khalid et al. (2017) [33] correlated the reason with increased density and viscosity of the mixture due to the water content inside the mixture. Park et al. (2016) [40] compared the emulsified diesel with 20% of water (DE20), 10% of water (DE10) and neat diesel. The study showed that DE20 had longer penetrations than DE10 and diesel with 800 bar injection pressure. Y. S. Lin and Lin (2011) [41] studied with emulsified castor biodiesel with 15% of water and increment in penetration length was observed with emulsified biodiesel. The reason was correlated to increment in the density. Also, A. Khalid et al. (2014) [42] examined spray characteristics of the emulsified diesel and diesel, and study emphasized that higher water

content due to higher viscosity leads to longer penetration lengths. Besides, Huo et al. (2014) [43] claimed that due to lower volatility and higher viscosity of the water resulted in longer penetration lengths under low ambient temperatures.

In addition to these, the studies of Yu et al. (2017) [34], Nguyen et al. (2020) [35], Gao et al. (2009) [37], Mohan et al. (2014) [38] and Wang et al. (2010) [46] examined the spray cone angles of diesel and biodiesel. Besides, Amir Khalid et al. (2017) [33], Y. S. Lin and Lin (2011) [41], A. Khalid et al. (2014) [42] and Emberson et al. (2016) [47] investigated the spray cone angle of emulsified fuels. Typically, cone angles of diesel were found out generally larger than that of biodiesel, and authors generally associated the reason with lower viscosity of the diesel which leads to disintegrate spray easier than biodiesel which promotes splitting to larger area, in turn induce increment in spray cone angle. In other words, it was claimed that biodiesel inhibits the disintegration of the spray due to its higher viscosity. Also, Yu et al. (2017) [34] found out that radial velocity of diesel at nozzle exit is higher than biodiesel at the same injection pressure and study concluded that diesel had larger cone angles than biodiesel at the same time due to lower viscosity and surface tension of the diesel. Also, Nguyen et al. (2020) [35] and Gao et al. (2009) [37] pointed out that increasing biodiesel concentration in the biodiesel blends causes narrower spray angles. For example, Nguyen et al. (2020) [35] found out that increasing biodiesel concentration resulted decrease in spray cone angles from 9.2% to 1.2% at 50 bar injection pressure. Also, Mohan et al. (2014) [38] compared the cone angle of B100, B20 and diesel. It was found out that B100 had narrower cone angles than B20 and diesel, and the reason was correlated with the higher viscosity and momentum of B100. Wang et al. (2010) [46] compared spray characteristics of the palm oil biodiesel, cooked oil biodiesel and diesel. They found out that, biodiesels had narrower spray angles than diesels while the palm oil had smallest spray angle between the fuels. Amir Khalid et al. (2017) [33] found out that, increasing water content in the mixture results in narrower spray cone angles, and they correlated the reason with the increased density of the mixture. Y. S. Lin and Lin (2011) [41] found out that spray angle of emulsified fuel had smaller than diesel until the middle of the injection however cone angle of emulsified fuel tend to increase sharply after middle of the injection, and it became larger than diesel. The reason was associated with the micro-explosion phenomenon due to water content inside of the mixture. A. Khalid et al. (2014) [42] compared to diesel and emulsified diesels (W5, W10, W15). They found out that increasing water concentration leads to smaller cone angles, and the smallest cone angle was obtained with W15. The reason was

correlated with the viscosity of the mixture. Emberson et al. (2016) [47] examined the cone angle of diesel fuel and water emulsions, (D10 and D20, containing 10% and 20% water by mass). They found out that emulsified fuel leads to reduction in the spray angle at 500 bar injection pressure.

Furthermore, Mohan et al. (2014) [38] found out that changing injection pressure has not remarkably effect on the spray cone angle while ambient pressure altering has effect on the cone angle significantly. Mohan et al. (2014) [38] correlated the reason that increase in ambient pressure causes the fuel exposing to higher resistance which inhibits its axial development in turn results in wider the spray cone angles.

According to Kadocsa (2007) [48], Sauter Mean Diameter (SMD) is the most commonly used mean quantity for diameter of sprays. Kadocsa (2007) [48] defined SMD as the diameter of a droplet which has same proportion between its volume and surface when the entire droplet population is taken consider. Carsten Baumgarten (2013) [24] stated that if SMD becomes smaller the surface per unit volume is increasing which has positive effect on the mixture formation however it is significant that droplet size distribution cannot be predicted with the SMD value. Carsten Baumgarten (2013) [24] expressed that droplet size of the distributions of two sprays with equal SMD may differ from each other. Also, it was stated that SMD decreases while the injection pressure increases.

Table 2.2 summarize the studies mentioned above with their conclusions and fuel types that is used during their studies.

Table 2.2: Summarization of studies related with spray characterization in CI engine [33-46]

No	Researcher	Fuel type	Conclusion	Ref. No.
1	Khalid et al.	EBB & Biodiesel Blends & Diesel	<ul style="list-style-type: none"> <li>- It was clarified that biodiesel blends have longer penetration lengths since they have higher viscosity than diesels.</li> <li>- The highest cone angle was observed by diesel because of lower viscosity.</li> <li>- Higher water content inside the emulsion leads longer spray tip length and smaller spray angle because of increment in the density of the mixture.</li> <li>- Mass flow rate of diesel was higher than biodiesel.</li> <li>- Diesel had higher average velocity at the exit of nozzle orifice than biodiesel.</li> <li>- Diesel had higher cavitation intensity compared to biodiesel at orifice inlet region at same injection pressure.</li> </ul>	[33]
2	Yu et al.	Biodiesel & Diesel	<ul style="list-style-type: none"> <li>- Diesel had greater radial velocity compared to biodiesel, which was tending to increment as injection pressure increased.</li> <li>- Biodiesel had longer spray tip penetration length compared to diesel at same injection pressure.</li> <li>- Biodiesel had smaller cone angles in contrast with diesel at same injection pressure because of high surface tension and viscosity of biodiesel.</li> </ul>	[34]
3	Nguyen et al.	Biodiesel Blends & Diesel	<ul style="list-style-type: none"> <li>- Spray penetration lengths of the biodiesel blends (B10, B20, B30) were found out higher than diesel due to higher viscosity, surface tension and density of biodiesel.</li> <li>- Spray cone angles of the biodiesel blends (B10, B20, B30) were found out narrower than diesel.</li> </ul>	[35]
4	Lee et al.	Biodiesel Blends & Diesel	<ul style="list-style-type: none"> <li>- The injection rate of the biodiesel had slightly lower than diesel at lower injection pressures. Vice versa occurred at higher injection pressures.</li> <li>- Spray development of diesel was faster than biodiesel at lower injection pressure under penetration length of 30 mm due to higher viscosity of biodiesel.</li> </ul>	[36]

Abbreviation: EBB: Emulsified Biodiesel Blends

(Cont. on next page)



**Table 2.2 (Cont.)**

<b>No</b>	<b>Researcher</b>	<b>Fuel type</b>	<b>Conclusion</b>	<b>Ref. No.</b>
5	Gao et al.	Biodiesel Blends & Diesel	<ul style="list-style-type: none"> <li>- Spray penetration length increased as biodiesel concentration was increased in the blended fuel since the higher viscosity prohibits disintegrating droplets of the spray.</li> <li>- Cone angle was narrowing as biodiesel content was increasing in the blended fuel.</li> <li>- Sauter Mean Diameter (SMD) was observed gradually raised as the concentration of biodiesel in the mixture increased.</li> </ul>	[37]
6	Mohan et al.	Biodiesel Blends & Diesel	<ul style="list-style-type: none"> <li>- Biodiesel had narrower angle in accordance with blend biodiesel and neat diesel. The angle was increasing with the ambient pressure while injection pressure did not affect significantly.</li> <li>- The longer spray penetration and higher velocity were obtained through utilizing biodiesel while there was no significant difference between biodiesel blend and diesel under high ambient pressure.</li> </ul>	[38]
7	Agarwal et al.	Biodiesel blends & Diesel	<ul style="list-style-type: none"> <li>- Spray penetration length was increasing as injection pressure was increasing.</li> <li>- On the other hand, it was observed that tip penetration was significantly reducing in accordance with increase in ambient pressure owing to increased friction between spray droplets and medium air.</li> </ul>	[39]
8	Park et al.	Emulsified Diesels & Diesel	<ul style="list-style-type: none"> <li>- In all conditions, the injection amount of emulsified diesel was lower than that of pure diesel and the injection amount decreased as the water content increased was associated with the kinematic viscosity.</li> <li>- Spray penetration length generally increased with the incrementation of injection pressure.</li> <li>- Spray penetration lengths of emulsified fuels were found out longer compared to neat diesel.</li> </ul>	[40]
9	Lin & Lin	Emulsified Biodiesel & Diesel	<ul style="list-style-type: none"> <li>- Biodiesel with 15% concentration of water led to higher penetration was associated with increased density.</li> <li>- At the beginning of the injection, cone angle of emulsified biodiesel was smaller than diesel due to water content inside emulsified fuel which results in higher viscosity. But, after 2ms of the injection, the angle of emulsified biodiesel tended to increase significantly was correlated with micro explosion.</li> </ul>	[41]

**(Cont. on next page)**

**Table 2.2 (Cont.)**

<b>No</b>	<b>Researcher</b>	<b>Fuel type</b>	<b>Conclusion</b>	<b>Ref. No.</b>
10	A. Khalid et al.	Emulsified Diesels & Diesel	- Higher concentration water inside the emulsified fuels led longer penetration length and narrower spray angles.	[42]
11	Huo et al.	Emulsified Diesels & Diesel	- Emulsified fuels resulted in longer penetration length at low chamber temperatures.	[43]
12	Song & Lee	Emulsified Diesels & Diesel	- At low Weber numbers, mean spray tip penetration increased while the concentration of water was increasing. - Increasing water concentration resulted in increment in calculated droplet particle size.	[44]
13	Huo et al.	Emulsified Diesel & Diesel	- It was concluded that at low ambient temperatures at the beginning of the injection emulsified fuel led longer penetration length.	[45]
14	Wang et al.	Biodiesels & Diesel	- At low ambient density, there were no significant difference in penetration lengths between diesel and biodiesels at the beginning of the injection. - The penetration difference between diesel and biodiesel was becoming closer as the ambient density was increased. - The cone angles of biodiesels were narrower than diesel due to the higher viscosity. - biodiesel was higher than diesel by the reason of high viscosity and surface tension.	[46]

### 2.3.5. Spray Measurement Methods

Soid and Zainal (2011) [31] emphasized that the interest on studies related about spray characterization has been increasing in recent years owing to incrementation of alternative fuels, and several optical test rigs have been utilized in order to analyse better the basic principles of spray characterization which is composed of two categories as macroscopic and microscopic parameters.

Srichai (2015) [49] indicated that several optical test rigs can be used to investigate the spray in diesel combustion. These are existed in literature as Rapid Compression Machines (RCM), Optical Research Engine (ORE), Constant Pressure Flow Rig (CPFR), Rapid Cycling Machine (RCYM), and Constant Volume Constant Chamber (CVCC) or Constant Volume Hot Cell (CVHC). The advantages and disadvantages of each test rig were examined detailly by Baert et al (2009) [50]. Besides, Munsin et al. (2013) [51] reported that CVCC has been differed compared to others due to providing a large amount of gas temperatures and pressures before the injection.

According to Soid and Zainal (2011) [31], there are several optical techniques have been used as diagnostic tools. Some of them are visualization, Laser Induced Fluorescence (LIF), Particle Image Velocimetry (PIV), and Phase Doppler Particle Anemometry (PDPA). Soid and Zainal (2011) [31] expressed that, visualization method is the most frequently used for measurement the spray cone angle and spray penetration length while the rest are utilized for microscopic parameters. As indicated in the Table 2.3. PIV and PDPA techniques are used to obtain measurement of velocity and droplet size respectively while LIF is utilized for visualizing the fuel vapor and drops of the liquid in the same time.

Bachalo (2000) [52] studied on the spray diagnostics and stated that shadowgraph systems can be used when the spray characteristics such as cone angle and breakup length are investigated according to study. In addition, Castrej (2011) [53] stated that shadowgraph imaging is predominance over other visualization techniques owing to fact that it allows various properties such as direction of movement, interface speed, and object dimensions to be recorded and measured.

Table 2.3: Comparison of optical techniques [31]

Technique	Application area	Drawbacks
Visualization	Spray penetration length & spray cone angle	Only macroscopic characteristics
PIV	Snap total area velocity	Hard to fulfil on dense sprays
LIF	Concentration of fuel	Quenching issues and hard to calibrate
PDPA	Measuring droplet size	Appropriate for only low-density sprays

Castrej (2011) [53] expressed that the utilization of shadowgraph technique is suitable for environments where the working environment is transparent and where there is a large difference in refractive index, and most of the shadowgraph systems contains two parts, the light source and recording item as shown in the Figure 2.16. Castrej (2011) [53] pointed out that the purpose of the light arrangement is to acquire a homogeneous background at the recording sensor and supply the illuminant refracted by the object or medium under examination meanwhile recording system has optical items such as CCD sensors in order to create and record the image of the object's silhouette or shadow.

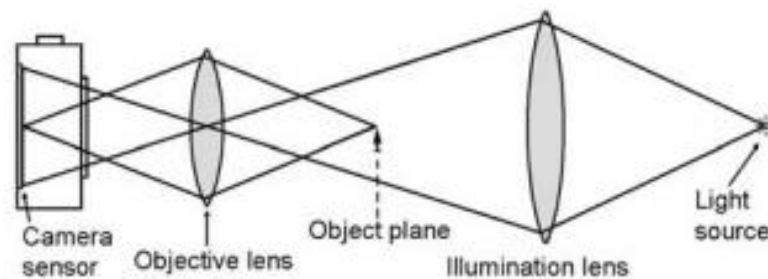


Figure 2.16 : Schematic view of a shadowgraph system [53]

In this study, CVCC and shadowgraph technique will be utilized in order to examine macroscopic spray characteristics such as spray tip penetration and spray cone angle. In addition to these, Braeuer (2015) [54] gives wide range knowledge about both schlieren and shadowgraph techniques. Besides, there are also other authors such as Zhao and Ladommatos (1998) which examines the measurement of the fuel vapor concentrations in IC engines by using different optical techniques.

## **2.4. Fuel types for CI Engine**

Diesel engines are preferred in the various of industries when its combustion efficiency and fuel economy is taken consider. As the emissions of diesel engines was discussed before, the emissions of diesel engines are HC, PM, NO<sub>x</sub>, and CO. Mohan et al. (2013) [56] emphasized that especially the amount of NO<sub>x</sub> and PM values are higher than spark ignition engines. All of these pollutants released from diesel fuels play a crucial role on human health and the environment.

Besides, increment in vehicle population, depletion of petroleum reserves and stricted regulations on emissions subsequently has been led many scientists to conduct various studies for an alternative fuel sources such as biodiesel and emulsified fuels in the recent years.

### **2.4.1. Emulsified Diesel**

According to studies of Fahd et al. (2013) [57], Armas et al. (2005) [58] and Maiboom and Tauzia (2011) [59], emulsified diesel with water has positive effect on the reducing NO<sub>x</sub> and PM emissions. For instance, Fahd et al. (2013) [57] investigated engine performance and emissions of diesel and emulsified diesel, containing 10% water by total (ED10). They observed reduction in NO<sub>x</sub> by using ED10 due to the water content inside the mixture which pretends as heat sink in the cylinder. However, they observed that emulsified fuel produced less engine efficiency and power output, also higher BSFC. Armas et al. (2005) [58] also examined emissions of emulsified diesel with water with 10%. They found that using ED10 resulted reduction in both NO<sub>x</sub> and PM. They observed increment in brake efficiency at some engine modes. Maiboom and Tauzia (2011) [59] investigated the effect of emulsified fuels with/without exhaust gas recirculation on the exhaust emissions. They found low emissions levels by combining emulsified fuels with exhaust gas recirculation which leads reduction in both NO<sub>x</sub> and PM.

## 2.4.2. Biodiesel

According to Aziz et al. (2014) [60], biodiesels are produced from the vegetable oil, waste cooking oil or animal fat and there are many advantages compared to diesel. Aziz et al. (2014) [60] stated that the advantages of the biodiesel are being renewable fuel and biodegradable. Besides, the harmful emissions released from diesels can be reduced by utilizing the biodiesel. Also, Aziz et al. (2014) [60] pointed out than it is applicable for the diesel engines without making any modification on the engine.

Figure 2.17 shows the feedstocks of the biodiesel used in the scientific articles. Pinto et al. (2005) [61] expressed that when the biodiesel is produced the availability of the feedstocks availability in each region is taken consider. It was stated that any fatty acid source can be used however usually soybean is preferred in the most scientific articles as shown in the Figure 2.17.

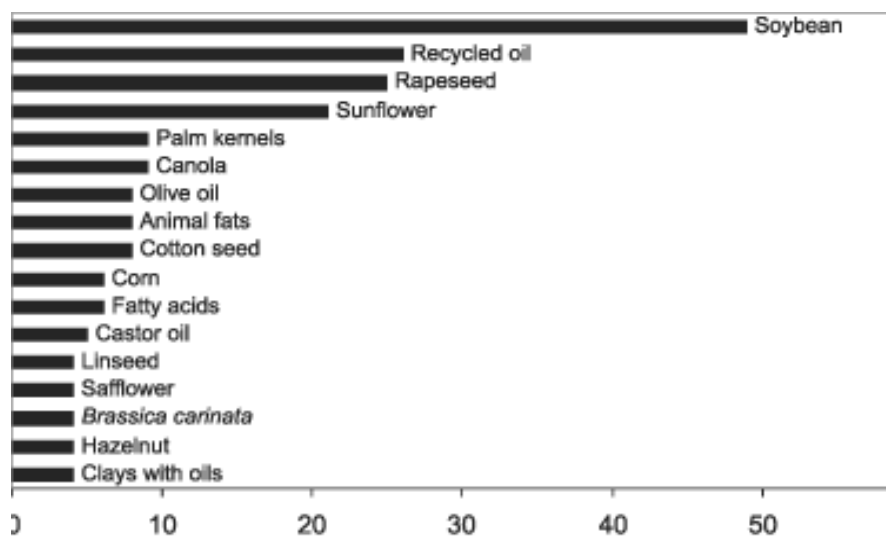


Figure 2.17: Distribution of feedstocks used in the scientific articles [61]

Pinto et al. (2005) [61] mentioned that waste vegetable oils are utilized as low expense biodiesel source when takes account of economy because the price of the soybean oils are higher than the diesel fuel. Meanwhile, Pinto et al. (2005) [61] stated that there is no difference in engine performance and emissions when the low quality underused feedstocks are utilized.

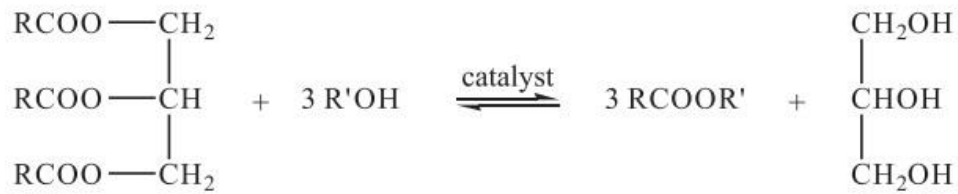


Figure 2.18: Transesterification reaction of triglyceride [61]

Huang et al. (2012) [62] reported that transesterification of the triglycerides with short chain alcohols is used when the biodiesel is produced in the presence of acid catalysts. Figure 2.18 shows the transesterification process of biodiesel. Huang et al. (2012) [62] indicated that methanol, ethanol, propanol, and butanol have been using as short chain alcohols however methanol is usually preferred due to its low price.

#### 2.4.2.1. Emissions of Biodiesel

As it is mentioned before, biodiesel releases less harmful emissions, so it can be said that more environmentally friendly compared to diesel fuel as shown in the Figure 2.19. Aziz et al. (2014) [60] notified that biodiesel generally consist of approximately 10 to 15% oxygen by weight. Hence, the combustion efficiency is improved, and emissions are reduced in comparison to diesel fuel.

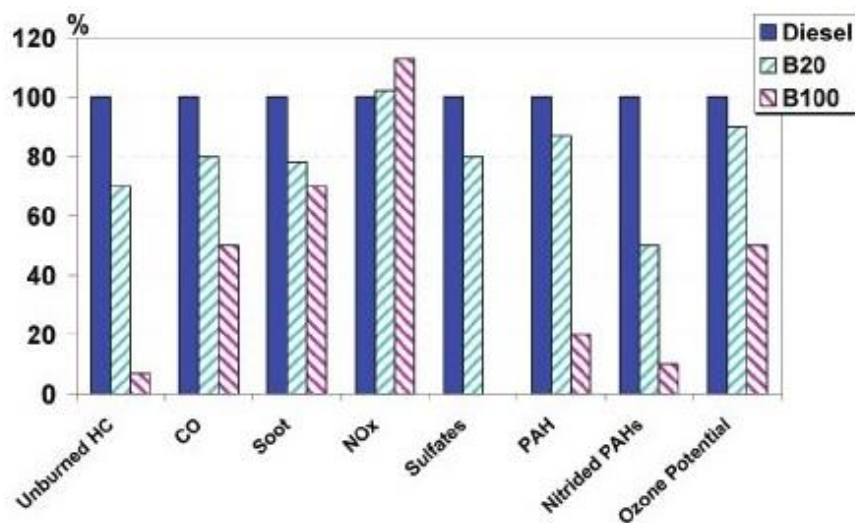


Figure 2.19: Emission difference between diesel, biodiesel and biodiesel blend [63]

Chauhan et al. (2012) [5], Nirmala et al. (2020) [13] and Raman et al. (2019) [22] investigate the engine performance and emissions of biodiesel. During their study, Chauhan et al. (2012) [5] utilized *Jatropha* biodiesel, Nirmala et al. (2020) [13] used two different biodiesels, which are algal oil biodiesel and waste cooking oil biodiesel while Raman et al. (2019) [22] used rapeseed oil biodiesel. They all found out that CO of the biodiesels and their blends are lower compared to diesel due to higher oxygen content in their structure since the more oxygen leads better combustion of carbons hence result in less CO emissions. Also, both Chauhan et al. (2012) [5] and Nirmala et al. (2020) [13] found that CO<sub>2</sub> released by biodiesel and its blends are higher than diesel. Nirmala et al. (2020) [13] explained the reason with higher oxygen content in biodiesel since the CO<sub>2</sub> is directly proportional the oxygen content of fuel the fuel.

Moreover, the particulate matters are based on the combustion temperature and oxygen content as discussed in the previous sections. Also, Huang et al. (2012) [62] stated that biodiesel contains less sulphur compared to diesel, which results in reducing SO<sub>2</sub> in the combustion process. Besides, both Chauhan et al. (2012) [5] and Nirmala et al. (2020) [13] found that biodiesels have lower smoke opacity than diesel. Also, Nirmala et al. (2020) [13] also observed that at lower loads the blended biodiesel contained higher oxygen content resulted in more smoke opacity than different biodiesel blend which contains lower oxygen content. At the higher load, it becomes opposite. This was associated with the importance of temperature in proper burning. However, Raman et al. (2019) [22] observed that biodiesel and their blends had higher smoke emissions than diesel. They associated the reason with the poor atomization and vaporization of the biodiesel and also it was correlated with heavier molecules of biodiesels in their structures which may result slow combustion.

In addition to these, more oxygen content results in less HC emissions as mentioned before. All Chauhan et al. (2012) [5], Nirmala et al. (2020) [13] and Raman et al. (2019) [22] found out that biodiesels have less HC in comparison with diesels due to availability of higher oxygen.

However, even biodiesels can reduce HC, PM and CO but they also lead to increase NO<sub>x</sub> emissions because of several factors. Hoekman and Robbins (2012) [3] reviewed and summarized the related studies that investigated the effects of biodiesels on NO<sub>x</sub> formation. According to Hoekman and Robbins (2012) [3], one of the reasons might



be having higher concentration of unsaturated compounds in biodiesels which makes the flame temperature higher than diesel which leads to increase NO<sub>x</sub> formation. Another reason might be that biodiesels have higher cetane number than diesel which results in shorter ignition delay. As a result of shorter ignition delay, higher temperatures are observed in the cylinder which could allow the increase in NO<sub>x</sub> formation. Besides, Chauhan et al. (2012) [5] found that biodiesel and its all blends had higher NO<sub>x</sub> than diesel. They associated the reason with shorter ignition delay of the biodiesel. Moreover, both Nirmala et al. (2020) [13] and Raman et al. (2019) [22] observed higher NO<sub>x</sub> emissions with biodiesels and their blends in comparison with diesel. Nirmala et al. (2020) [13] correlated the reason with higher viscosity of biodiesel, advanced injection timings and higher temperatures after combustion while Raman et al. (2019) [22] associated with the higher cetane number and oxygen content of the biodiesel.

#### **2.4.2.2. Engine Performance of Biodiesel**

Brake power (BP), brake specific fuel consumption (BSFC), and brake thermal efficiency (BTE) is taken consider while examining the engine performance of biodiesel. As mentioned in the previous sections, Nirmala et al. (2020) [13] defined BP as simply the total power generated by the engine at output shaft. Also, it was expressed as the total useful energy generated per second via an engine. It is directly related with BTE. Besides, Nirmala et al. (2020) [13] expressed BSFC as the ratio of the total fuel consumption to BP. Moreover, BTE was defined as the ratio of power output generated by the engine to chemical energy that supplied from the fuel. It was reported that the density, viscosity, and calorific value of the fuel takes a significant role while determining the BTE.

There are many studies investigated BSFC of the biodiesel which is found out that biodiesel had higher than diesel due to its lower heating value. Canakci (2007) [4] interpreted the reason with lower heating value of biodiesel. Also, Chauhan et al. (2012) [5] explained the reason with higher density, viscosity and lower heating value of the biodiesels. Meanwhile, Nirmala et al. (2020) [13] correlated with the same reasons like Chauhan et al. (2012) [5]. Besides, both Nguyen et al. (2020) [35] and Lee et al. (2017) [36] explained the reason with lower heating value of biodiesel.

Canakci (2007) [4], Chauhan et al. (2012) [5], Nirmala et al. (2020) [13] and Lee et al. (2017) [36] also compared the BTE of biodiesel with diesel, and Canakci (2007) [4] observed no significant difference between diesel and biodiesels while blended biodiesel had slightly lower than diesel. Meanwhile, Chauhan et al. (2012) [5] found out that biodiesel and its blends had lower BTE than diesel due to the lower calorific value. Also, Nirmala et al. (2020) [13] observed lower BTE with two different biodiesels and their blends because of lower calorific value and higher viscosity of biodiesel. In addition to these, Lee et al. (2017) [36] found slightly lower BTE for biodiesel in comparison with diesel.

Nirmala et al. (2020) [13] found out that neat diesels perform better performance in terms of brake power. They clarified that brake power is dependent with the calorific value and viscosity of the fuel and the reason why biodiesel result lower BP than diesel is associated with the higher density and lower calorific value of the biodiesel. Besides, Nguyen et al. (2020) [35] emphasized that increase in biodiesel concentration in blend biodiesel-diesel leads to reduce in brake power and increase in BSFC because increasing blending ratio results increment in the density and kinematic viscosity of the mixture which leads to reduction in fuel evaporation ability, thereby combustion efficiency is reduced and fuel consumption is increased.

Furthermore, Chauhan et al. (2012) [5] found out exhaust temperature of biodiesel is lower than diesel due to poor combustion characteristics of the *Jatropha* biodiesel however Raman et al. (2019) [22] pointed out that exhaust temperature of rapeseed biodiesel is higher than neat diesels due to high content of oxygen inside of the biodiesel which leads to improve combustion process that resulted in higher gas temperatures in the exhaust.

#### **2.4.2.3. Drawbacks of Biofuels**

Kumar et al. (2009) [6] reported that animal fats and vegetable oils are renewable, also they are easily available and can be obtained from different sources. Moreover, it was stated that biofuels can be directly utilized as fuel in diesel engines however they have also important disadvantageous. They emphasized that directly using biofuels in a

diesel engine cause some problems because of their high viscosity, molecular weight, and density. One of the important issues is poor atomization due to these reasons which causes incomplete combustion. Also, other problems such as injector coking, and piston ring sticking should be taken consider when directly utilizing the biofuels. Kumar et al. (2009) [6] indicated that fuel treatment techniques such as blending biofuels with diesel and alcohols, transesterification and use of some additives can be utilized in order to reduce emissions and increase performance of diesel engines with biofuels.

Also, as it is understood from previous section, many studies reported that different type of biodiesels and their blends tends to increase NO<sub>x</sub> formation due to the higher oxygen content of biodiesel and shorter ignition delay because of higher cetane numbers of biodiesel which are mentioned in the previous sections. Meanwhile, emulsified biodiesel-diesel blends with water can be utilized in order to reduce NO<sub>x</sub> emissions. Kumar et al. (2009) [6] stated that, the content of the water reduces the combustion temperature, and results in the reducing NO<sub>x</sub> formation on the exhaust, also another advantage of water is resulting micro-explosion phenomenon which will be investigated detailly in the following sections.

### **2.4.3. Emulsified Biodiesel-Diesel Blends**

According to studies as mentioned in the previous sections, utilizing biodiesel into diesel engine can reduce the emissions such HC, CO, and soot however it causes incrementation of the NO<sub>x</sub> which is undesired. Kumar et al. (2009) [6] mentioned that emulsification method by addition of water can reduce NO<sub>x</sub> formation with little or no modification in engine design.

There are various studies investigates the micro-explosion phenomenon which is resulted of emulsified fuels. For instance , Avulapati et al. (2016) [9] studied the micro-explosion phenomenon and puffing of diesel-biodiesel-ethanol blends. Meanwhile, Hagos et al. (2011) [10] investigated water in diesel emulsions and its micro-explosion phenomenon. Also, Vellaiyan and Amirthagadeswaran (2016) [64] reviewed the studies to examine the role of water in diesel emulsions on engine performance and emissions. Moreover, Yahaya Khan et al. (2014) [65] investigated effect of water in diesel on

combustion and emissions. According to these authors, utilizing water leads to micro explosion phenomenon which has a significant positive effect on the combustion. Basically, they stated that water drops within the emulsified fuel droplets vaporized rapidly due to high cylinder temperature which causes a spontaneous explosion which results in disintegration of the fuel droplets as very fine formation as illustrated in the Figure 2.20. Due to this secondary atomization, fuel and air mixture is enhanced, thereby combustion efficiency is improved.

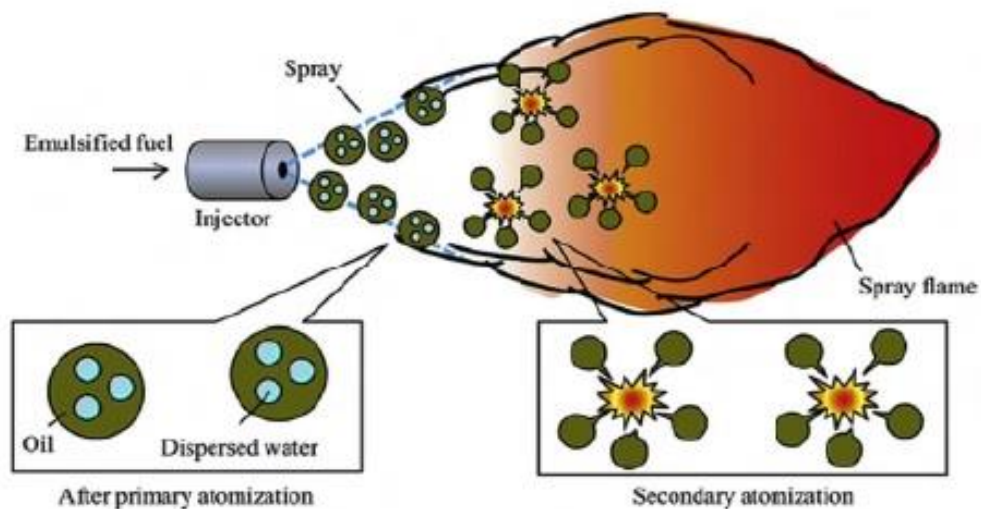


Figure 2.20: Illustration of secondary atomization due to micro explosion phenomenon [10]

### 2.4.3.1. Effect on Engine Performance

Brake power (BP), brake specific fuel consumption (BSFC), and brake thermal efficiency (BTE) is taken consider while examining the engine performance of emulsified biodiesel-diesel blends. Kumar et al. (2009) [6] investigated engine performance and emissions with different fuels including diesel, biodiesel and emulsified fuels. Elsanusi et al. (2017) [7] used diesel, B20 and B40 with three different levels of water concentration (5%, 10% and 15%). Also, Karabektas et al. (2016) [8] used two emulsified fuels, namely B20W10 and B20W15 containing 10% and 15% water by volume. Moreover, Raheman and Kumari (2014) [19] investigated the combustion characteristics

and emissions of emulsified Jatropha biodiesel blend containing 10% and 15% water (B10W10 and B10W15). In addition, Koc and Abdullah (2013) [66] utilized biodiesel nano-emulsions containing 5%, 15%, and 15% water and they compared combustion and emissions of them with B5, B20 and diesel. Furthermore, Reham et al. (2015) [67] reviewed papers related to biofuel emulsion in terms of their stability, combustion, emission and performance.

According to authors, Elsanusi et al. (2017) [7] found that BSFC of the each emulsified blend biodiesel is higher than diesel, and increasing water concentration resulted in increment in the BSFC. They explained the reason with lower heat content of the emulsified fuels. Also, Karabektas et al. (2016) [8] observed higher BSFC from the emulsified fuels. They claimed that water content inside the emulsified fuel leads to decrease in the calorific values, thereby this phenomenon increases the BSFC. Thus, more emulsified fuel is required in order to obtain same power produced by diesel, which leads to higher BSFC. Koc and Abdullah (2013) [66] found higher BSFC with biodiesel nano-emulsions in comparison with B5, B20 and diesel. They indicated that 15% water produced higher BSFC than %5 water, which means raise in the water concentration leads higher BSFC. The reason was correlated with the energy value of the emulsions which is lower than diesel.

According to Koc and Abdullah (2013) [66], BP of the biodiesel nano-emulsions was found lower than diesel, both B5 and B20. As predicted, they observed that increasing water concentration resulted in lower BP while diesel generally produced higher BP than biodiesel blends and emulsified biodiesel. The reason was associated with the higher energy of diesel.

The results from studies above are coherent in terms of BSFC, however they are not consistent when the BTE of the emulsified blend biodiesel are taken consider. For instance, Elsanusi et al. (2017) [7] found that emulsified biodiesel blends have higher BTE than diesel at all engine loads even they have lower calorific value than diesel fuels. The reason was associated with the higher oxygen content in biodiesel structure and micro explosion phenomenon of emulsified fuel which contributes the mixing of air and fuel. On the other hand, Karabektas et al. (2016) [8] found slightly lower BTE for B20W10 and B20W15 at all engine loads in comparison with diesel while B20 was highest BTE. Also, Raheman and Kumari (2014) [19] observed that B10W10 and B10W15 showed

lower BTE than diesel and B10 at lower engine loads, however the BTE of B10W10 becomes higher than B10 at higher engine loads while diesel has highest BTE at all engine loads. The reason why emulsified fuels have lower BTE than diesel was associated with their lower calorific value. Also, they correlated why B10W10 becomes higher than B10 even B10W10 has lower calorific value than B10 with the micro-explosion phenomenon which is occurred due to the volatility difference between of the water and fuels, which leads to enhance atomization of the spray.

In addition to these, Elsanusi et al. (2017) [7] reported that increasing water concentration reduce the exhaust gas temperature due to absorbed heat in the cylinder by water content. Also, Karabektas et al. (2016) [8] found that exhaust temperature of B20W10 and B20W15 has lower than diesel and B20 due to lower calorific value and higher heat vaporization of the emulsified fuels.

#### **2.4.3.2. Effect on Emissions**

For the CO, Elsanusi et al. (2017) [7] found out higher CO for emulsified biodiesel blends and increasing water concentration in the mixture tends to increase CO. The reason was explained with the water content in the emulsion which leads to reduce combustion temperatures. Also, Karabektas et al. (2016) [8] observed higher CO for B20W10 and B20W15 compared to B20 and diesel at lower engine loads. When the engine load between 80% and 100%, all test fuels tend to increase sharply, and CO of the emulsified fuel becomes lower than both B20 and diesel at maximum engine load. They explained with the lower cylinder temperatures at lower engine loads. To elaborate more, water content inside the emulsion absorbs more heat from cylinder, thereby reduces the cylinder temperatures and extend ignition delay. So that, CO is seen higher at lower engine loads due to the elongation combustion. However, decrease in CO compared to diesel and B20 was attributed to enhanced mixture formation due to increased cylinder temperatures and air turbulence. Besides, Raheman and Kumari (2014) [19] claimed that CO of the emulsified biodiesel blends were higher than diesel at lower engine loads however when engine load is increased up to 80% they observed 30-50% less CO than diesel because of burned fuel at higher temperatures and the availability of oxygen but

they observed 50-70% more CO than diesel at full engine load due to the lower air fuel ratio. In addition to these, Koc and Abdullah (2013) [66] found out lower CO for nano-emulsion biodiesels compared to diesel but they emphasized that increasing water concentration causes higher CO. The reason was attributed radical OH from water, which contributes to oxidation of carbon to CO.

For the CO<sub>2</sub>, Karabektas et al. (2016) [8] reported that emulsified biodiesel blends have slightly lower CO<sub>2</sub> than both diesel and biodiesel. The reason was attributed to water content of the emulsified fuel. Also, Raheman and Kumari (2014) [19] found out that emulsified blend fuel produced less CO<sub>2</sub> than diesel at higher engine loads due to better combustion. On the other side, Koc and Abdullah (2013) [66] found that nano-emulsion biodiesels produce more CO<sub>2</sub> than diesel and biodiesel blends. Also, they reported that increasing water concentrations leads to increase CO<sub>2</sub>. The reason of this attributed to increased oxygen atoms in the mixture with increasing water concentration.

For the HC, Elsanusi et al. (2017) [7] observed emulsified biodiesel blends emit lower HC than diesel at all engine loads. However, the study showed that emulsified biodiesel blends released slightly larger HC than their base biodiesel blend. On the other hand, Karabektas et al. (2016) [8] found higher HC for B20W15 and B20W10 than both B20 and diesel at all engine loads. The reason was correlated with that emulsified fuels tends to absorb more heat from cylinder in order to evaporate, which results in deteriorate in HC emissions. On the other hand, Raheman and Kumari (2014) [19] observed that emulsified fuels emit lower HC than diesel at all engine loads. They associated the reason with improved air fuel mixture due to the micro-explosion phenomenon.

For the PM emissions, Elsanusi et al. (2017) [7] showed that emulsified biodiesel blends release more smoke intensity than diesel, and study also shows that increasing water concentration leads to produce less smoke intensity. Besides, Koc and Abdullah (2013) [66] found that nano-emulsion biodiesels emit lower soot opacity than diesel, and also they reported that increasing water concentration in the mixture leads to reduce soot opacity. They attributed this to volatility difference between fuel and water which improves the fuel-air mixture.

For the NO<sub>x</sub> emissions, Elsanusi et al. (2017) [7] emphasized that emulsified biodiesel blends leads to reduce NO<sub>x</sub> emission significantly, also study shows that

increasing water concentration contributes the reduction of NO<sub>x</sub>. Emulsified biodiesel blend with 15% of water release less NO<sub>x</sub> was found out in the study. Also, in the same study average NO<sub>x</sub> reduction for emulsions with 15% of water concentration was found out approximately 30% in comparison with base fuel at 2100 rpm. The reason was attributed to heat energy absorbed by the water content which results in reduction in the peak flame temperature, thereby this phenomenon leads to produce less NO<sub>x</sub> emission for emulsified biodiesel blends. Karabektas et al. (2016) [8] also observed lower NO<sub>x</sub> emissions for emulsified fuels. They also attributed the same reason like Elsanusi et al. (2017) [7] which reduced cylinder temperatures due to water content in the mixture. In addition to these, they mentioned that delay in start of the combustion at low engine loads causes prolonged combustion process which results reduce in the NO<sub>x</sub> emissions. They achieved lowest NO<sub>x</sub> emissions by means of B20W15. Besides, Raheman and Kumari (2014) [19] observed that B10W10 and B10W15 release lower NO<sub>x</sub> emissions than B10, which was found to be between 3% and 28%. The reason was associated with the reduced flame temperature. In addition to these, Koc and Abdullah (2013) [66] showed that nano-emulsion biodiesel with 15% of water has less NO<sub>x</sub> emissions than both diesel and biodiesel blend.

## **2.5. Preparation of Blend Biodiesel-Diesel Emulsion**

C. Y. Lin and Lin (2007) [68] and C. Y. Lin and Wang (2003) [69] examined the stability of three phase biodiesel emulsions. According to authors, emulsions are composed of two non-miscible liquids. Generally, water is preferred as one of the fluids, and other one is represented as oil. It was stated that surfactants are utilized by adding to the mixture in order to reduce the surface tension between water and oil, maximize their contact areas and activates their surfaces. It was reported that the surfactant has hydrophilic and lipophilic group in which hydrophilic group absorbs the water phase while lipophilic group absorbs the oil phase. According to Kumar et al. (2009) [6], homogenizing machines such as mechanical, electric, or chemical are used to blend oil and water mixture.



Vellaiyan and Amirthagadeswaran (2016) [64] indicates that there are two types of emulsion techniques, which are two phase emulsion and three phase emulsion. Two phase emulsions contain one continuous phase and one dispersed phase. On the other side, three phase emulsions contain two dispersed phase and one continuous phase. Also, two phase emulsions are considered as two different forms, which are water in oil (W/O) and oil in water (O/W) while different forms of three phase emulsions are oil in water in oil (O/W/O), and water-in-oil-in-water (W/O/W) as shown in the Figure 2.21. Besides, if an emulsion comprises water drops dispersed in an oil phase is called as W/O while it comprises oil drops dispersed in a water phase is called as O/W emulsion. On the other side, multiple phases which contains three phases where the inner and outer phase is distinguished by a dispersed phase.

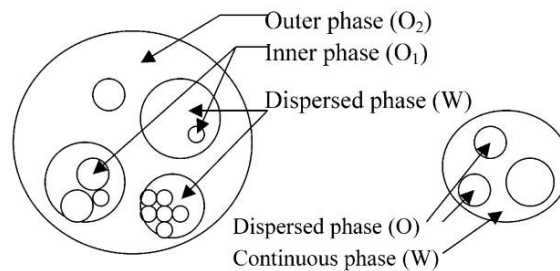


Figure 2.21: Illustration of three phase emulsion and two phase emulsion [69]

Kapadia et al. (2019) [70] mentioned that oil in water in oil (O/W/O) are recommended for fuel purposes while (W/O/W) emulsions have been utilized in food, cosmetics, or pharmaceutical applications. They also mentioned that three phase emulsions are more suitable than two phase emulsions when both emulsions are utilized as fuel even three phase emulsion results in higher CO<sub>2</sub>, CO emissions compared to neat diesel.

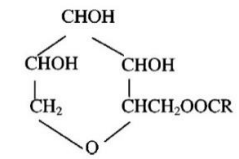
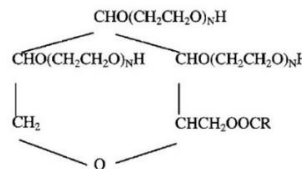
### 2.5.1. Emulsion Stability

C. Y. Lin and Wang (2003) [69] showed that emulsion stability relies on mixing speed of the homogenizer, HLB value, concentration of water and concentration of surfactant as following.

### 2.5.1.1. Role of Water & Surfactant Concentration on Emulsion Stability

Vellaiyan and Amirthagadeswaran (2016) [64] stated that one of the significant factors of obtaining stable emulsion is based on suitable hydrophilic-lipophilic balance (HLB). It was reported that SPAN 80 and TWEEN 80 are one of the common surfactants in the water in diesel emulsions. The properties of both surfactants are illustrated in the Table 2.4.

Table 2.4: Properties of Span 80 and Tween 80 [68]

Type	HLB	Specific Gravity	Chemical Structure
Span 80 (sorbitan monooleate)	4.3	0.98	
Tween 80 (polyoxyethylene sorbitan monooleate)	15	1.08	

According to C. Y. Lin and Wang (2003) [69], the total HLB value of the three phase emulsion is calculated by utilizing the each HLB value of the surfactants (H), and each weight of the surfactants (W) as follows, according to Tween 80 and Span 80;

$$HLB_{ST} = \frac{(H_S \times W_S) + (H_T \times W_T)}{(W_S + W_T)} \quad [\text{Eqn 2.6}]$$

Here,  $HLB_{ST}$  is combined HLB for Tween 80 and Span 80,  $H_S$  represents HLB of Span 80,  $H_T$  is HLB of Tween 80,  $W_S$  represents weight of Span 80, and  $W_T$  is weight of Tween 80.

C. Y. Lin and Wang (2003) [69] prepared various emulsions by changing the concentration of water and HLB in order to see the effect of water content and HLB on the O/W/O emulsion characteristics. During the preparation of the emulsions, different HLB values were applied, which were between 6 and 13, and different water concentrations were utilized such as 10%, 20% and 30%. Figure 2.22 shows the effect of water content and HLB on the stability of three phase emulsion. According to Figure 2.22, C. Y. Lin and Wang (2003) [69] reported that the most suitable surfactant values are found between 6~8 for O/WO. After the value of 10, the emulsion cannot stand stable even including 10% of water concentration. However, C. Y. Lin and Lin (2007) [68] found most appropriate HLB value as 13. Besides, Aziz et al. (2014) [60] investigated the effects of water concentration and Tween 80 on the stability of emulsified biodiesel blends. They also preferred to take HLB as 13 in their study. Besides, they reported that optimum concentration of Tween 80 was observed as 1.5g.

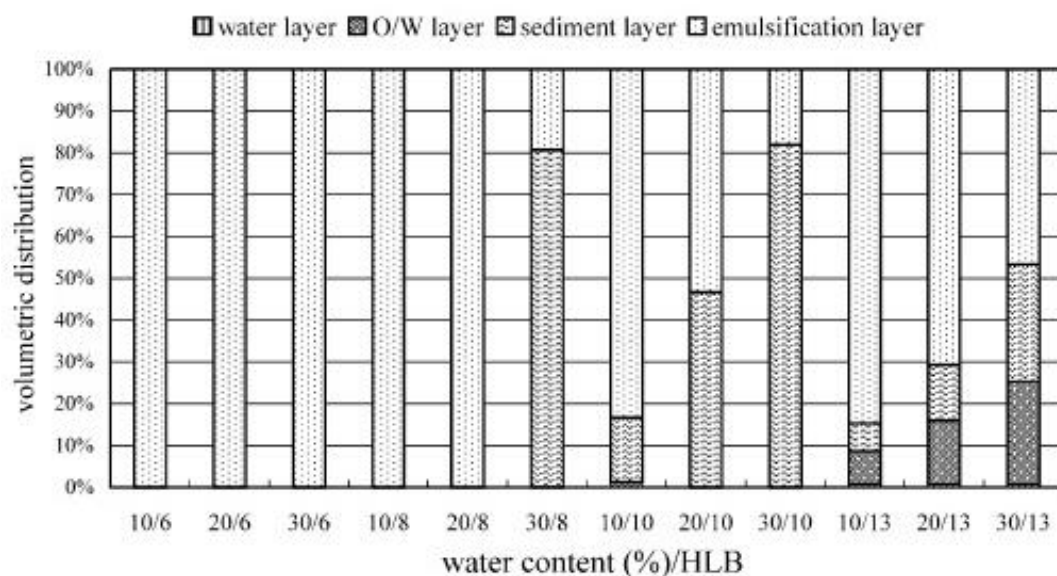


Figure 2.22: The stability of the three phase emulsion with respect to different HLB values and different water concentrations [69]

Furthermore, Elsanusi et al. (2017) [7] prepared various emulsified biodiesel blends with respect to HLB of 8.25 due to 8.25 gives better results in terms of stability. Besides, Rahman and Kumari (2014) [19] obtained HLB 5 provides better stability for the B10 emulsified fuel among the HLB 4.3, 5 and 6. Moreover, Kapadia et al. (2019)

[70] concluded that stability of three phase emulsion is better than two phase and surfactant having HLB of 9 is most suitable to make an emulsion. Also, Karim et al. (2018) [71] found that 10% surfactant with HLB of 9 resulted in deterioration in the viscosity of the mixture, and they reported that HLB of 9 is limited for higher surfactant concentrations. In addition to these, Abdul Karim et al. (2020) [72] produced favourable emulsion characteristics when HLB is equal to 8.

According to Elsanusi et al. (2017) [7], Aziz et al. (2014) [60], Kapadia et al. (2019) [70] and Patil (2017) [73], the stability of the emulsion tends to deterioration as the water concentration in the emulsion increases. Also, both Elsanusi et al. (2017) [7] and Maawa et al. (2020) [74] indicated that the diameter size of particles tends to increase when the water concentration is increased. In addition to these, Karim et al. (2018) [71], Abdul Karim et al. (2020) [72], Patil (2017) [73] and Ghannam and Selim (2009) [75] showed that increasing water concentrations result in increment in the density of the mixture. Moreover, Elsanusi et al. (2017) [7], C. Y. Lin and Wang (2003) [69], Karim et al. (2018) [71], Abdul Karim et al. (2020) [72], Patil (2017) [73] and Maawa et al. (2020) [74] found out that increment in water concentration in the emulsion leads to increase in kinematic viscosity of the mixture.

In addition, Karim et al. (2018) [71] reported that emulsified biodiesel blends that was prepared by ultrasonic stirrer resulted in larger number of smaller dispersed phase than that of prepared by mechanical homogeniser. Also, they mentioned that ultrasonic homogenised emulsified biodiesel blends resulted higher density values. Moreover, Sadhik Basha and Anand (2011) [76] compared emulsified biodiesels according to their engine performance and emissions. The emulsions were prepared by using mechanical agitator and ultrasonic stirrer. It was concluded that emulsions were stable more than four days.

In addition to these, Chu et al. (2012) [77] stated that supplying redundant water to the emulsion leads to lower temperature in the cylinder temperature which is not desired due to incomplete combustion because of large heat loss.

Table 2.5 examines and summarizes various researches which used the three phase emulsions during their studies.

Table 2.5 – O/W/O Emulsions with different concentration ratios of water, surfactant and HLB value [7,19,60,68-69,71-72,74,78-79]

No.	Researcher	Fuel Type	Water Conc.	Surfactant Conc.	Surfactant Type	HLB	Mixing Speed	Conclusion	Ref. No.
1	Elsanusi et al.	B10	5 %	2 %	Tween 80 & Span 80	8.25	4000 rpm & 15 min	- Increasing water and biodiesel concentration in emulsion caused deterioration in emulsion stability and led larger particle size of the droplets. - Increment on the water and biodiesel content led higher viscosity according to their base fuels.	[7]
		B20							
		B30							
		B40							
2	Raheman & Kumari	B10	10 %	0.5 %	Tween 80	4.3	2000 rpm	- Best stabilization is achieved when HLB is equal to 5 for B10. - 2500 rpm gave better results compared to 2000 and 3000 rpm in terms of stability.	[19]
			15 %	1 %	&	5	2500 rpm		
			20 %	2 %	Span 80	6	3000 rpm & 15 min		
3	Aziz et al.	B20	5 %	-	Tween 80 & Span 80	12.7 12.9 13 13.1	800 rpm & 15 min	- Utilization 1.5 <b>grams</b> of Tween 80 was found out as optimum concentration. - More than 1.5 grams of Tween 80 led deterioration on the stability. - Increasing water concentration caused reduction in the stability of the emulsions.	[60]
			10 %						
			15 %						
4	Lin & Lin	-	10 %	-	Tween 80 & Span 80	6 - 13	8000 rpm & N.A.	- The highest stability of O/W/O was achieved when HLB was equal to 13 while the lowest stability was observed when HLB was 6. - The kinematic viscosities of the biodiesel emulsions were acquired as higher than that of biodiesel.	[68]
5	Lin & Wang	-	10 %	2 %	Tween 80 & Span 80	6 - 13	3000, 5000, 8000 rpm & N.A.	- Most stability was achieved when HLB was between 6-8 for O/W/O emulsions. - Increasing water content resulted increase in viscosity of O/W/O emulsions.	[69]
			20 %						
			30 %						

Abbreviation: Conc.: Concentration

(Cont. on next page)

**Table 2.5 (Cont.)**

No.	Researcher	Fuel Type	Water Conc.	Surfactant Conc.	Surfactant Type	HLB	Mixing Speed	Conclusion	Ref. No.
6	Karim et al.	B5	9 %	5 % 10 %	Tween 85 & Span 80	6	Ultrasonic & Mechanic & 30 min	<ul style="list-style-type: none"> <li>- The SMD was ascertained as lower when ultrasonic homogenizer was used instead of mechanical. Besides, the densities of the emulsions prepared by ultrasonic homogenizer were higher than mechanical one.</li> <li>- Increased water concentration generally resulted in increment in the viscosity.</li> <li>- Increased water concentration resulted in increment in the density.</li> <li>- All SMD values of ultrasonic homogenised emulsions were observed less than 2 <math>\mu\text{m}</math>.</li> <li>- HLB 9 was determined as limit for higher concentration of surfactant due to viscosity restrictions.</li> </ul>	[71]
			12 %			7			
			15 %			8			
						9			
7	Abdul Karim et al.	B5	9 %	5 % 7 % 9 %	Tween 85 & Span 80	6	Ultrasonic (30kHz) & N.A.	<ul style="list-style-type: none"> <li>- The better emulsion characteristics was achieved with the HLB 8.</li> <li>- Changing water content significantly affected the density of the emulsion.</li> <li>- Lowest mean density (852.98 kg/m<sup>3</sup>) was observed at 11% water, 9% surfactant with HLB 8.</li> <li>- Increasing water content caused in increase viscosity.</li> <li>- 9% surfactant, 11% water with HLB 7 and with 11% or 13% water, 7% surfactants with HLB 8 were indicated as optimum water in biodiesel emulsion.</li> </ul>	[72]
			11 %			7			
			13 %			8			
			15 %			9			

Abbreviation: Conc.: Concentration

(Cont. on next page)

**Table 2.5 (Cont.)**

No.	Researcher	Fuel Type	Water Conc.	Surfactant Conc.	Surfactant Type	HLB	Mixing Speed	Conclusion	Ref. No.
8	Maawa et al.	B20	5 % 10 % 20 % 30 %	2 %	Tween 80 & Span 80	N.A.	800 rpm & 15 min	- The stability periods of the emulsion fuels were observed tending to decrease as water concentration increase. - Mean droplet size and kinematics viscosity are increased with the increment of water content.	[74]
9	Senthil et al.	B20	5 % 7.5 %	2 %	Tween 80 & Span 80	8	5000 rpm & 10 min	- Stability of emulsions was indicated as 5 hours. - It was found out that the density of B20 with 5% water concentration is 845 kg/m <sup>3</sup> while B20 with 7.5% water concentration is 848 kg/m <sup>3</sup> .	[78]
10	Kumar Patidar & Raheman	B20	10 %	1 %	Tween 80 & Span 80	5	2500 rpm & 15 min	- The separation layer was not observed up to 48 hours.	[79]

**Abbreviation:** Conc.: Concentration

## CHAPTER 3

### EXPERIMENTAL DESIGN & METHODOLOGY

The test rig consists of electrical and mechanical components with several systems, which are constant volume combustion chamber, fuel injection system, optical system, and control system. The schematic of the experimental test rig is illustrated in the Figure 3.1 below.

During the experiments, all process was recorded by a high-speed camera via shadowgraph technique. In this chapter, the experimental apparatus and its compenents, image processing aloratihm, and experimental methodology will be explained respectively. In addition to these, the method of the preparation of blended biodiesel emulsions with water is going to be expressed.

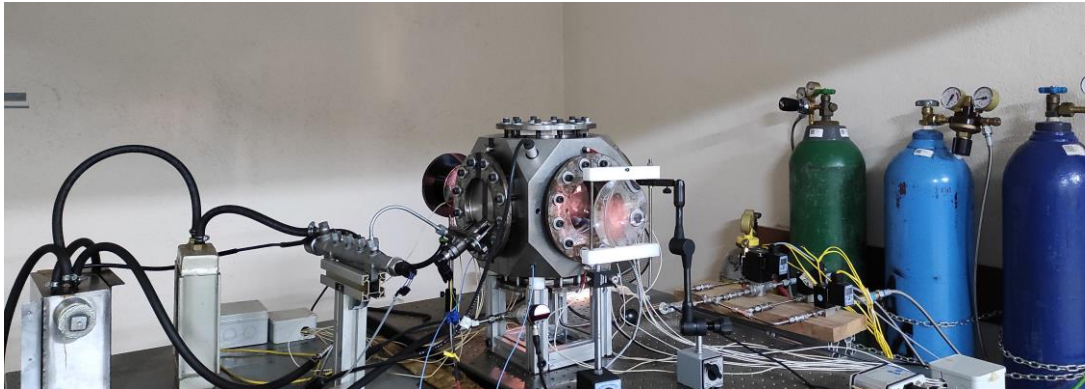


Figure 3.1: Illustration of experimental test apparatus

Constant volume combustion chamber with an optical access was utilized in order to obtain non-evaporative spray characterization for this experimental study. An injector, a common rail, and fuel pump are used for injection system. Gas tubes were performed to provide efficient and suitable pressure inside of the combustion chamber required for observing spray formation. A high-speed camera is used for the recording data. Finally,



a computer with data-acquisition module is used to generate signals to operate drivers and sensors and to monitor the obtained data. The whole schematic experimental apparatus can be seen on the Figure 3.2.

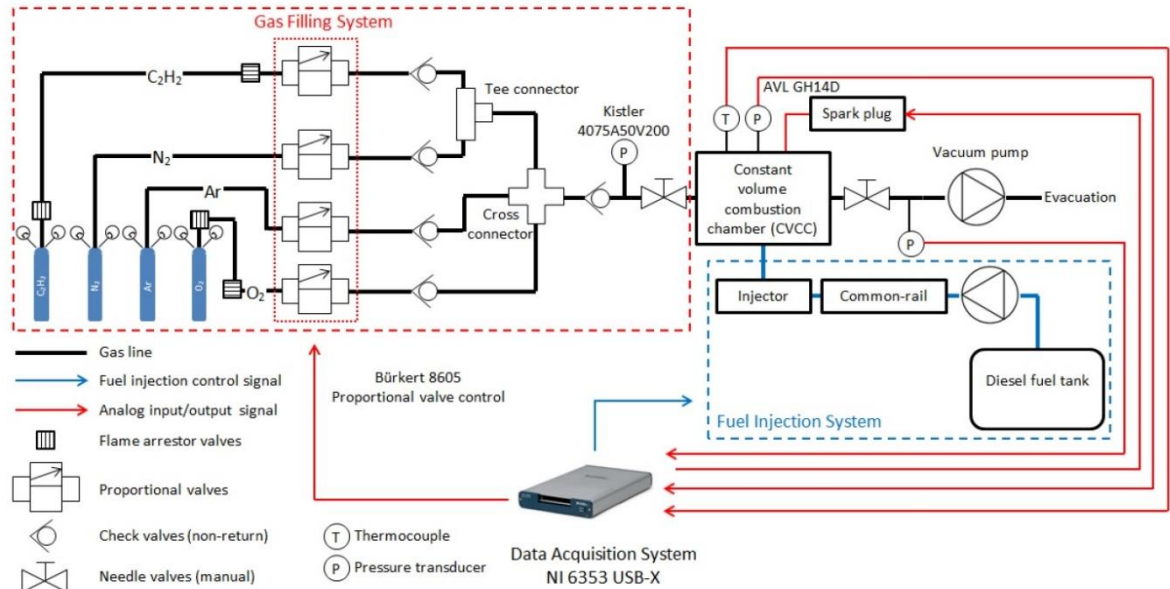


Figure 3.2: Schematic of the experimental test apparatus

### 3.1. Experimental Test Apparatus

Constant volume combustion chambers are generally used to make simulations of wide range thermodynamic conditions for the engines because of composing thick steel wall container on its structure. The chamber was composed of a single piece stainless steel aiming to endure reliable under tough conditions. Also, Figure 3.3 shows the CVCC that was utilized during the experiments. It has two quartz windows, stand on the opposite which attached to the main body via the flanges. The diameter of the windows is 120 mm, and the thickness is 30 mm. There are six gaps with 105 mm diameter on the chamber allowing to connection with ambient. One of them is used for the gas filling and ejaculate. Meanwhile, other two gaps are used for the windows and one of them is used for the injector mounting. The rest are not used in this experiment however they can be used for future works.

It is possible to obtain combustion simulation and spray formation through CVCC. Basically, gaseous mixture with combination of  $C_2H_2$ ,  $O_2$ ,  $Ar$  and  $N_2$  is sent to CVCC to

provide efficient and suitable pressure inside of the combustion chamber for the pre-combustion.

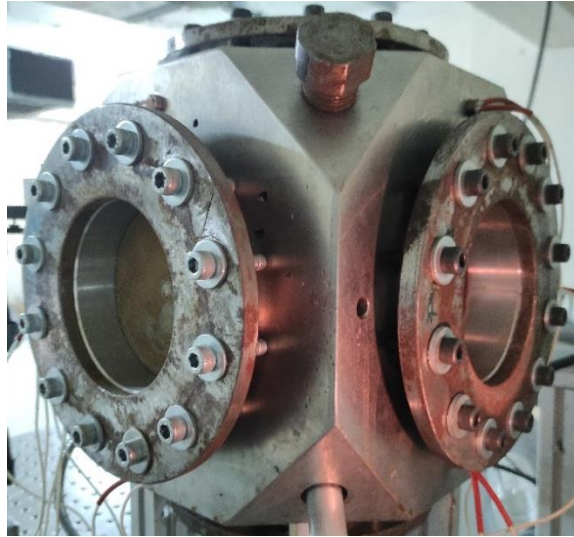


Figure 3.3: The demonstration of CVCC

After that, mixture is ignited by the spark plugs. So that, the temperature and pressure are both increased. Then, fuel is injected to the chamber. The circumstances for the pre-combustion can be obtained since the fuel ignition point is lower than the chamber. Therefore, an auto ignition starts. However, pre-combustion method is not appropriate for the spray measurement since there is no ignition during the experiment. Only requirement for the spray measurement is to have required level of pressure inside of the chamber to observe the spray formation. Hence, only nitrogen was used during the experiment. The required pressure is supplied by the regulator mounted on the industrial pressurized gas cylinder and then nitrogen gas is presented by the proportional valve. Finally, nitrogen is sent to the chamber through pipes. During the experiment, check valve and sensors are mounted on the pipes in order to prevent undesired hazardous circumstances.

The purpose of the fuel injection system is to deliver fuel into CVCC from fuel tank. The main parts of the system are fuel tank, high pressure pump, common rail and injector are going to be explained, respectively.

Basically, a fuel tank is used to storage the flammable fuel. The volume of the tank is 10 litter. The reason behind of it is in order to prevent reaching high temperature issues during the experiment. The temperature can be cooled down rapidly by keeping the volume as 10 litter.

The pressurization of the fuel is carried though high-pressure fuel pump, which is located at the bottom of the table as can be seen in the Figure 3.4. Fuel is transferred into common rail from fuel tank. The high pressure is controlled by the valves which are Pressure Control Valve (PCV) and Volume Control Valve (VCV), which were mounted left-side of the common-rail and at the inlet of the high-pressure pump. Pulse width modulated signals (PWM) are generated by the data acquisition card (DAQ) and transmitted to the valves on the pump.

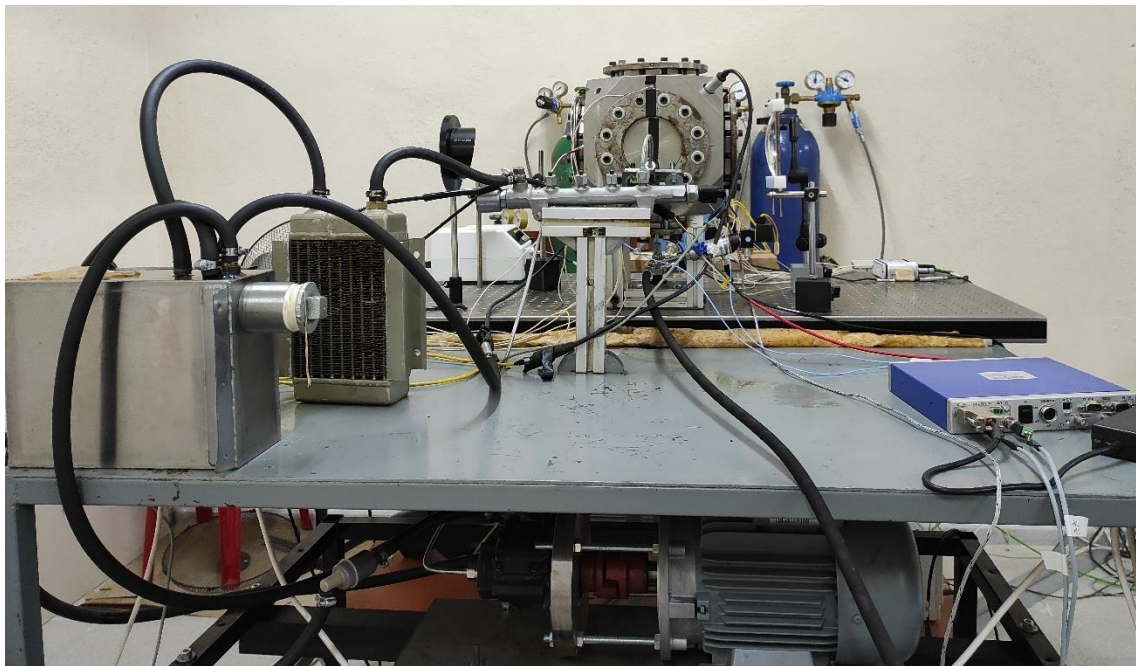


Figure 3.4: The components of fuel injection system, respectively; fuel pump (at the bottom of the table), fuel tank (on the left of the table), common rail (at the middle of the table)

The pressure inside of the common-rail is measured by the pressure sensor which is mounted at the end of the common-rail. PCV is running according to pressurized value. Basically, PCV starts to close the valve if high pressure is required. On the other hand, it

starts to open the valve if low pressure is required according to data coming from pressure sensor.

The high pressure fuel inside the common rail is transmitted to piezoelectric injector. Originally, the type of the injector utilized during the experiment was multi-hole nozzle. However, because of one hole is adequate to observe spray formation the rests were closed by welding process. The injector is mounted to CVCC as angle of  $45^\circ$  horizontally to observe spray penetration better due to the larger area as illustrated in the Figure 3.5. The signal that enables to trigger injector at desired time is carried through the injector driver, and value of the signal is DC 5V and signal is transmitted for 1ms. So that, injection time is adjusted as 1ms according to this signal.

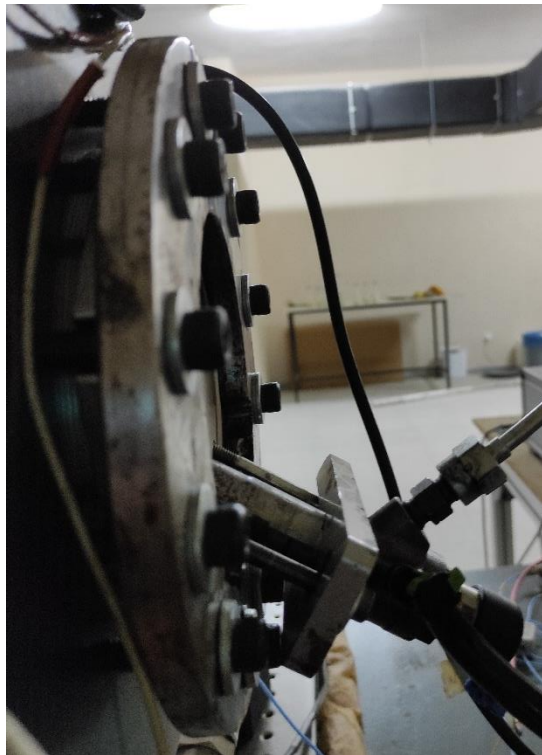


Figure 3.5: Indication of located injector as horizontally

During the spray formation occurrence in the combustion chamber, the light source is used in order to visualize the spray formation. The model of the light source is MI-150 Fiber Light Source. The intensity of the light source is adjusted by the diagram with a diameter of 30.8mm. After that, the light comes from diagram is passed through

parabolic mirror (101.6 x 152.4 mm) to make adequate angle according to chamber window. After light is passing through the combustion chamber, it is focused on a certain point by a convex lens of 125mm diameter and 250mm focal length. All the components are illustrated in the Figure 3.6. Finally, a high-speed camera which capture 20000 frame per second is used to record the data.

Also, a vacuum pump, which is 0,75kW, is used in order to draw away exhaust gases and fuel vapour inside of the chamber.

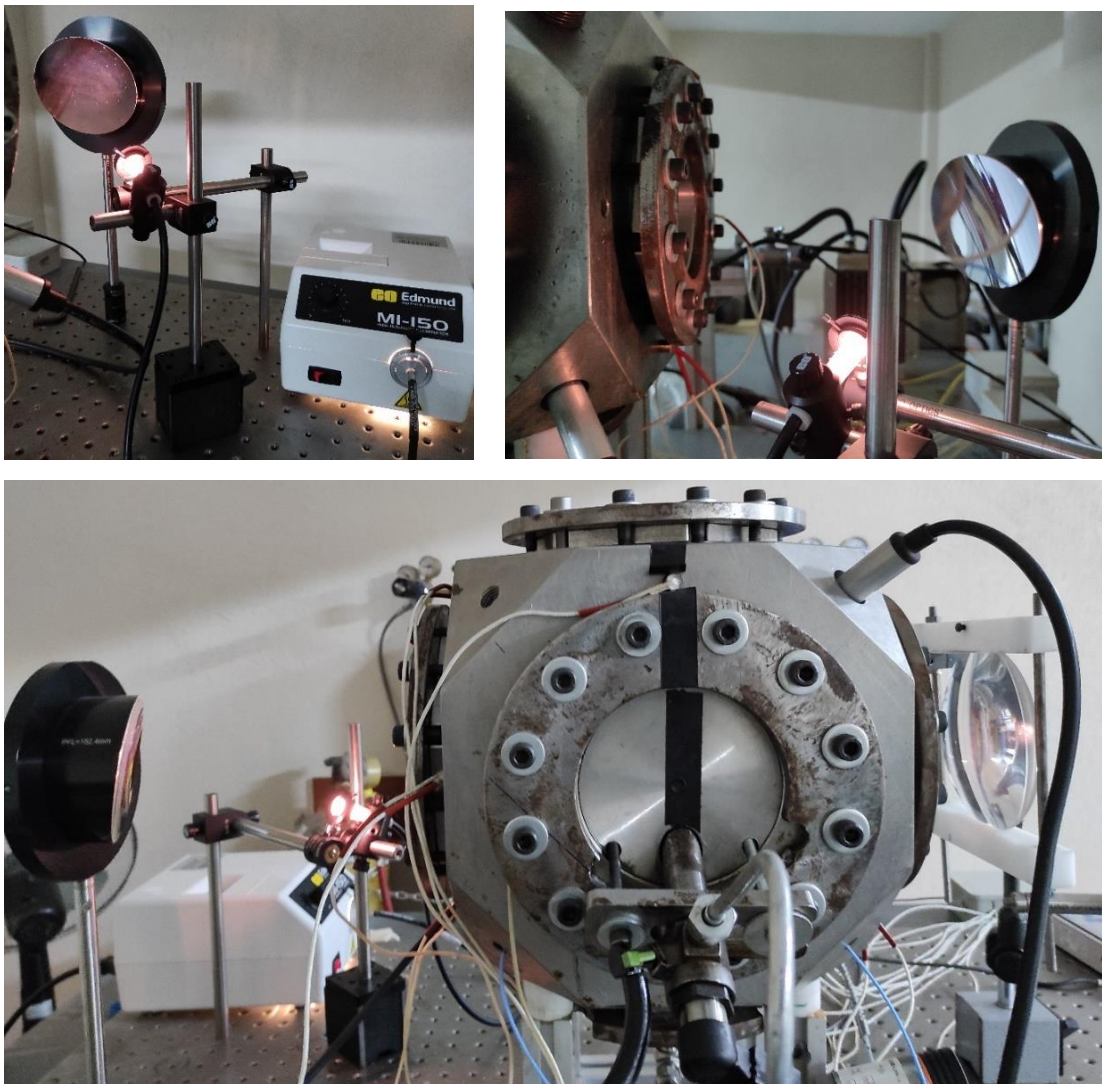


Figure 3.6: Illustration of optical system from different views

During the experiment, components of the experimental setup such drivers and sensors are controlled by two DAQ card (NI USB 6353) and a PC with LabView software. The signals sent to drivers and sensors is also generated by computer and that signal is passed to the DAQ cards. Also, thanks for the LabView software, the data comes from sensor and drivers can be monitored through easily.

### 3.2. The Preparation of Emulsion of Biodiesel-Diesel Blend

The preparation of emulsion of blended biodiesel-diesel with water (B20W5 and B20W15) are prepared according to methods applied in the study of Aziz et al. (2014) [60], which consists of two steps. During the preparation, mechanical agitator is utilized as stirrer, TWEEN 80 and SPAN 80 are used as surfactants, diesel fuel is supplied from gas station near university, and biodiesel is provided from company named DB Tarimsal Energy [80].

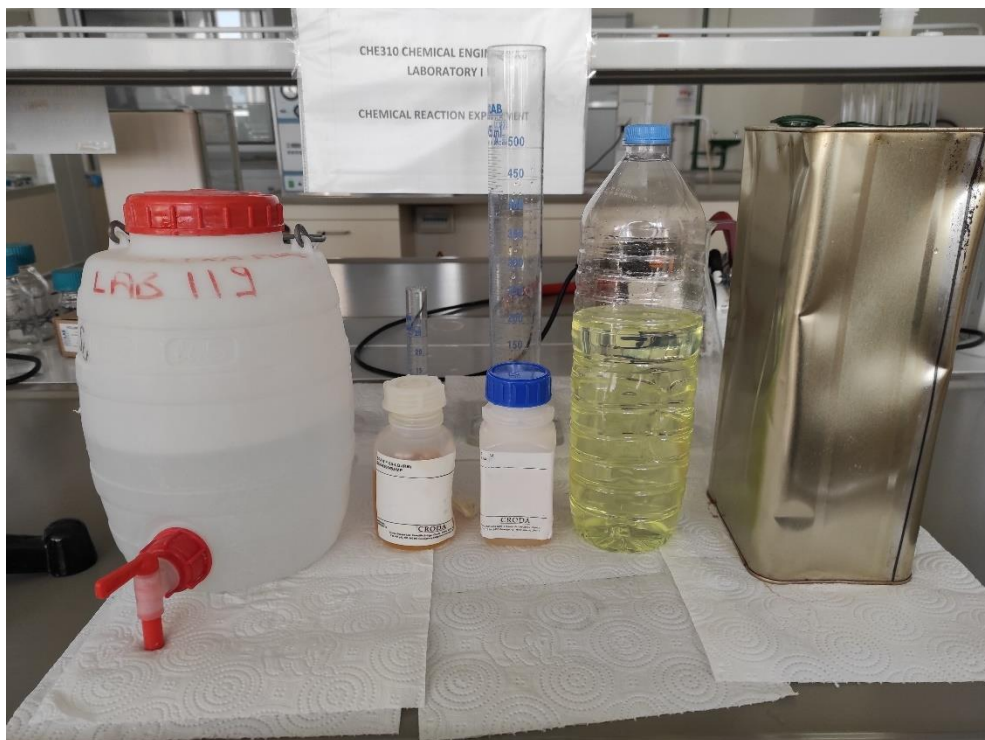


Figure 3.7: Materials for preparation B20W15 and B20W5; distilled water, surfactants, diesel and biodiesel

Even there are many studies prepared the emulsion with different values of HLB (see the section 2.5.1.1) the appropriate HLB was preferred as 8 according to experimental results which is discussed in the Chapter 4.

In the first step, surfactants are added into the blended diesel-biodiesel mixture according to formulation which is given in the section 2.5.1.1. Next, the mixture is stirred at 800 rpm for 5 minutes via mechanical agitator. In the second step, distilled water is added to the mixture of blended diesel-biodiesel and surfactants. While the adding water, the mixture begun to change into a creamy formation as illustrated in the Figure 3.8.



Figure 3.8: Changing colour of the mixture during the addition of water

After that, mixture is stirred at constant 6000 rpm for 20 minutes. Next, stirring speed is set to 10000 rpm for 10 minutes to make the mixture more homogeneous and stable. At the end of the stirring processes, the blended emulsion is obtained as a creamy colour. One of the emulsion samples is shown in the Figure 3.9.

Finally, emulsion of blend diesel-biodiesel with 5% and 15% concentration of water (B20W5 and B20W15) is obtained with the same methodology as above, respectively.



Figure 3.9: The sample of blended emulsion fuel at the end of the preparation process

### 3.3. Methodology

In this section, the whole method performing the experiment are taken consider from beginning of the experiment to its end.

First, 2 litter of blended diesel-biodiesel with water emulsion as regards to concentration ratios mentioned in the previous section was prepared to be utilized in the experiments. After obtained B20W5 and B20W15, the high-speed camera was located toward to combustion chamber window to obtain greatest angle for recording. Also, it was cabled to the injection driver to communicate with it in order to start recording when the injection begun. Shutter speed of the camera and resolution were adjusted as 1/62000 and 512x512 to achieve higher qualities.

Secondly, all gases combustion chamber includes were vacuumed until pressure inside of the chamber was equal to zero. Next, the nitrogen gas filled into the combustion chamber through proportional valves mentioned in the previous section. PID control system via Labview program was used to make sure that there will be no error during the filling process. The desired value was set to the program. The current value was checked



by the help of sensors and the error will be compensated through PID system if there were any difference between the desired value and current value. The proportional valve was closed when the desired amount of nitrogen was obtained in the chamber.

Next, the system was started to operate in order to drain existing fuel inside of the injection and fuel tank to prohibit misleading results during the experiments. After that, the test fuel was added to the fuel tank whereafter all existing fuel consumed inside of the test components. Then, the light source was turned on and the mirrors and lens are checked. So that, system become ready to perform spray formation of the test fuel.

After that, desired pressure value was set on the program. Hence, PWM signals were generated through DAQ card and these signals were sent to valves mounted on the fuel pump and common rail. So that, fuel pump was started to pressurize the test fuel until it reached to desired set value. When the required pressure was obtained, the injector was triggered via signals that come from DAQ card. Therefore, injection was immediately begun after trigger process had done, and it ended after a while later. During the injection process, the camera started shooting with 20000 frames per second and whole recording is saved to the computer to investigate the spray angle and penetration by processing the images.

As final step for the experiment, the gas and fuel vapor within the combustion chamber was vacuumed by the pump to make the system ready for the next experiment. So, the method of performing spray formation of the test fuel was achieved at the end of the vacuum process.

The experiments were performed when the injection pressure was set 600 bar and 800 bar respectively while the ambient pressures were determined as 0 bar, 5 bar and 10 bar. As mentioned before, the injector type was single hole piezoelectric injector, and it was mounted to the combustion chamber with a 45° angle. Also, injection duration was set as 1 ms. All experiments were repeated in three times, as repeatability of tests was taken into account.

The spray images of the emulsified biodiesel-diesel blends were saved to the computer to explore their spray penetration lengths and spray cone angles after spray formation of the emulsified fuels was recorded by the high-speed camera. The measurements of both spray cone angle and spray penetration length were carried out

with the ImageJ program [81] which is a public domain Java image processing program inspired by NIH Image.

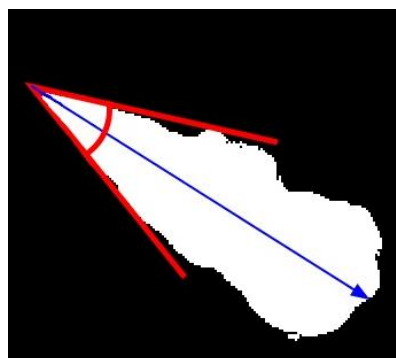
After the experiments were carried out, the spray penetration length was measured firstly. The raw frames come from the recorded video was converted to greyscale. Then, background of the each of these frames were subtracted. Also, the greyscale was converted to binary scale to obtain white and black images. After the conversion process was finished, the required frames to observe the spray formation of the test fuel was acquired. Next, the line between nozzle exit and the end of the spray was drawn, and the known distance was entered to the program in order to take as a reference distance while measuring the distance between pixels. Hence, spray penetration length was measured through with utilizing the blue line as in the Figure 3.10 and reference distance.



- Raw image



- Greyscale image



- Spray cone angle and penetration length

Figure 3.10: Demonstration of images during the measurement process

Secondly, spray cone angle was measured with the angle tool via the same program. In the first part, the same subtraction process and conversion processes were applied to each frame comes from the recorded video to be able to measure the spray cone angle. For the next step, three arbitrary points were marked on the image which creates two arbitrary lines with respect to three points where one of the points specified the nozzle and the rests specified the outer of spray boundaries. So that, the spray cone angle was achieved through the angle between these red lines as it can be seen on the Figure 3.10.

As a result, the all spray penetration lengths and cone angles of B20W5 and B20W15 which occurred under 0 bar, 5 bar and 10 bar ambient pressure with 600 bar and 800 bar injection pressure were measured by applying mentioned spray measurement process as shown in the Figure 3.10.

## CHAPTER 4

### RESULTS & DISCUSSIONS

In this section, the results obtained from the experiments will be discussed and compared to other studies in the literature. In the first part, the results of these studies which show the stabilities of the different emulsions are presented. In the next part, the macroscopic spray characteristics such as spray penetration length (SPL) and spray cone angle (SCA) of the B20W5 and B20W15, which are the main goals of this study, will be presented in several graphs.

#### 4.1. Stabilities of Emulsions

As mentioned in the previous section, there are many studies which used different values of HLB, water concentration, and fuel concentration while preparing the blended diesel-biodiesel emulsions. Table 4.1 indicates several trials which were made according to these studies to obtain stable emulsion of B20W5 and B20W15 which can stand stable during performing the experiments. Also, in order to understand better the effect of different ratio of water and surfactant, and different HLB values on the emulsion stability. During the whole trials, stirring speed of each step was kept same, and TWEEN 80 and SPAN 80 were utilized as surfactants in order to compare results each other's. The HLB range and concentration of surfactants range were chosen to be between 8~9 and 2~5 respectively depending on the studies of C. Y. Lin and Wang (2003) [69] and Abdul Karim et al. (2020) [72]. Stabilizations were calculated based on the moment when the first separation in the mixture was observed. Generally, the first separation was occurred at the bottom of the mixture as a sediment layer. It was observed that there was no separation between oil and water until the first sediment layer was formed.

The calculations of the concentrations were proportioned according to overall volume of the mixture which was determined as 100mL.

Table 4.1: Stabilization of emulsions with different concentration of ingredients

Sample No	Fuel	HLB	Conc. of surfactants (%)	Conc. of water (%)	Conc. of diesel (%)	Conc. of biodiesel (%)	Stability (days)
1	B10W5	9	2	5	83.7	9.3	5
2	B20W5	9	2	5	74.4	18.6	3
3	B40W5	9	2	5	55.8	37.2	<1
4	B10W5	9	5	5	81	9	6
5	B10W10	9	5	10	76.5	8.5	5
6	B10W15	9	5	15	72	8	3
7	B20W5	9	5	5	72	18	5
8	B20W10	9	5	10	68	17	3
9	B20W15	9	5	15	64	16	2
10	B30W10	9	5	10	59.5	25.5	<1
11	B40W10	9	5	10	51	34	<1
12	B50W10	9	5	10	42.5	42.5	<1
13	B20W5	8.25	2	5	74.4	18.6	2
14	B30W5	8.25	2	5	65.1	27.9	<1
15	B40W5	8.25	2	5	55.8	37.2	<1
16	B50W5	8.25	2	5	46.5	46.5	<1
17	B20W5	8	5	5	72	18	8
18	B20W15	8	5	15	64	16	5

**Abbreviation:** Conc.: Concentration.

Table 4.1 shows that increasing water concentration in emulsion caused deterioration in emulsion stability. The stabilities of the samples between 4 and 6 are shown as 6 days, 5 days and 3 days, respectively. Similarly, between the sample of 17 and 18 while keeping the same concentration of surfactant and HLB, the stability of the emulsion is decreasing from 8 days to 5 days. Besides, increment in the concentration of biodiesel has adverse effect on the emulsion stabilities as can be seen from samples between 1 and 3. Also, samples between 8 and 10 shows that more than 20% of biodiesel concentration gives negative effect on stability of the emulsion. In addition, 5% concentration of surfactant and HLB 8 give better stabilization on the emulsion compared %2 concentration of surfactant as the samples between 1 and 4, 7 and 17, and between 9 and 18 are considered.

As a result, the most stable emulsion among the trials is obtained when the surfactant concentration is equal to 5% and HLB is equal to 8 which is consistent with other results in literature like C. Y. Lin and Wang (2003) [69] and Abdul Karim et al. (2020) [72]. In the literature, there are many studies related to emulsions of biodiesels and their stabilities as indicated in the chapter 3. The optimum values of HLB,

concentrations of water and surfactants of these studies may vary, in turn the stability of those emulsions results differently. The reason of this is most likely due to the large variety of biodiesel and hence the changing chemical properties of it. Another possible reason may be different types of agitators utilized in the studies, some of them used different mechanical types while some of them used ultrasonic ones.

The properties of prepared B20W5 and B20W15 can be seen in the Table 4.2 below. During the measurement of density of the emulsified blend fuels, the calibrated pycnometer was used. Firstly, empty weight of the pycnometer was measured and, room temperature fuel was added and the excess overflow was wiped with acetone. After that, the average weight was measured by measuring the weight 10 samples and pycnometer's own weight was subtracted from average weight. Finally, the weight of the fuel obtained was divided by the volume of the pycnometer which was 25,066 ml. Also, the viscosity values of these emulsified biodiesel blends were measured by using AR 2000ex rheometer. In order to compare density and viscosity of emulsified blend biodiesels with those of diesel and biodiesel, the viscosity and density of reference diesel and reference biodiesel were taken from study of A. Ulu (2020) [82].

Table 4.2: Properties of fuels

<b>Fuel type</b>	<b>Density at 25°C (kg/m<sup>3</sup>)</b>	<b>Viscosity at 40°C (cSt)</b>
Diesel (ref) [82]	829.5	3.07
B20W5	855.6	3.55
B20W15	869.3	3.92
Biodiesel (ref) [82]	884.01	4.24

Table 4.2 shows that viscosity and density of B20W15 is higher than B20W5. The results are align with the study of Elsanusi et al. (2017) [7], Karim et al. (2018) [71], Abdul Karim et al. (2020) [72] and Patil (2017) [73] since these authors also found out that increase in content of water inside of the emulsion leads higher viscosity in the emulsion. Also, Karim et al. (2018) [71] and Patil (2017) [73] reported that increasing

water concentration leads increment in the density of the mixture. Besides, when the results are compared to study of A. Ulu (2020) [82], it was understood that, emulsified fuels have higher viscosities and densities than diesel while they have smaller viscosities and densities compared to that of biodiesel. For the following sections, the SPL and SCA of the B20W5 and B20W15 will be investigated, respectively.

## 4.2. Examination of Spray Penetration Length

In order to investigate SPL and SCA of B20W5 and B20W15, the experiments conditions were preferred as 0 bar, 5 bar and 10 bar for the CVCC while the injection pressures were adjusted as 600 bar and 800 bar. All experiments were repeated three times, to check the repeatability of tests. The data in the graphs were presented by averaging the results of each test. The repeatability according to maximum difference was calculated to be in 5% for both SPL and SCA. Also, uncertainty of the SCA was found out as  $\pm 0.9^\circ$  while that of SPL was found out as  $\pm 5$  mm, which are shown in the graphs. In order to better understand the effect of 600 bar and 800 bar injection pressure on the spray length depending on the pressure change in the combustion chamber, spray lengths at 0 bar, 5 bar and 10 bar ambient pressure are respectively shown as follows. Also, the effect of ambient pressures on the penetration lengths at each injection pressure under 0 bar, 5 bar and 10 bar pressure are shown respectively. In order to compare spray penetration lengths of the emulsified biodiesel blends with that of diesel and biodiesel, all reference diesel and reference biodiesel values in the graphs which are shown with bold red and green lines were taken from study of A. Ulu (2020) [82] which conducted the experiments with the same apparatus under the same test conditions in order to investigate the spray characteristics of diesel and biodiesel. During that study, repeatability and uncertainty of the penetration length for diesel and biodiesel was found out as 3% and  $\pm 4$  mm.

The repeatability and uncertainty of SPL for B20W5 and B20W15 are 5% and  $\pm 5$  mm respectively while the repeatability and uncertainty of SPL for reference diesel and reference biodiesel are 3% and  $\pm 4$  mm respectively in all graphs within both Figure 4.1 and Figure 4.2.

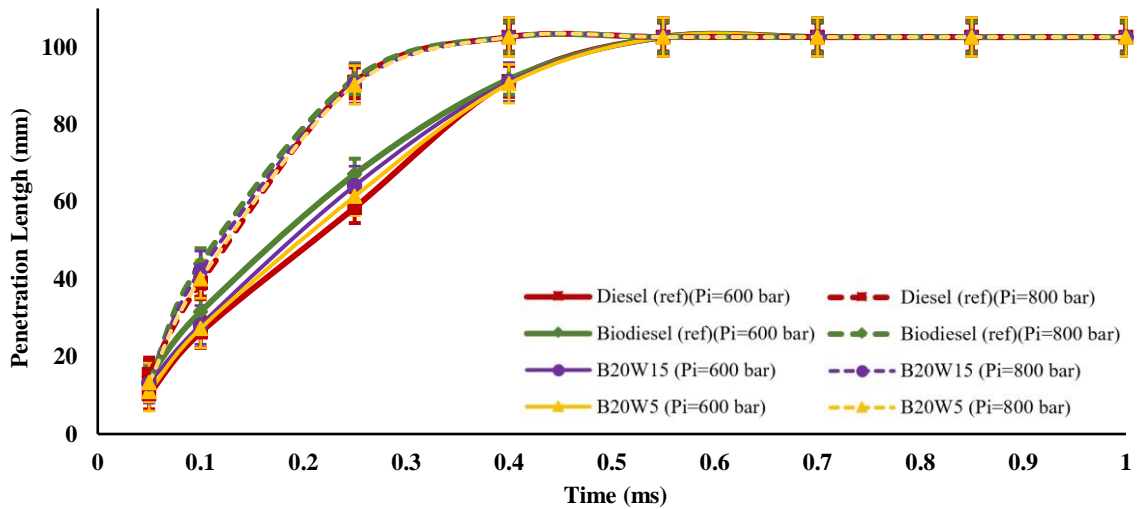


Figure 4.1 (a): Spray penetration lengths with injection pressures of 600 bar and 800 bar at 0 bar ambient pressure

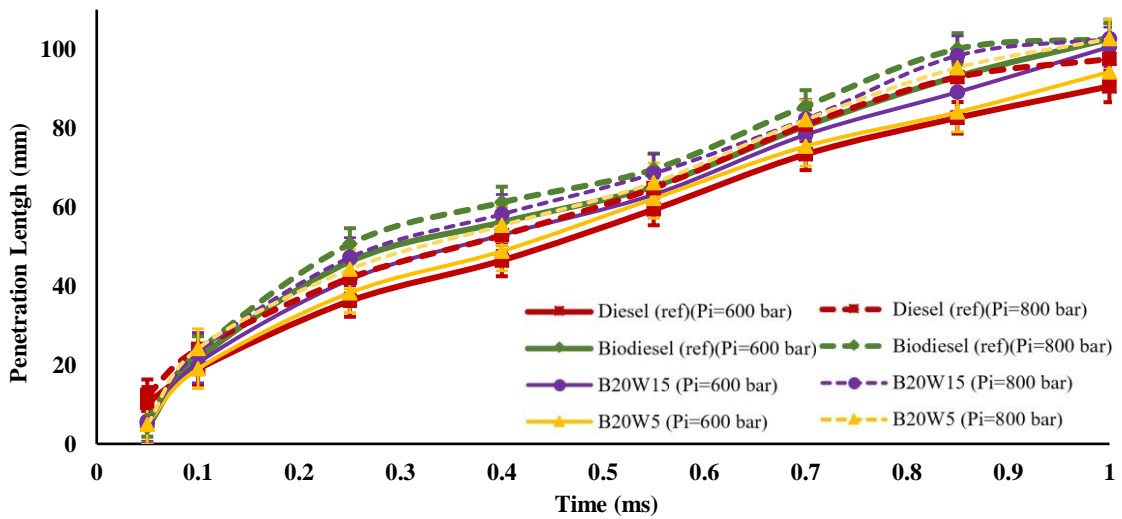


Figure 4.1 (b): Spray penetration lengths with injection pressures of 600 bar and 800 bar at 5 bar ambient pressure

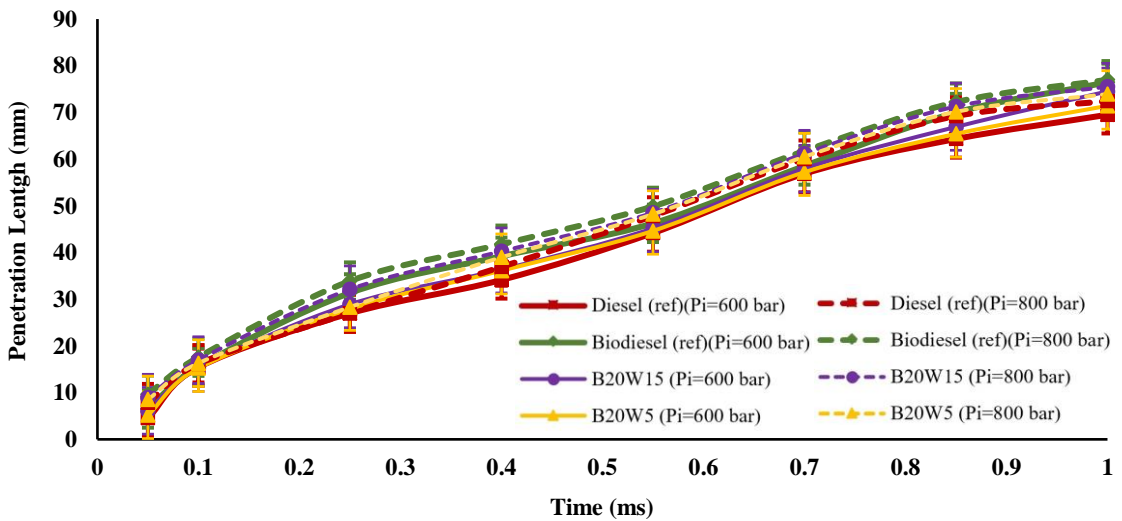


Figure 4.1 (c): Spray penetration lengths with injection pressures of 600 bar and 800 bar at 10 bar ambient pressure



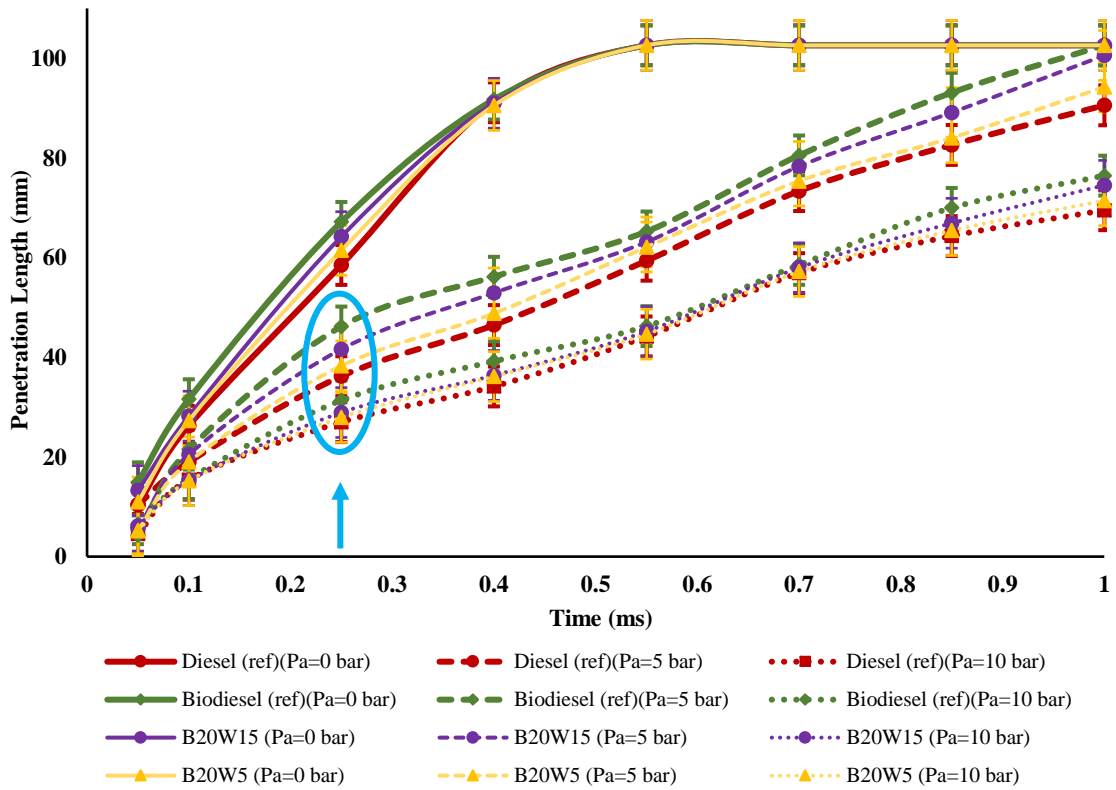


Figure 4.2 (a): Spray penetration lengths with 600 bar injection pressure under 0 bar, 5 bar and 10 bar ambient pressure

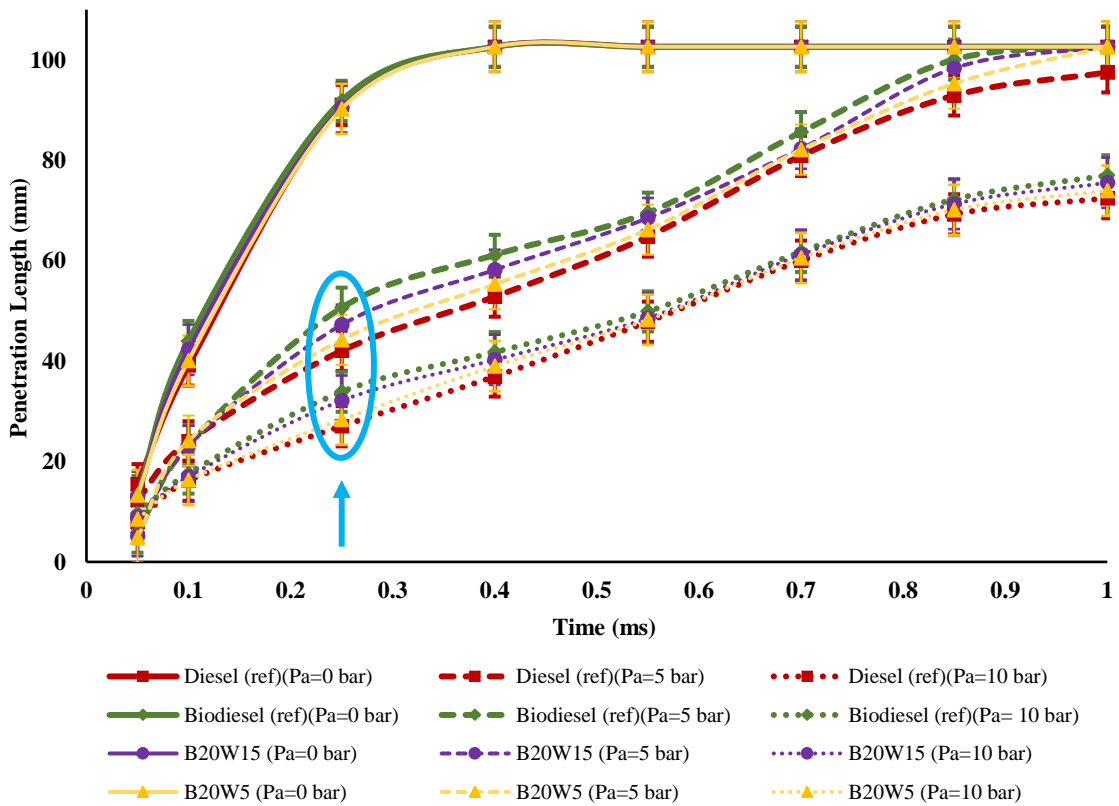


Figure 4.2 (b): Spray penetration lengths with 800 bar injection pressure under 0 bar, 5 bar and 10 bar ambient pressure

Figure 4.1 and Figure 4.2 show that at the same time reference biodiesel was slightly longer tip penetrations compared to both emulsified biodiesel-diesel blends and reference diesel for 600 bar and 800 bar injection pressures under 0 and 10 bar ambient pressures while the difference was higher under 5 bar chamber pressure. Also, B20W5 and B20W15 (emulsions of blended diesel and biodiesel with water concentration %5 and 15%) had longer penetrations than reference diesel while B20W15 had longer penetrations compared to B20W5. Meanwhile, reference diesel had smaller penetrations in comparison with reference biodiesel and emulsions for both injection pressures at all ambient pressures.

Besides, it was observed that, increasing ambient pressure takes an essential role on the spray penetration length while the injection pressure takes less than chamber pressure. It can be seen that the spray penetration of all fuels decreases as ambient pressures increases for both 600 and 800 bar injection pressure. Agarwal et al. (2014) [39] explained this with increased flow resistance between the spray and air within the chamber. So that, spray may be exposed more resistance force as the ambient pressure increased which may inhibit its propagation on movement axis, in turn results in smaller spray penetrations. Also, increased injection pressure from 600 bar to 800 bar led more longer penetrations. According to Nguyen et al. (2020) [35] increasing injection pressures lead to increase initial velocity and momentum of the spray. This phenomenon may have resulted fuels in longer penetrations with injection pressure of 800 bar. Especially, raising the injection pressure under zero bar ambient pressure had a remarkable effect on the spray penetration lengths compared to other ambient pressures, in particular at the beginnings of the injection. For example, penetration length of B20W15 at 0.25 ms under 0 bar chamber pressure with 600 bar injection pressure was measured as 64.2 mm but when the injection pressure was increased to 800 bar under same ambient pressure the penetration length became 90.5 mm. However, its effect seems much less than chamber pressure when the 5 bar and 10 bar of ambient pressures are taken consider. To elaborate more, as it is shown with blue circles in the both Figure 4.2(a) and Figure 4.2(b), the penetration length of the B20W15 with 600 bar injection pressure under 5 bar ambient pressure was measured as 41.6 mm after 0.25 ms injection started, while the injection pressure was increased to 800 bar under same ambient pressure at the same time it was measured as to be 47,2 mm. And penetration length under 10 bar ambient pressure while keeping the same conditions were measured as 28,9 mm and 32,1mm respectively.

Consequently, it can be said that chamber pressure has stronger effect on the penetration length than injection pressure.

In addition to these, it was observed that, at 600 bar injection pressure under zero bar ambient pressure, all fuels hit the wall after approximately 0.55 ms injection time, while they all hit the wall after 4 ms injection time at 800 bar under the same ambient pressure. But when the ambient pressure was 5 bar, reference diesel could not reach the wall for both injection pressures while reference biodiesel was the only one hitting the wall under both injection pressures. B20W15 and B20W5 also could not touch the wall under 600 bar injection while they both impinge to the wall under 800 bar injection towards the end of the enjection. In addition to these, reference biodiesel and both emulsions could not hit the wall for both injection pressures under 10 bar chamber pressure.

To compare emulsions, in general the lengths of B20W15 was closer to reference biodiesel while B20W5 was closer reference diesel. As it is shown in Figure 4.1 and Figure 4.2, B20W15 had longer penetrations than B20W5 under both injection pressure and ambient chamber. For instance, at 600 bar injection pressure under 5 bar at 0.4 ms of injection, the difference between B20W15 and B20W5 was 4.1 mm while the difference was 5.1 mm at 0.85 ms of injection. At the end of the injection the difference became 6.3 mm. The results became slightly smaller at 800 bar injection pressure under 5 bar chamber pressure, and both emulsions impinge the wall at the end of the injection. In addition to these, the most distinctive differences at each ambient pressure for 600 bar injection pressure between them occurred at the end of the injection except zero bar chamber pressure since all fuel impinged the wall earlier due to the low resistance. For instance, the differences between them were 6.3 mm and 3.1 mm respectively at 600 bar injection pressure and under 5 bar and 10 bar ambient pressure.

The penetration differences between fuels can be associated with the viscosities and densities of the fuels and increment on the ambient pressure as mentioned. Yu et al. (2017) [34] reported that the average velocity at the end of the nozzle for diesel is higher than that of biodiesel because of lower viscosity of diesel. Therefore, the average velocity at the end of the nozzle for reference diesel might become higher than that of reference biodiesel, B20W15 and B20W5 because of its lower viscosity. However, these features of reference diesel may lead to speed up breaking up the spray results in better

atomization, but it may result in lower penetration lengths by preventing the development of spray propagation. This phenomenon can be seen better on the Figure 4.1.(b) while the ambient pressure was 5 bar. At the beginning of the injection reference diesel had longer penetration than reference biodiesel and both emulsions, while it can be seen that it takes the same distance with other fuels 0.1 ms after the start of injection, soon after that the penetration length of diesel becomes less than all other fuels.

In addition to these, both Nguyen et al. (2020) [35] and Gao et al. (2009) [37] stated that increase in biodiesel concentration in the mixture makes the spray more resistance to break up due to raised viscosity in the mixture, which resulted larger size of droplets. Larger size with bigger momentum spray droplets due to higher density results in longer penetration lengths. According to this reason, why both emulsified fuels had longer penetration lengths than that of reference diesel can be associated with their higher viscosities and densities compared to diesel since water content leads to increase viscosity and density of the mixture. Meanwhile, according to same reason, why both emulsified fuels had shorter penetration lengths than that of reference biodiesel can be attributed to their lower viscosities and densities compared to reference biodiesel. Furthermore, the reason why B20W15 had longer penetrations than B20W5 can also be associated with higher viscosity and density of B20W15 since increasing water concentrations results in higher density and viscosity in the mixture.

To sum up, it was found out that B20W15 resulted longer penetration lengths than B20W5 under the same test conditions. Besides, it was understood that both emulsified biodiesel-diesel blends lead longer spray penetration lengths compared to reference diesel, but they lead shorter penetration lengths than reference biodiesel when the result of this study is compared to result of A. Ulu (2020) [82], however it was understood that there is no distinctive difference between B20W5 and reference diesel. Also, the results found out in this study were coherent with the studies in the literature. To explain, increment in chamber pressure reduces the penetration length was observed like study of Agarwal et al. (2014) [39] while increase in injection pressure leads longer penetrations align with studies of Nguyen et al. (2020) [35], Agarwal et al. (2014) [39] and Park et al. (2016) [40]. Also, increment in water concentration in the mixture results in longer spray penetrations was found out like the studies of Amir Khalid et al. (2017) [33], Park et al. (2016) [40], A. Khalid et al. (2014) [42].

### 4.3. Examination of Spray Cone Angle

In order to better understand the effect of 600 bar and 800 bar injection pressures on the spray cone angle depending on the pressure change in the combustion chamber, spray angles of fuels at 0 bar, 5 bar and 10 bar ambient pressures are respectively shown in Figure 4.3 as follows. Besides, the effect of ambient pressures on the spray angle at each injection pressure under 0 bar, 5 bar and 10 bar pressure are shown together in Figure 4.4 for easier comparison. Besides, in order to compare spray cone angles of the emulsified blend biodiesels with those of diesel and biodiesel, all reference diesel and reference biodiesel values in the graphs which are shown with bold red and green lines were taken from study of A. Ulu (2020) [82] which carried out the experiments with same test equipments under the same test conditions to investigate the spray cone angle of diesel and biodiesel. During that study, repeatability and uncertainty of the spray cone angle for diesel and biodiesel was found out as 3% and  $\pm 0.7^\circ$ .

The repeatability and uncertainty of SCA for B20W5 and B20W15 are 5% and  $\pm 0.9^\circ$  respectively while repeatability and uncertainty of SCA for reference diesel and reference biodiesel are 3% and  $\pm 0.7^\circ$  in all graphs within in Figure 4.3 and Figure 4.4.

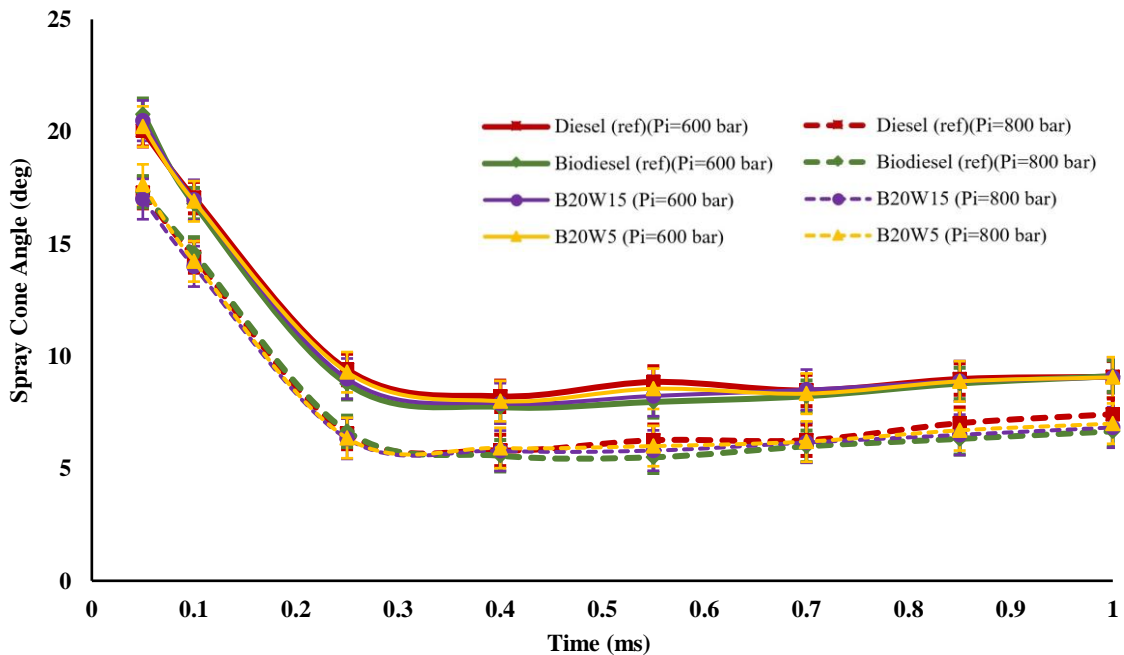


Figure 4.3 (a): Spray cone angles with injection pressures of 600 bar and 800 bar at 0 bar ambient pressure

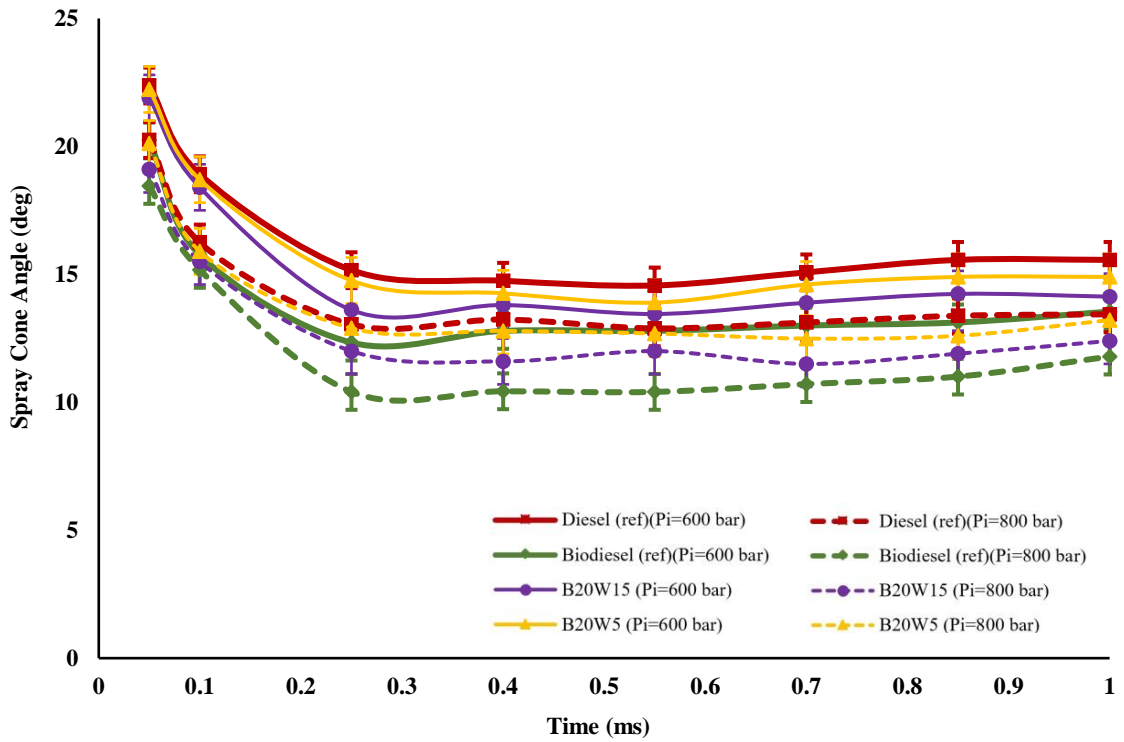


Figure 4.3 (b): Spray cone angles with injection pressures of 600 bar and 800 bar at 5 bar ambient pressure

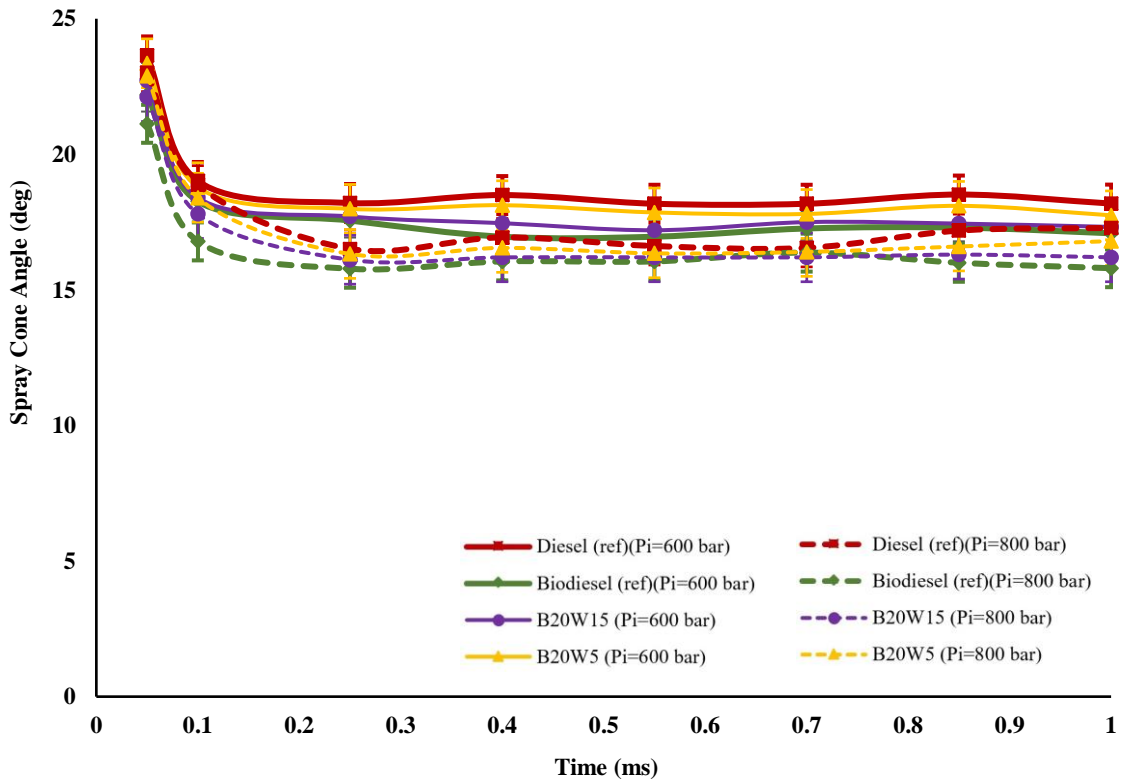


Figure 4.3 (c): Spray cone angles with injection pressures of 600 bar and 800 bar at 10 bar ambient pressure

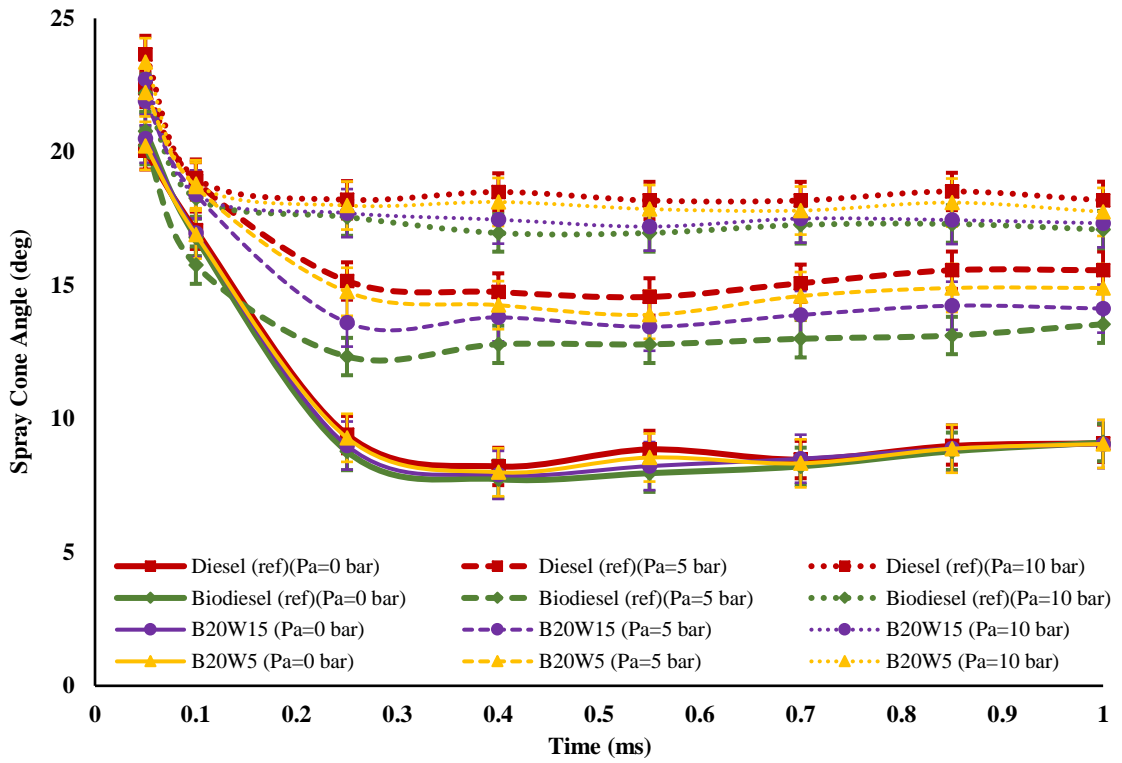


Figure 4.4 (a): Spray cone angles with 600 bar injection pressure under 0 bar, 5 bar, 10 bar ambient pressure

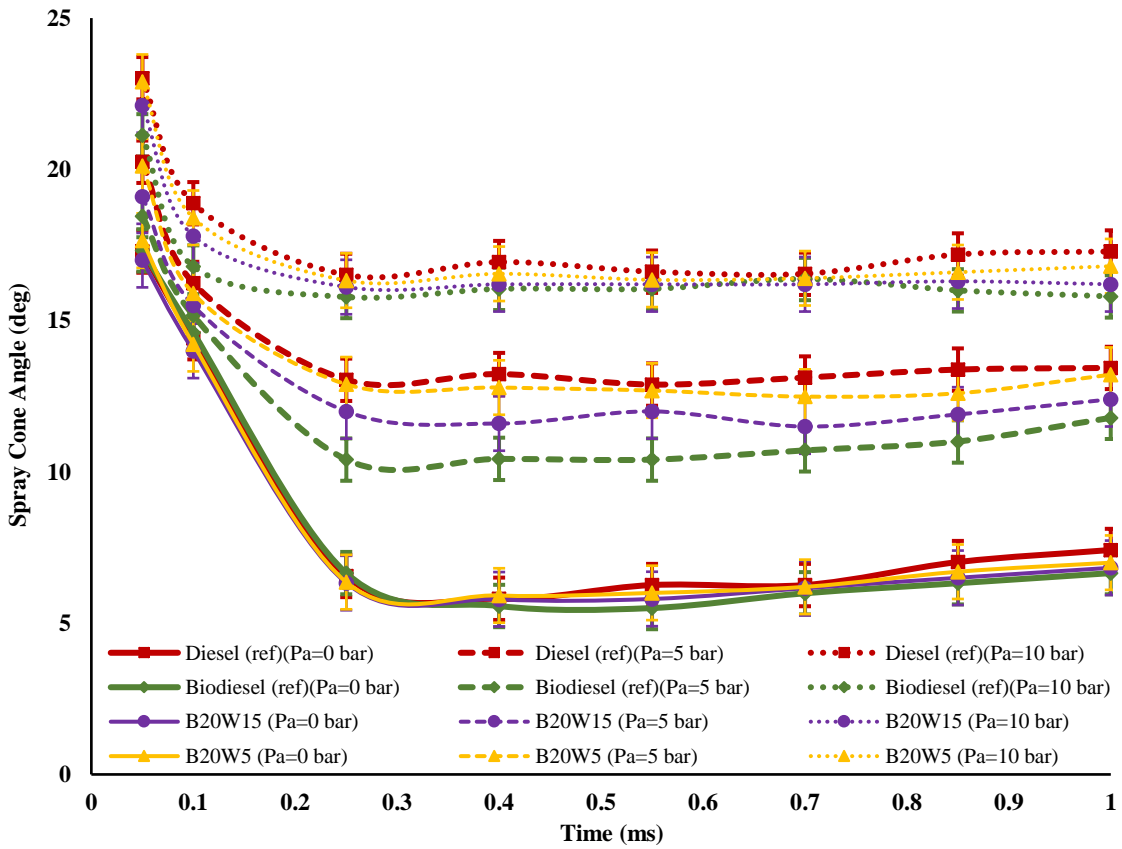


Figure 4.4 (b): Spray cone angles with 800 bar injection pressure under 0 bar, 5 bar, 10 bar ambient pressure

Figure 4.3 and Figure 4.4 indicate that injection pressure and ambient pressure take significant role on the spray cone angle. It was observed that, increasing ambient pressure results in significant increase in spray cone angle while increasing injection pressure from 600 bar to 800 bar results in less reduce on spray cone angle. To explain, the maximum difference in spray cone angle caused by increased injection pressure from 600 bar to 800 bar after 0.4 ms of the injection under 0 bar ambient pressure was measured  $2.1^\circ$  for B20W15 fuel while angles of both injection pressures were respectively  $7.9^\circ$  and  $5.8^\circ$ . When the 5 bar chamber pressure was taken consider at same time under same injection pressures, the angles became respectively  $13.8^\circ$  and  $11.6^\circ$  while the difference caused by changing injection pressure was  $2.2^\circ$ . The effect of increasing ambient pressure was found out more than twice of increasing injection pressure according to this conditions. Under the same conditions at same time, larger differences were observed for reference diesel fuel followed by B20W5, B20W15 and reference biodiesel. Mohan et al. (2014) [38] explained the reason why increasing ambient pressure causes increment in spray cone angle is that raised ambient pressure causes fuel exposed to higher resistance which inhibits its axial devoplement therefore it results in wider spray cone angles.

In addition to these, reference diesel has the largest angles under all conditision except under zero bar ambient pressure since all types of fuel strike to wall surface in earlier. Also, reference biodiesel has narrower spray cone angles compared to all fuels. In general, the angle of B20W5 was closer to reference diesel while B20W15 was closer to reference biodiesel. In other words, the spray angles of B20W5 had larger than B20W15, which shows that increment in water concentration results in narrower spray angles. For example, spray angles of B20W5 and B20W15 at 600 bar injection pressure exposed 5 bar chamber pressure after 0.4 ms injection started was measured respectively  $14.2^\circ$  and  $13.8^\circ$ . However, it was observed that, there were no obvious distinction between spray angle of the fuels when the sprays became steady, which results in stabile angle for the rest of the injection. To elaborate more, at 0.85 ms of injection under the same conditions (0.45 ms later) the angles of sprays became  $14.9^\circ$  and  $14.2^\circ$ . Hence, it can be seen that, the difference in the spray angle of the each emulsified fuel is not exceeding  $1^\circ$  during steady state. Moreover, as the ambient pressure increases the spray cone angle of fuels becomes stable earlier as shown in Figure 4.3 and 4.4. For example, when the ambient pressure was 10 bar, the time for angles to become stable was



aproximately after 0.1 ms injection started. Meanwhile, it was approximately 0.25 ms for 5 bar chamber pressure.

Yu et al. (2017) [34] reported that the lower viscosity of diesel may lead the spray disintegrate easier than higher viscosity of biodiesel which promotes diesel splitting to larger area, thereby it leads to increase in spray cone angle. Meanwhile, biodiesel inhibits the disintegration of the spray which leads to smaller cone angles due to higher viscosity of biodiesel. The reason why B20W5 had wider cone angles compared to B20W15 under the same conditions may be correlated with the lower viscosity of B20W5. Also, for the same reason, why emulsified fuels have narrower angles compared to reference diesel and larger angles compared to reference biodiesel can be associated with their higher viscosities compared to reference diesel and their lower viscosities in comparison with reference biodiesel.

To sum up, it was observed that, B20W5 have wider cone angles than B20W15 under the same conditions. Also, it was understood that under the same conditions emulsified biodiesel-diesel blends resulted smaller cone angles compared to reference diesel, but they resulted larger cone angles than reference biodiesel when the result of this study is compared to result of A. Ulu (2020) [82], but it was understood that there is no significant difference between B20W5 and reference diesel. Besides, the results obtained in this study are in harmony with other studies in the literature. It was observed that increment water concentration in the emulsion caused narrower spray angles like the research in Amir Khalid et al. (2017) [33] and A. Khalid et al. (2014) [42]. In addition, it was observed that, increase in chamber pressure leads increase in spray cone angle like studies of Mohan et al. (2014) [38] and Emberson et al. (2016) [47]. On the other hand, raise in injection pressure resulted in decrease in spray cone angle. However, changing injection pressure did not significantly effect the spray cone angle while changing ambient pressure affected remarkably spray cone angle like research of Mohan et al. (2014) [38].

## CHAPTER 5

### CONCLUSION

#### 5.1. Conclusions

Since the exhaust emissions caused by diesel fuel adversely affect human health and environment, many researches have been carried out by the researchers in order to find out an alternative fuel that can replace diesel fuel. Studies indicate that emulsified biofuels with water do not only reduce the pollutant emissions, and also contribute to the combustion efficiency. The aim of this study is to examine the macroscopic spray parameters such as spray penetration length and cone angle of emulsified fuels, which directly play an essential role on emission level and combustion efficiency when the air and fuel mixture is taken into consideration.

In order to investigate macrospray characteristics of emulsified fuels, two emulsion fuels, namely B20W5 and B20W15 (containing 5% and 15% water by volume) were prepared. The emulsification process was carried out by utilizing Tween 80 and Span 80 as surfactants via mechanical agitator. In order to conduct the experiment, a Constant Volume Combustion Chamber (CVCC) was used for the test rig and the shadowgraph technique was applied to visualize the spray propagation. A high speed camera that captures 20000 frames per second was utilized for recording.

The experiments were performed under 0 bar, 5 bar and 10 bar ambient chamber pressure provided by nitrogen gas while injection pressures were adjusted to 600 bar and 800 bar respectively via fuel pump. Before starting the experiments, B20W5 and B20W15 were prepared and their density at room temperature and viscosity at 40°C were measured through pycnometer and rheometer, respectively. After the experiments were completed, the spray images of the test fuels recorded by high speed camera. Then, the recorded images were processed through ImageJ program and the results were analyzed.

According to results obtained during this study, it can be said that water concentration in the emulsion has significant effect on the emulsion stability. To explain, increment in water concentration in blended biodiesel-diesel causes deterioration in the emulsion stability. In addition, value of HLB and concentration of surfactant is also important for emulsion stability. According to trials, best stabilization was obtained when the HLB of the mixture was 8, both concentration of surfactant and water were 5% by volume. However, it was observed that, it is possible to make stable mixtures with HLB 9 although it has less stabilization compared to HLB 8. Besides, it was also found that increasing water content led to raise in density and viscosity of the emulsion.

When the spray characteristics of emulsified biodiesel blends were examined, the following results were obtained. Under the same conditions, B20W15 had longer penetrations and narrower angle than B20W5. In other words, it was found out that, increment in water concentration in the emulsion resulted in smaller spray angles and longer spray penetrations. For instance, spray penetration of B20W15 was found as 7% higher than that of B20W5 at the end of the injection with 600 bar injection pressure under 5 bar ambient pressure. On the other hand, spray cone angle of B20W5 was obtained as 6% higher than that of B20W15 under the same condition. The reason of this may be because of the higher viscosity and density of B20W15. While the higher viscosities may cause poor atomization which may result in longer spray penetration lengths and narrower spray cone angles. Meanwhile, higher density may promote increment in momentum of the fluid, which may result in longer penetrations.

Moreover, it was found that, increase in ambient pressure led remarkable reduce in spray penetration length and increment in spray cone angle. The reason for this may be explained by the fact that the fuel is exposed to higher resistance at the end of the nozzle exit may cause inhibition its axial development which results in wider spray cone angles and shorter penetration. Besides, raise in injection pressure caused longer penetration lengths, probably due to increase in velocity at nozzle exit however it did not affect spray cone angles significantly.

To sum up, it was observed that the physical properties of fuels, changing ambient pressure and injection pressure take an important role on the spray penetration length and spray cone angle. The result showed that increasing water concentration in the emulsion resulted higher kinematic viscosity, higher density and deterioration in the stability of the

emulsion. Also, it resulted in longer spray penetration lengths and smaller spray cone angles. It was found out that B20W15 led longer spray penetrations and narrower spray cone angles compared to B20W5 under the same test conditions. Besides, it was understood that there is no distinctive difference between B20W5 and reference diesel in terms of spray geometry when the result of this study is compared to another study which performed the experiments with same test apparatus under the same test conditions in order to investigate spray characteristics of diesel and biodiesel. As a result, considering the ability of B20W5 to reduce the use of fossil oil and no significant difference in terms of spray geometry when compared to diesel, it can be said that B20W5 may be a promising alternative fuel for future.

## **5.2. Suggestions for Future Works**

The effect of mixer type on the emulsion stability can be analyzed by preparing the emulsions via ultrasonic homogenizer instead of mechanical stirrer. Thus, the stability of emulsion produced by ultrasonic homogenizer can be compared to emulsion produced by mechanical agitator. Also, microscopic examination can be carried out on the emulsions in order to observe which mixer type provides larger or smaller particle size. So that, emulsions contain different size of particles can be used in the experiments and the results can be compared in terms of their spray characteristics.

Besides, emulsions can be prepared by utilizing different surfactants. So that, different types of emulsions can be acquired which could be beneficial when investigating the spray characteristics of these different emulsions, especially when their viscosities are taken consider. Also, effect of using different type of surfactants on emulsion stability can be examined.

Moreover, since the viscosity and density takes an significant role on the spray characteristics of the fuel, the emulsion blends can be prepared by various of biodiesel and water concentrations, and their properties can be compared between each others.

Furthermore, the experiments can be conduct with higher injection pressure under higher chamber pressures to better understand effect of these on the spray penetration length and spray cone angle.

## REFERENCES

- [1] Thangavelu, Saravana Kannan; Ahmed, Abu Saleh; Ani, Farid Nasir. Review on bioethanol as alternative fuel for spark ignition engines. *Renewable and Sustainable Energy Reviews* (2016), 56, 820–835
- [2] Borovalı, Selçuk. Dünya’da ve Türkiye’de Biyodizel Sektörünün Bugünü ve Yarını. *Biyodizel Sanayi Derneği* (2019).
- [3] Hoekman, Kent; Robbins, Curtis. Review of the effects of biodiesel on NOx emissions. *Fuel Processing Technology* (2012), 96, 237–249.
- [4] Canakci, Mustafa. Combustion characteristics of a turbocharged DI compression ignition engine fueled with petroleum diesel fuels and biodiesel. *Bioresource Technology* (2007), 98(6), 1167–1175.
- [5] Chauhan, Bhupendra Sing; Kumar, Naveen; Cho, Haeng Muk. A study on the performance and emission of a diesel engine fueled with Jatropha biodiesel oil and its blends. *Energy* (2012), 37(1), 616–622.
- [6] Kumar, Senthil; Bellettre, Jérôme; Tazerout, Mohand. The use of biofuel emulsions as fuel for diesel engines: A review. *Proceedings of the Institution of Mechanical Engineers, Part A: Journal of Power and Energy* (2009), 223(7), 729–742
- [7] Elsanusi, Osama Ahmed; Roy, Muhari Mohon; Sidhu, Manpreet Singh. Experimental Investigation on a Diesel Engine Fueled by Diesel-Biodiesel Blends and their Emulsions at Various Engine Operating Conditions. *Applied Energy* (2017), 203, 582-593

- [8] Murat Karabektas; Gokhan Ergen; Can Hasimoglu; Ahmet Murcak. Performance and Emission Characteristics of a Diesel Engine Fuelled with Emulsified Biodiesel-Diesel Fuel Blends, *International Journal of Automotive Engineering and Technologies* (2016), 176-185
- [9] Avulapati, Mohan Madan; Ganippa, Lionel Christopher; Xia, Jun; Megaritis, Athanasios. Puffing and micro-explosion of diesel-biodiesel-ethanol blends. *Fuel* (2016), 166, 59–66.
- [10] Hagos, Ftwi Y.; Aziz, A. Rashid A.; Tan, Isa M. Water-in-diesel emulsion and its micro-explosion phenomenon-review. *2011 IEEE 3rd International Conference on Communication Software and Networks* (2011), *ICCSN 2011*, 314–318
- [11] Naber, Jeffrey D.; Johnson, Jaclyn E. Internal combustion engine cycles and concepts. *Alternative Fuels and Advanced Vehicle Technologies for Improved Environmental Performance: Towards Zero Carbon Transportation* (2014), 1–224.
- [12] Tindal, M. J.; Uyehara, O. A. Chapter Three Diesel Engines. In *Internal Combustion Engines*, (1988).
- [13] Nirmala, N.; Dawn, S. S.; Harindra, C. Analysis of performance and emission characteristics of Waste cooking oil and *Chlorella variabilis* MK039712.1 biodieselblends in a single cylinder, four strokes diesel engine. *Renewable Energy* (2020), 147, 284–292.
- [14] Heywood, John B. *Internal combustion engine fundamentals*; McGraw-Hill: New York, (1998).

- [15] Salmani, Mahir. H.; Rehman, S.; Zaidi, K.; Hasan, Ahmad. K. Study of ignition characteristics of microemulsion of coconut oil under off diesel engine conditions. *Engineering Science and Technology, an International Journal* (2015), 18(3), 318–324.
- [16] Rounce, Paul; Tsolakis, Athanasios; York, Andrew Peter Edward. Speciation of particulate matter and hydrocarbon emissions from biodiesel combustion and its reduction by aftertreatment. *Fuel* (2012), 96, 90–99.
- [17] Sayin, Cenk; Ilhan, Murat; Canakci, Mustafa; Gumus, Metin. Effect of injection timing on the exhaust emissions of a diesel engine using diesel-methanol blends. *Renewable Energy* (2009), 34(5), 1261–1269.
- [18] Mohamed Shameer, P.; Ramesh, Kasimani; Sakthivel, Rajamohan; Purnachandran, Ramakrishnan. Effects of fuel injection parameters on emission characteristics of diesel engines operating on various biodiesel: A review. *Renewable and Sustainable Energy Reviews* (2017)., 67(3), 1267–1281.
- [19] Raheman, Hijfur; Kumari, Sweeti. Combustion characteristics and emissions of a compression ignition engine using emulsified jatropha biodiesel blend. *Biosystems Engineering* (2014), 123(x), 29–39.
- [20] Panneerselvam, N.; Murugesan, A.; Vijayakumar, C.; Kumaravel, Arumugam; Subramaniam, Dhanakotti; Avinash, A. Effects of injection timing on bio-diesel fuelled engine characteristics - An overview. *Renewable and Sustainable Energy Reviews* (2015), 50, 17–31.
- [21] Canakci, Mustafa; Ozsezen, Ahmet Necati; Alptekin, Ertan; Eyidogan, Muharrem. Impact of alcohol-gasoline fuel blends on the exhaust emission of an SI engine. *Renewable Energy* (2013)., 52(x), 111-117

- [22] Raman, L. Anantha.; Deepanraj, Balakrishman.; Rajakumar, S.; Sivasubramanian, Velmurugan. Experimental investigation on performance, combustion and emission analysis of a direct injection diesel engine fuelled with rapeseed oil biodiesel. *Fuel* (2019), 246(March 2018), 69–74.
- [23] Gupta, Vivek Kumar; Zhang, Zhen; Sun, Zongxuan. Modeling and control of a novel pressure regulation mechanism for common rail fuel injection systems. *Applied Mathematical Modelling* (2011), 35(7), 3473–3483.
- [24] Carsten Baumgarten. *Mixture Formation in Internal Combustion Engines; Heat and mass transfer*; Springer-Verlag Berlin Heidelberg: Berlin, (2006)
- [25] Fuel Injection Systems. <https://nathbeke.files.wordpress.com/2013/11/fuel-injection.pdf> (accessed Oct 18, 2020).
- [26] Horrocks, R. W.; Lawther, R.; Hatfield, L. Fuel injection systems for high-speed direct injection diesel engines. *Advanced Direct Injection Combustion Engine Technologies and Development: Diesel Engines* (2009), 61–104.
- [27] Helge von Helldorff; Micklow, Gerald. J. Micklow. Primary and Secondary Spray Breakup Modelling for Internal Combustion Engine Applications. *Journal of Multidisciplinary Engineering Science and Technology* (2019), 6(4).
- [28] Trinh, Huu. P.; Chen, C. P. Modeling of turbulence effects on liquid jet atomization and breakup. *43rd AIAA Aerospace Sciences Meeting and Exhibit Meeting Papers, December* (2005), 5781–5801.
- [29] Bekdemir, Cemil. Numerical Modeling of Diesel Spray Formation and Combustion. *Master Thesis*, (2008).



- [30] Yao, Jiafeng. F.; Tanaka, Keiichi; Kawahara, Akimaro; Sadatomi, Michio. Development of Resource-Driven Scheduling Model for Mass Housing Construction Projects. *International Journal of Engineering and Technology* (2015), 7(5), 424–431.
- [31] Soid, Shahril Nizam Mohamed; Zainal, Z. Alimuddin. Spray and combustion characterization for internal combustion engines using optical measuring techniques - A review. *Energy* (2011), 36(2), 724–741.
- [32] Suh, Hyun Kyu; Park, Sung Wook; Lee, Chang. Effect of piezo-driven injection system on the macroscopic and microscopic atomization characteristics of diesel fuel spray. *Fuel* (2007), 86(17–18), 2833–2845.
- [33] Khalid, Amir; Suardi, Mirnah; Chin, Ronny Yii Shi; Amirnordin, Shahrin Hisham. Effect of Biodiesel-water-air Derived from Biodiesel Crude Palm Oil Using Premix Injector and Mixture Formation in Burner Combustion. *Energy Procedia* (2017), 111(September 2016), 877–884.
- [34] Yu, Shenghao; Yin, Bifeng; Jia, Hekun; Wen, Shuai; Li, Xifeng; Yu, Jianda. Theoretical and experimental comparison of internal flow and spray characteristics between diesel and biodiesel. *Fuel* (2017), 208, 20–29.
- [35] Nguyen, Tuannghia; Pham, Minh Hieu; Anh, Tuan Le. Spray, combustion, performance and emission characteristics of a common rail diesel engine fueled by fish-oil biodiesel blends. *Fuel* (2020), 269(January).
- [36] Lee, Sanghoon; Lee, Chang S.; Park, Sungwook; Gupta, Jai Gopal; Maurya, Rakesh Kumar; Agarwal, Avinash Kumar. Spray characteristics, engine performance and emissions analysis for Karanja biodiesel and its blends. *Energy* (2017), 119, 138–151.

- [37] Gao, Yuan; Deng, Jun; Li, Chunwang; Dang, Fengling; Liao, Zhuo; Wu, Zhijun; Li, Liguang. Experimental study of the spray characteristics of biodiesel based on inedible oil. *Biotechnology Advances* (2009), 27(5), 616–624.
- [38] Mohan, Balaji; Yang, Wenming; Tay, Kun Lin; Yu, Wenbin. Experimental study of spray characteristics of biodiesel derived from waste cooking oil. *Energy Conversion and Management* (2014), 88, 622–632.
- [39] Agarwal, Avinash Kumar; Dhar, Aatul; Gupta, Jai Gopal; Kim, Woong Il; Lee, Chang S.; Park, Sungwook. Effect of fuel injection pressure and injection timing on spray characteristics and particulate size-number distribution in a biodiesel fuelled common rail direct injection diesel engine. *Applied Energy* (2014), 130, 212–221.
- [40] Park, Sangki; Woo, Seungchul; Kim, Hyungik; Lee, Kihung. The characteristic of spray using diesel water emulsified fuel in a diesel engine. *Applied Energy* (2016), 176, 209–220.
- [41] Lin, Yuang-Shin; Lin, Hai-Ping. Spray characteristics of emulsified castor biodiesel on engine emissions and deposit formation. *Renewable Energy* (2011), 36(12), 3507–3516.
- [42] Khalid, A.; Amirnordin; Shahrin Hisham; Hamidon, Lambosi; Lambosi, Latip; Manshoor, B.; Sies, Mohamad Farid; Salleh, Hamidon; Spray characteristic of diesel-water injector for burner system. *Advanced Materials Research* (2014), 845, 66–70.
- [43] Huo, Ming; Lin, Shenlun; Liu, Haifeng; Lee, Chia-fon F. Study on the spray and combustion characteristics of water-emulsified diesel. *Fuel* (2014), 123, 218–229.

- [44] Song, Jinkwan; Lee, Jong Guen. Characterization of spray formed by diesel-water mixture jet injection into an air crossflow. *Fuel* (2020), 282(August), 118818.
- [45] Huo, Ming; Wu, Han; Zhou, Nan; Nithyanandan, Karthik; Lee, Chia-fon F. Effects of Spray Characteristics of Emulsified Diesel on Soot Emissions in a Constant Volume Chamber. *Department of Mechanical Science and Engineering University of Illinois at Urbana-Champaign, Urbana, IL 61801, USA State Key Laboratory of Automotive* (2013).
- [46] Wang, Xiangang; Huang, Zuohua; Kuti, Olawole Abiola; Zhang, Wu; Nishida, Keiya. Experimental and analytical study on biodiesel and diesel spray characteristics under ultra-high injection pressure. *International Journal of Heat and Fluid Flow* (2010), 31(4), 659–666.
- [47] Emberson, David R.; Ihracska, Balazs Alexis; Imran, Shahid; Diez, Alvaro. Optical characterization of Diesel and water emulsion fuel injection sprays using shadowgraphy. *Fuel* (2016), 172(x), 253–262.
- [48] Kadocsa, András. *Modeling of Spray Formation in Diesel Engines*, (2007).
- [49] Srichai, Prathan. Design Concept of Biodiesel Direct Injection Constant Volume Combustion Chamber (October 2012).
- [50] Baert, Rik S. G.; Frijters, Peter J. M.; Somers, Bart; Luijten, Carlo; De Boer, Wout. Design and operation of a high pressure, high temperature cell for HD diesel spray diagnostics: Guidelines and results. *SAE Technical Papers* (2009), 4970.

- [51] Munsin, Ronnachart; Shing, Bodin Chung Lim; Phunpheeranurak, Khansorn; Thanisorn, Phongphankasem; Laonual, Yossapong; Jugjai, Sumrerng; Chanchaona, Somchai. Design of Constant Volume Combustion Chamber (CVCC) with Pre-Combustion Technique for Simulation of CI Engine Conditions. *The 4th TSME International Conference on Mechanical Engineering* (2013)
- [52] Bachalo, W. D. (2000). Spray diagnostics for the twenty-first century. *Atomization and Sprays*, 10(3–5), 439–474.
- [53] Castrej, R. *The shadowgraph imaging technique and its modern application to fluid jets and drops - ProQuest SciTech Collection – ProQuest* (2011), 57(3), 266–275.
- [54] Braeuer, Andreas. Shadowgraph and Schlieren Techniques. *Supercritical Fluid Science and Technology* (2015), 7, 283–312.
- [55] Zhao, Hua; Ladommatos, Nicos (1998). Optical diagnostics for in-cylinder mixture formation measurements in IC engines. *Progress in Energy and Combustion Science*, 24(4), 297–336.
- [56] Mohan, Balaji; Yang, Wemning; Chou, Siaw Kiang. Fuel injection strategies for performance improvement and emissions reduction in compression ignition engines - A review. *Renewable and Sustainable Energy Reviews* (2013), 28(x), 664–676.
- [57] Fahd, M. Ebna Alam; Wenming, Yang; Lee, Poh Seng; Chou, Siaw Kiang; Yap, Christopher R. Experimental investigation of the performance and emission characteristics of direct injection diesel engine by water emulsion diesel under varying engine load condition. *Applied Energy* (2013), 102, 1042–1049.

- [58] Armas, Octavio; Ballesteros, Rosario; Martos, Ramos F. J.; Agudelo, John R. Characterization of light duty Diesel engine pollutant emissions using water-emulsified fuel. *Fuel* (2005), 84(7–8), 1011–1018.
- [59] Maiboom, Alain; Tauzia, Xavier. NOx and PM emissions reduction on an automotive HSDI Diesel engine with water-in-diesel emulsion and EGR: An experimental study. *Fuel* (2011), 90(11), 3179–3192.
- [60] Aziz, Amir; Jusoh, Asraf; Mamat, Rizalman; Abdullah, Adam. Effect of water content and tween 80 to the stability of emulsified biodiesel. *Applied Mechanics and Materials* (2014), 465–466(March 2015), 191–195.
- [61] Pinto, Angelo. C.; Guarieiro, Lilian L. N.; Rezende, Michelle J. C.; Ribeiro, Núbia M.; Ednildo, A. Torres; Lopes, Wilson A., Pereira, Pedro A. de P.; Andrade, Jailson B. de. *Biodiesel: An Overview*. (2005), 16(6), 1313–1330.
- [62] Huang, Daming; Zhou, Haining; Lin, Lin. Biodiesel: an Alternative to Conventional Fuel. *Energy Procedia* (2012), 16, 1874–1885.
- [63] Kiss, Anton. A., Dimian; Alexandre C. Dimian; Rothenberg, Gadi. Biodiesel by catalytic reactive distillation powered by metal oxides. *Energy and Fuels* (2008), 22(1), 598–604.
- [64] Vellaiyan, Suresh; Amirthagadeswaran, Sankaranarayanan. The role of water-in-diesel emulsion and its additives on diesel engine performance and emission levels: A retrospective review. *Alexandria Engineering Journal* (2016), 55(3), 2463–2472.
- [65] Yahaya Khan, Mohammed; Abdul Karim, Zainal Ambri, Hagos, Ftwi Yohanness; Aziz, A. Rashid A.; Tan, Isa Mohd. Current trends in water-in-diesel emulsion as a fuel. *The Scientific World Journal*, (2014).

- [66] Koc, A. Bulent; Abdullah, Mudhafar. Performance and NO<sub>x</sub> emissions of a diesel engine fueled with biodiesel-diesel-water nanoemulsions. *Fuel Processing Technology* (2013), 109(x), 70–77.
- [67] Reham, S. S.; Masjuki, Hassan Hassan; Kalam, Mohammed Abul; Shancita, I.; Rizwanul Fattah, I. M.; Ruhul, A. M. Study on stability, fuel properties, engine combustion, performance and emission characteristics of biofuel emulsion. *Renewable and Sustainable Energy Reviews* (2015), 52, 1566–1579.
- [68] Lin, Cherng-Yuan; Lin, Shiou-An. Effects of emulsification variables on fuel properties of two- and three-phase biodiesel emulsions. *Fuel* (2007), 86(1–2), 210–217.
- [69] Lin, Cherng-Yuan; Wang, Kuo-Hua. The fuel properties of three-phase emulsions as an alternative fuel for diesel engines. *Fuel* (2003), 82(11), 1367–1375.
- [70] Kapadia, Harsh; Brahmabhatt, Hardik; Dabhi, Yuvrajsinh; Chourasia, Sajan. Investigation of emulsion and effect on emission in CI engine by using diesel and bio-diesel fuel: A review. *Egyptian Journal of Petroleum* (2019), 28(4), 323–337.
- [71] Karim, Zainal Ambri Abdul; Tee, Degen; Khan, Mohamed Yahaya; Hagos, Ftwi Yohannes. Investigation of Water-in-Biodiesel Emulsion Characteristics Produced by Ultrasonic Homogenizer. *MATEC Web of Conferences* (2018), 225.
- [72] Karim, Zainal Ambri Abdul; Kaur, Esha; Syed Masharuddin, Syed Masharuddin; Khan, Mohammed Yahaya; Hagos, Ftwi Yohannes. The characteristics of water-in-biodiesel emulsions produced using ultrasonic homogenizer. *Alexandria Engineering Journal* (2020), Vol. 59, Issue 1, pp. 227–237.

- [73] Patil, Harshal; Waghnamre, Jyotsana. Biodiesel-water emulsions: An alternative approach for conventional fuels. *International Research Journal of Engineering and Technology (IRJET)* (2017), 4(7), 1200–1204.
- [74] Maawa, Wan Nor; Mamat, Rizalman; Najafi, Gholamhassan; De Goey, L. P. H. Performance, combustion, and emission characteristics of a CI engine fueled with emulsified diesel-biodiesel blends at different water contents. *Fuel* (2020), 267.
- [75] Ghannam, Mamdouh T.; Selim, Mohamed Y. E. Stability behavior of water-in-diesel fuel emulsion. *Petroleum Science and Technology* (2009), 27(4), 396–411.
- [76] Sathik Basha, J.; Anand, R. B. Role of nanoadditive blended biodiesel emulsion fuel on the working characteristics of a diesel engine. *Journal of Renewable and Sustainable Energy* (2011), 3(2).
- [77] Chu, Ningning; Xu, Yan; Ma, Yujiu; Wang, Jianxun; Li, Xuebing; Wang, Lisheng. Fuel properties of a two-phase biodiesel emulsion. *Advanced Materials Research* (2012), 418–420, 254–259.
- [78] Senthil, Ramalingam; Arunan, K.; Silambarasan, Rajendran. Experimental investigation of a diesel engine fueled with emulsified biodiesel. *International Journal of ChemTech Research* (2015), 8(1), 190–195.
- [79] Kumar Patidar, Sonu; Raheman, Hifjur. Performance and durability analysis of a single-cylinder direct injection diesel engine operated with water emulsified biodiesel-diesel fuel blend. *Fuel* (2020), 273, 117779.

- [80] DB Tarımsal Enerji. <https://dbtarımsalenerji.com.tr/iletisim>  
(Accessed July 12, 2020)
- [81] ImageJ. <https://imagej.nih.gov/ij/docs/intro.html> (Accessed Oct 19, 2020)
- [82] Ulu, Anılcan. Experimental Investigation of Methyl Ester and Ethyl Ester Type Biodiesel Fuels in a Constant Volume Combustion Chamber, *Master Thesis*, (2020).
- [83] Fuel Injection System. <https://www.slideshare.net/JanardhanReddyBommiR/types-of-fuel-injection-system-and-nozzles> (Accessed Oct 11, 2020)